

**DEVELOPMENT OF A COMPUTER CONTROLLED
MULTICHANNEL POTENTIOSTAT FOR
APPLICATIONS WITH FLOWING SOLUTION ANALYSIS**



**DUBLIN CITY
UNIVERSITY**

Ollscoil Chathair Bhaile Atha Chath

By

Tang Fang B.Eng.

**A thesis submitted to Dublin City University for the degree of
Master of Science**

at

**The School of Chemical Sciences
Dublin City University**

May 1994

DEDICATION

I would like to dedicate this work to many people I love

In particular

My

Father, Mother

Brother

Wife

DECLARATION

I hereby certify that this material, which I now submit for assessment on the programme of study leading to the award of Master of Science is entirely my own, save and to the extent that such work has been cited and acknowledged within the text of my work.

Signed: Tang Fang
Tang Fang

Date: 20 May, 1994

School of Chemical Sciences
Dublin City University

ACKNOWLEDGMENTS

First and foremost I sincerely thank my supervisors Professors Malcolm R. Smyth and Doctor Dermot Diamond for their help and advice during the course of this work

I am grateful to my colleague Michael McGrath for his help and understanding

I am also indebted to all the staff, both academic and technical of the School of Chemical Sciences, Dublin City University, for their valuable assistance during my stay in Ireland

I would like to thank Doctor Peter Filelden for the donation of glassy carbon rods

ABSTRACT

A 16-channel computer controlled potentiostat has been designed for use with an amperometric array for analysis in flowing streams. The instrumentation developed to date has been used with both linear and radial flow cell configurations which have been constructed "in-house". Analogue and digital circuits for the independent control of 4 working electrodes have been fabricated, tested and integrated successfully to give an amperometric array. The design is based on the utilisation of common reference and counter electrodes to reduce the complexity of the electrode arrangement. Control of the purpose built instrumentation was effected with a 486-33 personal computer and Analog Devices RTI-815 and RTI-817 data acquisition/control cards, which are responsible for hardware control functions and data acquisition via digital and analogue control lines. Software for instrumentation control, data display (2- or 3-dimensional formats), on-line and post-run data processing and storage has been developed using the QuickBASIC software environment. The user interface utilises a Windows style display to achieve user friendliness with an on-line help facility. Data is stored in a spreadsheet compatible format (ASCII with "," column delimiter) to facilitate post-run processing with standard applications packages such as Microsoft EXCEL. The system has been applied to the determination of well characterised electroactive compounds using flow-injection analysis. Linearity over the range 10^{-2} - 10^{-7} M has been obtained with a detection limit of 2×10^{-7} M (S/N = 3.0) for potassium ferricyanide. The array has been applied to the simultaneous measurement of both oxidation and reduction currents of ferricyanide and hydroquinone.

CONTENTS

DEDICATION	I
DECLARATION	II
ACKNOWLEDGMENTS	III
ABSTRACT	IV
CONTENTS	V
CHAPTER 1. INTRODUCTION	1
1 1 Voltammetry	1
1 1 1 Hydrodynamic Voltammetry	4
1 2 The Potentiostat	5
1 2 1 Computerised Single Channel Potentiostats	7
1 2 2 The Bi-Potentiostat	9
1 2 3 Multichannel Potentiostats	10
1 3 Electrochemical Detection	13
1 3 1 FIA and Single Channel Potentiostats	14
1 3 2 Dual Electrodes	14
1 3 3 Flow Injection Analysis and Dual Channel Potentiostats	16
1 4 Multichannel Detection	17
CHAPTER 2. COMPOSITION AND FUNCTION OF SYSTEM	21
2 1 Introduction	21
2 2 Composition of Detection System	22
2 3 Technical Performance Criteria	23
2 4 System Functions	24
CHAPTER 3. DESIGN OF MULTICHANNEL POTENTIOSTAT	25
3 1 Introduction	25

3 2	Composition of Multichannel Potentiostat	25
3 3	Counter\Reference Electrode CE\RE Unit	26
3 3 1	Feedback Circuit of CE\RE Unit	27
3 3 2	Counter Electrode\Reference Electrode Unit Circuit	27
3 4	Current to Voltage (I/E) Converter Unit	29
3 4 1	Current to Voltage Converter	30
3 4 2	Gain and Sensitivity Selection	30
3 4 3	Current Offset	31
3 4 4	Analogue Filter	33
3 4 5	Differential Amplifier	36
3 4 6	Current to Voltage Converter Unit Circuit	38
3 5	D/A Converter and Control Units	40
3 5 1	AD7237 Introduction	41
3 5 2	AD7237 - Digital I/O Port Interface	41
3 5 3	Interface Logic Information - AD7237	42
3 5 4	DAC Units to RTI 817 Digital I/O Map and Function	45
3 5 5	Control Flow Chart	48
3 5 6	DAC Unit Circuit	49
3 6	Control Unit	50
3 6 1	Analogue Switch (DC411, DG419 and H13-0509)	51
3 6 2	Analogue Switch - Digital I/O Port Interface	52
3 6 3	Sensitivity Select and Control Truth Table	53
3 6 4	Control Unit Circuit	54
3 7	Power supply	55
CHAPTER 4. COMPUTER AND INSTRUMENTATION INTERFACE		56
4 1	Computer and hardware configuration	56
4 2	Interface card	56

4 2 1 RTI 815 Board	57
4 2 2 RTI 817 Board	58
4 2 3 RTI 817 Digital I/O Port Byte	58
4 2 4 Computer I/O Address Selection	63
4 2 5 RTI 815 and RTI 817 Software Drivers	63
CHAPTER 5. DEVELOPMENT FOR SOFTWARE OF SYSTEM	64
5 1 Introduction	64
5 2 Software Selection	65
5 2 1 Assembly Language Toolbox Operation	65
5 2 2 RTI Software Routines	67
5 3 Software Design	67
5 3 1 Structural Composition of Program	68
5 3 2 Program Flowchart	69
5 3 3 Initializing Routine	70
5 3 4 Detection System Program Menu	70
5 3 5 Graphical Display	73
5 3 6 Data File Import and Export	75
5 3 7 Potential Step Sequences	77
5 4 Data Acquisition and I/O Control Routines	77
5 4 1 Data Acquisition	77
5 4 2 Analog I/O Routine	78
5 4 3 Digital I/O Control Routine	81
5 5 Data Processing	86
5 5 1 Baseline Correction	86
5 5 2 Digital Filter	86
5 5 2 1 Boxcar Averaging	88
5 5 2 2 Ensemble Averaging	88

5 5 2 3 Smoothing (Weighted Digital Filtering)	88
5 5 2 4 Digital Filter Design for Detection System	89
5 5 3 Normalisation of the Signals	90
5 5 4 Peak Analysis	91
CHAPTER 6. DESIGN OF FLOW CELL AND ELECTRODE ARRAYS	93
6 1 Introduction	93
6 2 Design and Fabrication of Flow Cell	94
6 2 1 Multi-electrode array	94
6 2 2 Flow Cell body (Counter electrode)	95
6 2 3 Thin Flow Directing Spacer	95
6 2 4 Reference Electrode Holder	95
6 3 Design and Fabrication of Radial Flow Cell	97
6 3 1 Design and Construction of Radial Flow Cell	97
6 3 2 Production and Assembly	97
CHAPTER 7. FLOWING SOLUTION ANALYSIS	99
7 1 Experimental	99
7 1 1 Chemicals	99
7 1 2 Flow-Injection Analysis System	99
7 1 3 Working Electrode Preparation	100
7 2 Results and Discussion	100
7 2 1 Linearity	100
7 2 2 Filters	102
7 2 3 Electrode Response Weighting	103
7 2 4 Array Normalisation Procedure Evaluation	104
7 2 5 Three-Dimensional Results	112
7 2 6 Metal Analysis	116

CHAPTER 8. CONCLUSIONS AND FURTHER WORK	120
8 1 Conclusion	120
8 2 Further Work	121
REFERENCES	122
APPENDICES	127

CHAPTER 1

INTRODUCTION

Analytical techniques based on electrochemical principles make up one of the three major divisions of instrumental analytical chemistry. Each basic electrical measurement of current, resistance and voltage has been used alone or in combination for analytical purposes. If these electrical properties are measured as a function of time, many additional electroanalytical methods of analysis are possible. The individual techniques are best recognised by their excitation response characteristics. An example of one such technique is voltammetry [1-2]. Historically, voltammetry developed from the discovery of polarography by the Czechoslovakian chemist Jaroslav Heyrovsky [3] in the early 1920's. Polarography, which is still the most widely used of all the voltammetric methods, differs from the others in the respect that a dropping mercury electrode is used as the working electrode [4].

1.1 Voltammetry

Voltammetry comprises a group of electroanalytical techniques e.g. square wave voltammetry [5], normal pulse voltammetry [6] and cyclic voltammetry [7]. These techniques are based on the current-potential relationship in an electrochemical cell and in particular with the current-time response of an electrode at a controlled potential. In voltammetry an electron-transfer reaction can take place at the electrode if the potential is appropriate, its magnitude being determined by the surface concentration of some electroactive species. The current is recorded as a function of applied potential. The resultant current will only be transient, decaying rapidly to zero, unless some mechanism is present to bring a continuously renewed supply of the electroactive

material to the surface. A similar mechanism must be generally available to remove the product of reaction from the surface.

Three major modes of mass transport are usually in operation [8], due to

- 1 convective motion of the solvent (and supporting electrolyte), carrying the active species with it,
- 2 movement of the active species through the solvent by diffusion,
- 3 migration, the effect of an electrical potential gradient

Voltammetric experiments may be carried out with or without mechanical stirring. If the solution is stirred, the dominant transport mechanism is convection. In other cases, the cell is protected from mechanical forces that might cause convective motion of the solution. As the electrolysis proceeds, the active species in the vicinity of the electrode are depleted by being reduced or oxidised, creating a concentration gradient between the surface of the electrode and the bulk solution. Provided the applied potential is small, the active species from the bulk of the solution can diffuse rapidly enough to the electrode surface to maintain the electrolysis current. But as the potential is increased, the current is increased, creating a larger concentration gradient. Therefore the analyte must diffuse at a more rapid rate in order to maintain the current. The concentration gradient, and hence the rate of diffusion, is proportional to the bulk concentration. If the solution is dilute, a potential will eventually be reached at which the rate of diffusion reaches a maximum and all the analyte molecules are reduced or oxidised as fast as it can diffuse to the electrode surface. Hence a limiting current value, i_l , is reached, and further increases in potential will not result in increased current. If the solution is stirred or the electrode is rotated, a sigmoidal plot is obtained (see Figure 11(a)), that is, the limiting current remains constant once it is established. This occurs because the diffusion layer, or the thickness of the concentration gradient across which the analyte must

diffuse, remains small and constant, since the analyte is continually brought near to the electrode surface by mass transfer (stirring). But if the electrode is unstirred and in a quiescent solution, the diffusion layer will extend farther out into the solution with time, with the result that the limiting current decreases exponentially with time and a "peaked" wave is recorded (see Figure 1.1(b)) [9]

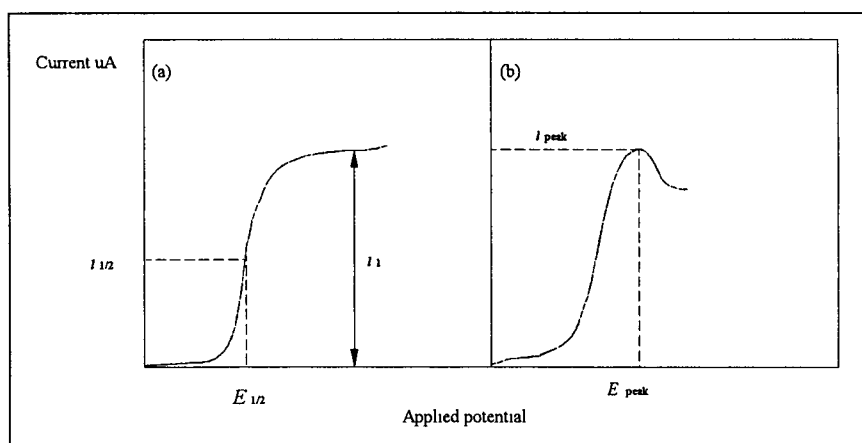


Figure 1.1 Different types of voltammetric curves (a) Stirred solution, (b) Unstirred solution

Of all the mass transport mechanisms, diffusion and migration are most readily susceptible to detailed theoretical treatment. In the presence of supporting electrolyte, migration becomes of negligible importance. In an unstirred solution, the surface concentrations change rapidly in the sense to diminish the current. This is given by the Cottrell equation

$$I = \frac{nFAD^{1/2}C^*}{(\pi t)^{1/2}} \quad (1.1)$$

where n is the number of electrons transferred, F is the Faraday constant (96,495 coulomb mole⁻¹), A is the area of the electrode (cm²), D is the diffusion coefficient (cm² s⁻¹) and c^* is the bulk concentration of analyte species. Thus the current drops off as the inverse square root of the time t .

In the case of a well-stirred solution, fresh active material is always available to the electrode, so the current stays at a nearly constant value. The magnitude of the current is proportional to concentration, which diminishes slowly because of the charge-transfer reaction, and the curve drops exponentially with time at a slow rate. In the absence of stirring, there is no noticeable change of bulk concentration, simply because during all but the first small fraction of time, the current continues at a higher level, and appreciable changes in concentration may occur [8-10]

1.1.1 Hydrodynamic Voltammetry

When voltammetric experiments are carried out in unstirred solutions, the current response is a transient that decays with time. As the current approaches zero, the information available disappears. In order to obtain more information, the redox process must be forced to continue. One possible answer is to provide fresh solution to the electrode by mechanical means. The term "hydrodynamic" is used to describe this procedure, since solution flow is invariably associated with it. Hydrodynamic methods take advantage of enhanced sensitivity resulting from the enhanced mass transfer of the electroactive substance to the electrode that occurs under hydrodynamic conditions. A steady state is attained rather quickly and measurements can be made with high precision. At steady state, double layer charging does not enter into the measurements.

For flowing solutions, such as the carrier stream from a high performance liquid chromatographic (HPLC) column, electrochemical detectors possess advantages of sensitivity and simplicity over many alternative devices. Detectors in such applications must have a small internal volume, since the time needed to replace the volume of the detector with fresh sample determines the limit of resolution for flow systems. Normally the detector volume for monitoring chromatographic peaks must be at least ten times smaller than the volume of the chromatographic peak to ensure satisfactory resolution [1, 8, 11-12]

1.2 The Potentiostat

A characteristic of modern voltammetric instrumentation is potentiostat control of the working electrode potential accompanied by the measurement of the current at that electrode. The potentiostat must perform these two functions with electrodes of varying conductivity. The potential may be pulsed very rapidly or scanned very slowly, and the resulting cell current may be extremely high or low. The potentiostat has the capability to maintain a set potential to within an accuracy of a few millivolts while only causing a minimal current of the order of a few picoamps to be drawn through the reference electrode. It also has a very rapid response time, typically of the order of a few microseconds when driving a resistive load [1].

Early designs of direct current (dc) polarographs used a motor driven potentiometer to apply the working potential to a two-electrode cell. By using a large area reference anode such as a mercury pool, the reference electrode potential remained essentially constant while the working electrode was polarised. In this arrangement the polarising potential was applied to the dropping mercury electrode (DME) through the reference electrode and across the cell. The overall cell potential could be defined as

$$E_{\text{cell}} = E_{\text{working}} - E_{\text{reference}} - iR \quad (12)$$

where the iR term, known as the ohmic drop, is the potential required to overcome the resistance of the experimental system, mainly of the cell. At low current levels in highly conducting media, this system works well. Unfortunately, at higher current levels, it is possible to polarise the reference electrode. A further complication is that in poorly conducting media such as organic solvents, the resistance across the cell is included in the measurements and causes distortion of the polarogram. The first solution to this problem was the development of the three electrode manual potentiostat. In this system the cell

voltage was applied between the working and reference electrodes, while the true working potential was measured (with a second reference electrode) in a separate circuit with a high impedance voltmeter. This device provided a means for controlling the potential between the electrodes, but had the serious disadvantage that it required constant adjustment of the control voltage during the measurement of a polarogram. A schematic of a typical modern electronic potentiostat is shown in Figure 1.2. Operational amplifier (op-amp) 1 is the control amplifier which supplies the input signal (dc level, voltage ramp etc.) to the cell. Op-amp 2 is a high impedance, unity gain, non-inverting voltage follower, while op-amp 3 is a variable gain current follower which serves to

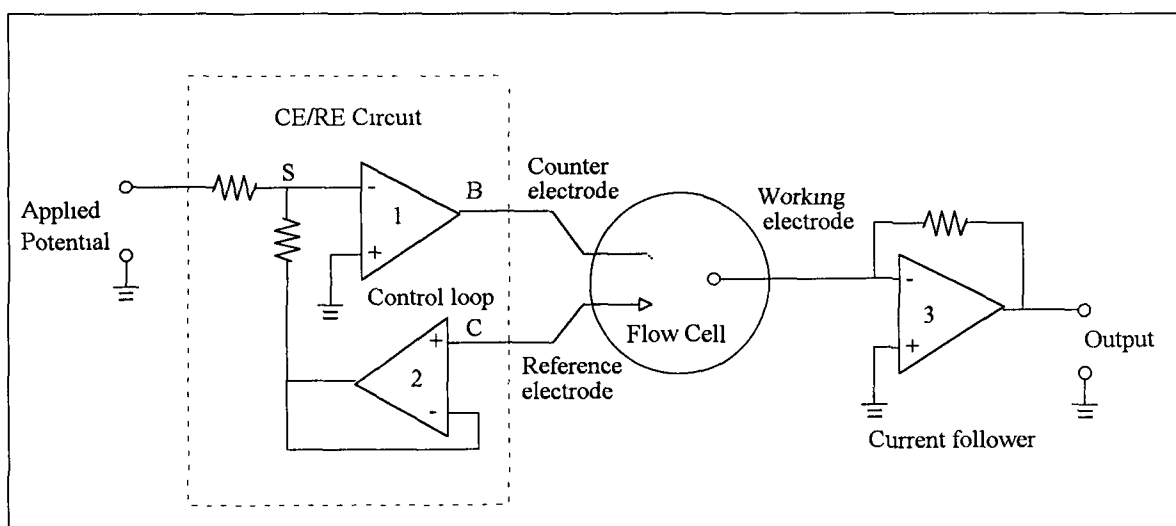


Figure 1.2 Schematic circuit for a three-electrode potentiostat

maintain the working electrode at zero volts (virtual ground) and provide an output proportional to the polarographic current. The operation of this circuit can be best visualised realising that an operational amplifier reacts in a manner required to maintain zero potential difference between its inputs. The stable condition for the loop containing op-amps 1 and 2 is when the output from op-amp 2 is equal in magnitude but opposite in polarity to the sum of the input voltages. This means that the voltage at point S (the

summing junction) will always be at zero volts. Thus, the voltage measured at point C should always be the same as that applied to point S, and if momentarily it is not, the voltage at point B will automatically increase to maintain point C equal to point S.

Although the potentiostat must control the potential at the working electrode surface, the potential is actually measured at the reference electrode. The three-electrode potentiostat automatically compensates for the resistance of the solution between the counter and reference electrodes. This makes it possible to use non-aqueous solvents of high resistance and quite dilute aqueous electrolytes. Distortion of the wave shape and slope of the current-voltage signal is much less pronounced, if not entirely eliminated. For extremely small electrodes (ultramicroelectrodes) and extremely small currents, a two-electrode cell suffices [1,11,13].

The operational amplifier (op-amp) circuit is the basic component of most analogue signal modifiers. The first op-amp circuits were composed of vacuum tube amplifiers and other necessary elements such as diodes, resistors and capacitors. Discrete transistors later replaced vacuum tubes, and finally entire operational amplifier circuits became available as IC (integrated circuit) chips. About one-third of all IC's are op-amps. More than 2000 types are commercially available. An IC op-amp consumes little power and operates at relatively low voltages (usually 10 to 15V) with power supplies that need not be highly regulated. The IC op-amps have very low drift with both temperature and time, and can withstand short circuits on the output without damage [14].

1.2.1 Computerised Single Channel Potentiostats

Faced with a perceived necessity of joining the computer age, many electrochemists have designed and built their own computer-based or microprocessor-based electrochemical systems [15]. Developments in both computer and interface hardware have both contributed to this evolution. The use of the computer strongly affects the ease of

instrument operation and the degree of functional adaptability [16] These systems provide power and flexibility for experimental control of functions such as waveform generation, digital filtering and data acquisition

Bond and Grabaric [17] have described a computerised potentiostat which was used to carry out differential polarography for the determination of cadmium in the concentration range 10^{-6} - 10^{-8} M The electrochemical instrumentation consisted of a PAR Model 174 polarographic analyser interfaced to a PDP 11/10 mini-computer used in conjunction with a CAPS-11 operating system The computer was equipped with a DR-11 general purpose interface which could provide the logic and buffer register necessary for program controlled parallel transfer of 16-bit data between the PDP-11 system and the polarographic analyser Sampling of the current output from the polarographic analyser was performed using an AR-11 real-time analogue sub-system Software for the operation of the polarographic analyser, data acquisition, data analysis and display was written in Basic and PAL-11 assembly language A program for background correction based on a quadratic least-squares fit of the data was developed [17] The development of a remote controlled potentiostat interfaced to a microcomputer for use in chemically hazardous or radiation laboratories was also later reported by Bond et al [18]

The power and flexibility of computer controlled potentiostats have continued to increase in parallel to developments in both computer/interface hardware and software Wieck et al have described a system which could be easily interfaced to many standard potentiostats [19] An ADALAB analogue interface card was used as the interface between an Apple-II Plus computer and the potentiostat Software routines written in Microsoft Basic supervised functions such as waveform generation and data acquisition A further development in this area was reported by Stefani et al [20] Their system comprised of a PDP 11/23 Plus computer and a home made interface The purpose built interface included both D/A and A/D convertors and programmable timers allowing fast data transfer The software written in FORTRAN 77 was capable of performing cyclic

voltammetry and chronoamperometry. The system as a unit could provide the user with computer-aided execution of experiments, including potential waveform synthesis, collection and evaluation of responses. Continued developments in terms of increased hardware performance have been reported by Heand Faulkner [21] and Kankare et al [22].

1.2.2 The Bi-Potentiostat

Electrochemical detectors which utilise dual working electrodes require the use of a special potentiostat referred to as a bipotentiostat. The basic circuit is outlined in Figure 1.3. One electrode is controlled in the same manner as the single channel potentiostat. The circuitry devoted to it is shown in the left half of the figure.

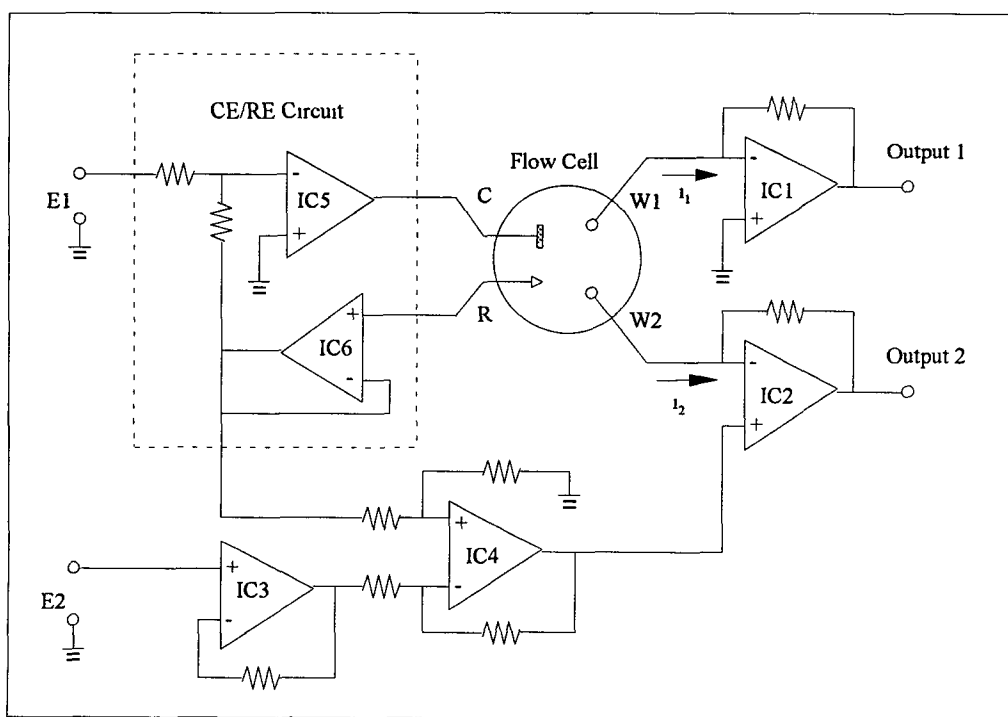


Figure 1.3 Schematic circuit for a bi-potentiostat

The second electrode is controlled by a current follower (IC2) with a summing point held away from ground by some voltage difference ΔE , because its noninverting input is away from ground by ΔE . This circuit has the effect of using the first electrode as a reference point for the second. The first electrode can be set at any desired potential, E_1 , with respect to the reference, then the second working electrode is offset with respect to the first by $\Delta E = E_2 - E_1$ where E_2 is the potential of the second electrode with respect to the reference. The counter electrode passes the sum of the current i_1 and i_2 . The remaining amplifiers (IC3 and IC4) serve as inverting and zero-shifting stages. Their function is to supply the desired potential E_2 without concern for the value of E_1 [11,23]. This feature is important when E_1 and E_2 are to be varied independently with time.

1.2.3 Multichannel Potentiostats

A number of hardware variations have been used in the construction of multichannel potentiostats. Matsue et al. [24] based their hardware design on an extension of the conventional bi-potentiostat. A resistor ladder was used to divide an input voltage into 16 evenly spaced potentials which were applied to the working electrode via a voltage follower. The analogue control circuits for each channel, except for channel 1, consisted of a 3 op-amp arrangement. Op-amp 1 was used as a voltage follower while op-amp 2 served a two-fold purpose. Firstly to polarise the working electrode at the input potential, and secondly to monitor, convert and amplify any changes in current to voltage at the electrode surface due to any redox processes taking place. Op-amp 3 was utilised in a differential configuration to subtract the applied polarisation potential from the signal output from op-amp 2. The signal sampled therefore by the ADC was solely from any response at the working electrode. Common reference and counter electrodes were used in a standard feedback loop and were held at a constant potential. Therefore the difference in potential between the working electrodes and the counter electrode potential

was used. A schematic of this design is outlined in Figure 1.4. The 16 responses from the current-to-voltage converters in the multipotentiostat were drawn into two-channel multiplexers, with the resulting two sets of eight signals being digitised successively by an eight-channel analog-to-digital (12-bit) converter system. The instrumentation was controlled by an NEC 9801 VX2 PC.

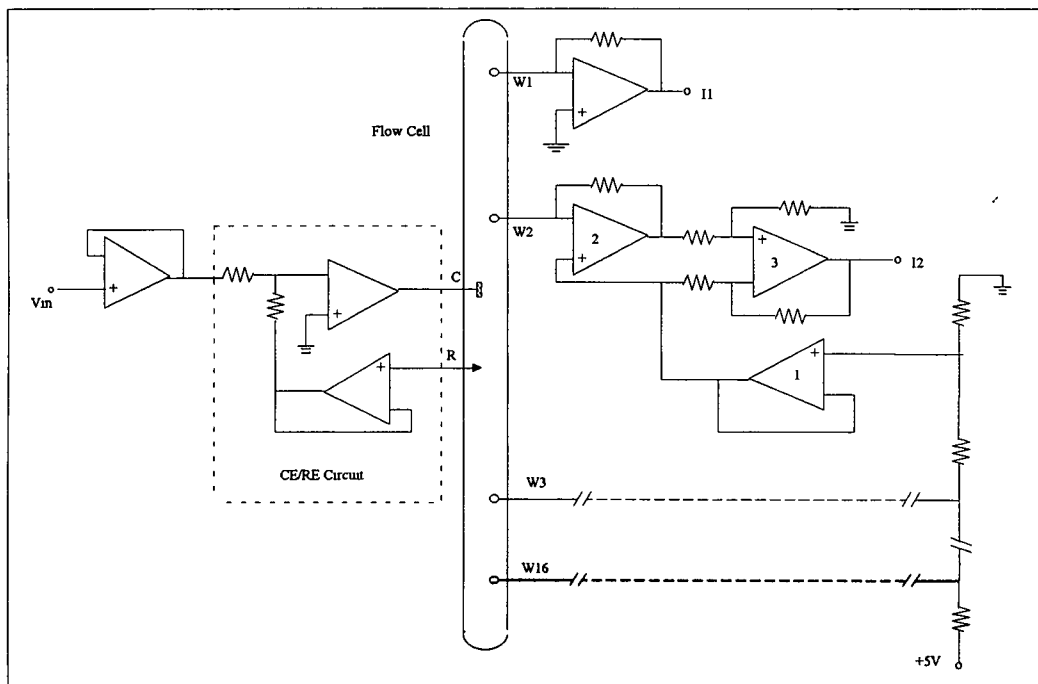


Figure 1.4 Basic circuit of a multipotentiostat (from Matsue et al in reference 24)

The multichannel potentiostat constructed by Hoogvliet et al [25] was based on the use of a dedicated dual channel DAC (AD 7547) for each channel of the potentiostat. The DAC's were responsible for background current offsetting ($0.2 \mu\text{A}$) and working electrode polarisation. The principle of maintaining the reference electrode at system ground as described by Fielden et al [26] was applied. Software selectable sensitivity between 1 mA and 1 nA (7 decades) was available. An analog low-pass (third order Bessel) filter with a cut-off frequency of 3.2 Hz was incorporated into each channel for noise reduction. An IBM-AT personal computer was used for data acquisition and control of the multipotentiostat via a Burr-Brown PCI-2000 interface.

An extension of the bi-potentiostat was also used the basis for the design adopted by Fielden et al [26] when constructing their multi-electrode potentiostat (see Figure 1.5). Each channel was provided with its own current follower which polarised the working electrode via a 12-bit DAC. Multiplexed analogue to digital conversion was used to monitor the outputs of each channel. The potentiostat uses a single reference and counter electrode. The reference electrode was maintained at virtual ground by the action of the counter electrode responding to the current demands of the array. Each working electrode (W_1, W_2, \dots, W_{16}) was polarised relative to the reference electrode so that the actual applied potential to working electrode is used rather than a difference potential. Fixed value resistors R were used with the current followers which limited the operating range of the potentiostat to about three orders of magnitude.

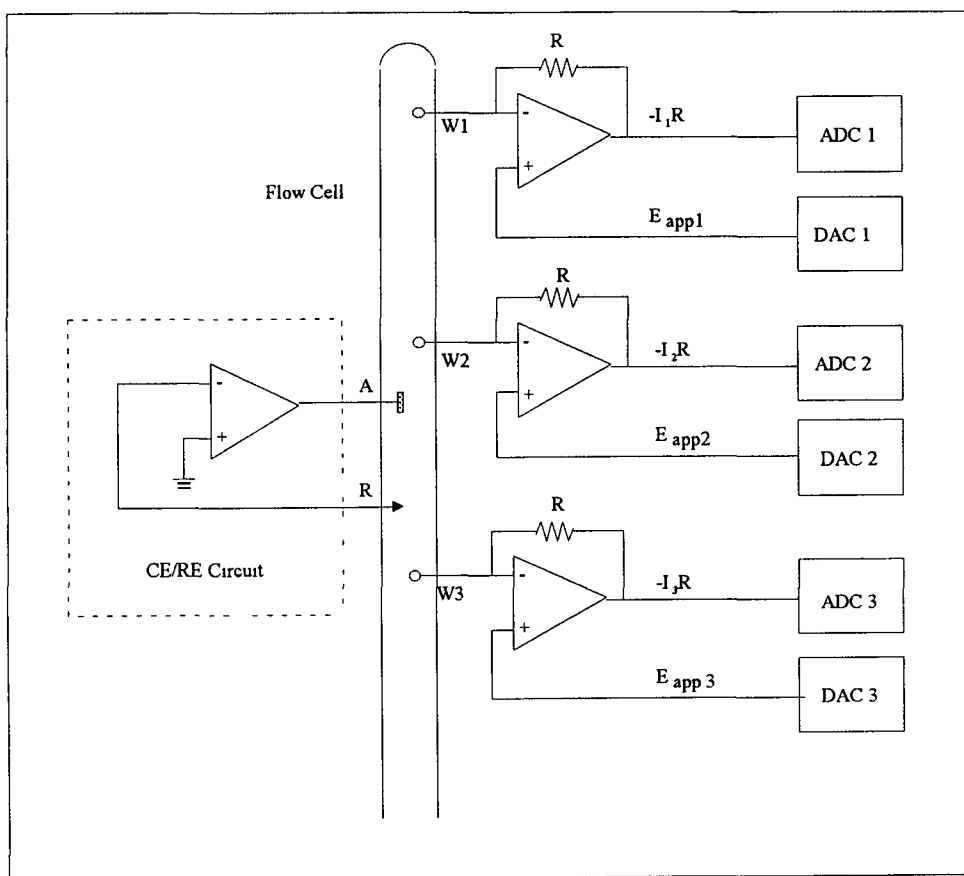


Figure 1.5 Schematic of multi-electrode potentiostat (from Fielden et al, in reference 26)

1.3 Electrochemical Detection

Electrochemical detection in flow systems has been widely used for trace analysis of electroactive materials. There are two main types of electrochemical (EC) detectors utilised in analytical systems. The first type is the planar surface (usually glassy carbon) amperometric detectors mounted in thin layer flow or wall jet cells which oxidise or reduce about 5% of the compounds passing over it after separation on a HPLC column. The second type are large area porous flow through coulometric detectors which oxidise approximately 100% of electroactive compounds flowing through it [27]. However, with conventional HPLC columns, coulometric detectors have limited application, as the requirement of complete electrolysis necessitates a large working electrode area and the mobile phase flow-rate must be very low, it is then difficult to maintain an effective volume in the detector and attain flow-rates optimal from the point of view of separation in the column [12].

Liquid chromatography with electrochemical detection has become a popular technique for trace organic analysis because of its ease of use, high sensitivity and excellent selectivity [28]. A wide spectrum of applications with electrochemical detectors have been reported in the literature. These include a variety of compounds at trace levels such as pesticides, aromatic amines, phenolic compounds and amino acids [28-34].

Normal single channel amperometric detection, however, gives poor information on the electrochemical properties of the species being detected. Recently, much attention has been focused on electrochemical flow-through voltammetric detection in order to obtain three-dimensional information (time, potential and current). This method usually requires a rapid potential scan to detect species flowing in and out of the detector, resulting in increases in the background due to charging current and also in distortion of the voltammetric shape. To overcome this problem several techniques have been reported including square-wave voltammetry [35,36], staircase voltammetry [37,38], normal

voltammetry [39] and differential pulse [40] techniques. However, the detection limits obtained are 2 to 3 orders of magnitude higher than those obtained by conventional amperometric detection systems.

1.3.1 FIA and Single Channel Potentiostats

The use of scanning electrochemical detectors with flow analysis systems have been reported. Janta et al. have described a flow injection analysis system for cyclic voltammetry (CV) [41]. By careful selection of both the flow and scan rates it was possible to obtain either the hydrodynamic or cyclic voltammogram of the analyte. The system consisted of a single line, flow injection analysis system driven by low pressure nitrogen. The potentiostatic cell comprised of a mercury working electrode, a reference electrode (Ag/AgCl), and a counter electrode (stainless steel).

An IBM EC255 voltammetric analyser with an internal triangular voltage waveform generator was utilised for potential application. It was concluded that the combination of FIA and cyclic voltammetry was attractive because of the flexibility of FIA and the diagnostic power of CV.

1.3.2 Dual Electrodes

The application of two independently controlled working electrodes in a thin layer flow cell have been reviewed by Roston et al. [42]. These dual electrode arrangements are based on the thin layer single working electrode cells that incorporate downstream reference and counter electrodes. The dual electrode detector offers additional selectivity compared to a single electrode detector. In the first configuration the working electrodes are placed parallel to the flowing stream with each electrode being held at different potentials. The two simultaneous chromatograms can then be rationed for peak

confirmation. The working electrodes are arranged in series in the second configuration. The upstream working electrode generates an electroactive product which is detected at the second electrode. The series arrangement limits the number of electroactive compounds that can be detected because only those electroactive products that are stable in the time required to reach the working electrode are detected [1,43].

The ability to redox cycle between two parallel-opposed working electrodes in a thin layer cell was demonstrated by Anderson and Reilly [44]. Their design was based on a cofacial twin-electrode thin-layer geometry. The use of redox cycling was further investigated by Weber and Purdy [45] and Clmtock and Purdy [46].

A dual electrode detector for liquid chromatography, with enhanced capabilities designed to obtain a three-dimensional data array of current responses as a function of both time and potential, has been described by Lunte et al [47]. By displaying the entire chromatovoltammogram allowed post-run choice of the optimal detection potential. Voltammetric detection of 10 to 100 μmol injected of gentisic acid and caffeic acid were possible. The voltammetric data also provide a second method of peak identification for greater certainty in peak assignments. Waveform generation and data acquisition and analysis were controlled by a Zenith 158 personal computer which interfaced with an ADALAB-PC interface card. The utilisation of dual-electrode detector in a series configuration for the detection of phenolic compounds in commercial beverages and the determination of metabolites of the analgesic acetaminophen in urine was reported by Roston et al [48]. The upstream working electrode was used to oxidise the compounds of interest which were then detected by reduction at the downstream working electrode. The use of redox cycling allows improvements in selectivity, peak identification and high detection at extreme potentials.

The use of a dual electrode arrangement to detect thiols and disulphides has been reported by Allison and Shoup [49]. The thiols and disulphides were determined simultaneously by using thin-layer dual mercury amalgam electrodes in a series configuration coupled to

a HPLC After chromatographic separation of the sample, disulphides were first converted to their corresponding thiols at the upstream electrode (-1.0V vs Ag/AgCl). Both the thiols and disulphides were then detected as thiols downstream at +0.15V via their catalytic oxidation of the mercury surface. The application of this method to the determination of phenols in environmental samples which have been chromatographically separated by HPLC was described by Shoup and Mayer [50].

Electrochemical characterisation of two microarray electrodes, an interdigitated microarray electrode (IDAE) and a single potential microarray electrode (SAE), was investigated in flowing stream [51]. A comparison between the IDAE and a dual-series rectangular electrode with the same area demonstrated a current amplification of current responses by a factor of 2.8-3.9 due to redox cycling. The application of the IDAE to the selective determination of reversible catecholamines in high performance liquid chromatography was demonstrated. A thin layer cell was fabricated by Sanderson and Anderson [52] containing two interdigitated electrodes constructed by etching a gold film which had been vapour deposited on a quartz window. The electrode used a spacing of 100 μm between anode and cathode and reached virtual steady state in 1 minute. Semi-empirical equations from steady-state electrochemical and spectrochemical experiments on model redox couples were presented.

1.3.3 Flow Injection Analysis and Dual Channel Potentiostats

Dual-electrode detection has normally found applications with HPLC. However, a number of applications with flow injection analysis systems have been reported. A FIA system with a dual-electrode amperometric detector has been developed by Lunte et al [53]. The dual electrodes were used with a thin layer cell in a series configuration. The potential at the upstream electrode was scanned while the downstream electrode was maintained at a constant potential. The downstream electrode was used to monitor the

redox reaction occurring at the upstream electrode without the charging current associated with scanning the potential. Therefore, voltammetric information can be obtained at an electrode operating in an amperometric mode. The system was used to determine hexacyanoferrate (III) and ascorbic acid. It was possible to distinguish between their responses based on their electrochemical reversibility or irreversibility at the electrode surface.

A FIA system combined with cyclic voltammetry was developed by Cante et al. [54] which performed fast i - E scans. The system consisted of a triangular wave generator and a potentiostat constructed as described by Albahadily and Mottola [55]. The information collected by the system could be presented in a number of formats. First, x - y recordings as in cyclic voltammetry could be presented as i - E recordings or derivative recordings. Secondly, x - t plots could be recorded. The system had possible applications in both qualitative and quantitative analysis through utilisation of the halfwave potential of the voltammetric process. The future application of the system to multicomponent analysis was also discussed.

1.4 Multichannel Detection

Two approaches have been adopted for the development of multichannel electrochemical detection systems (more than two independently controlled working electrodes) based on the two types of electrochemical detectors, namely coulometric and amperometric. A number of publications have described the application of coulometric array detectors to HPLC systems [56-58]. These systems are based on conventional technology with each working electrode having both its own reference and counter electrodes resulting in an instrument which is large and cumbersome. The most common detection mode is amperometric detection with a single working electrode maintained at a constant potential. However, this approach only provides limited information about the

electrochemical properties of a species being detected, namely a particular current value at one potential as a function of time, which gives the user no confirmation as to whether peaks are arising from one or more electroactive species. On the other hand, an extra measurement dimension can provide additional information regarding the number of components contributing to a signal. This has already been very successfully exploited via detectors such as the photodiode array detector and excitation-emission fluorescence detectors in HPLC [59,60]. This goal has partially been achieved with the use of dual electrode potentiostats as demonstrated by Lunte et al [47]. However, the development of multichannel potentiostats with arrays of working electrodes have for the first time made the acquisition of three-dimensional electrochemical information in real-time possible.

Wang et al have reported on an amperometric array consisting of 4 chemically modified electrodes in a thin layer flow cell. However, the electrodes were monitored sequentially, rather than simultaneously, as in normal amperometric arrays [61]. Fabrication of single and multiple electrode arrays by photolithography have been reported [62-64]. These arrays are also known as interdigitated microelectrode arrays and can be defined as an electrode array geometry consisting of rectangular active elements separated by narrow gaps with alternating elements held at different potentials [65,66].

Harrington et al [67] have described a general purpose, multiple working electrode potentiostat, capable of controlling up to 11 working electrodes. The potentiostat was capable of controlling independently the electrode potentials over a continuous range from -2.5 to +2.5 V with current sensitivities in the range 1 mA-100 μ A. Low noise performance was achieved through appropriate power isolation and null balancing techniques. For automated data acquisition and control, the multiple electrode potentiostat was interfaced to an Apple IIe microcomputer. All control lines between the microcomputer and the potentiostat were provided by the secondary input/output devices located on the I/O socket of the Apple IIe motherboard. The potentiostat was used with

an interdigitated filar microelectrode array for the determination of ferrocene. The instrumentation was designed for either stand alone operation or for computer controlled operation and was capable of implementing either stepped potential or scanned potential programs.

Matsue et al [24,68] have described the design and fabrication of an interdigitated array and multichannel potentiostat capable of the independent control of up to 16 separate working electrodes. The design was based on the use of analogue circuits to control functions such as working electrode polarisation and signal amplification. The interdigitated array was polarised via an input potential which was divided over a resistor ladder into 16 evenly spaced potentials. No hardware facilities for background current offsetting were incorporated into the design. The necessary background corrections were achieved by subtraction of background voltammograms obtained prior to sample injection. The multichannel potentiostat was utilised with an FIA system to generate 3-dimensional hydrodynamic voltammograms. By applying a stepwise voltage sequence at the working electrode array it was possible to obtain measurements at 80 different potentials, thus improving the resolution of the data obtained. The detection system was applied to FIA and HPLC of a mixture of several electroactive chemicals, such as ferrocene derivatives, ascorbic acid, uric acid and catecholamines. A detection limit of $1 \times 10^{-8} \text{M}$ for a ferrocene derivative was obtained.

A considerable advance in the development of multichannel potentiostat hardware has been made by Hoogvliet et al [25]. Their design incorporated independent control of each working electrode through the utilisation of a dual channel DAC (AD 7547) for each working electrode. One channel was dedicated to working electrode polarisation between -2.0 and +2.0 V vs the reference electrode potential (resolution ca. 1 mV), while current offsetting was controlled via the second channel (resolution ca. 50 pA). Data acquisition and control of the multichannel potentiostat on an IBM-AT PC was used. Interface of the instrumentation was via a Burr-Brown PCI-20000 interface. Software for instrumental

control, data acquisition, storage, display and data processing was written in Turbo-Pascal V 5.0. The instrumentation developed was an improvement over the design reported by Matsue et al [24,68] in terms of improved potentiostatic control and current offsetting capabilities, i.e. each working electrode in the array is both polarised and offset ($\pm 0.2 \mu\text{A}$) for back current independently of each other. Efficient and versatile current setting capabilities are important in high sensitivity situations (1 nA-10 μA) where low level analytical signals are often superimposed on much higher background currents. The potentiostat was used with a radial flow cell design consisting of a 16 carbon paste working electrode array and was applied to the determination of epinephrine with a LOD of $1 \times 10^{-9} \text{M}$ by HPLC. While the limit of detection achieved was comparable to a conventional single working electrode systems, the 3-d chromatogram generated by the array is obviously much more comprehensive in terms of information content.

Fielden et al have reported the design of an 8-channel amperometric array using a radial flow configuration operating under wall jet conditions. However, their hardware did not demonstrate the same degree of instrumental flexibility as the design reported by Hoogvliet et al [25]. The hardware design was similar to an extended bi-potentiostat. Control of the instrumentation was effected via a Compaq 386/20 PC and software routines written in Turbo Pascal. Their system was applied to determination of mixtures of metal ions such as Cu^{2+} and Cd^{2+} in aqueous solutions using FIA and HPLC. The signal obtained for the reduction of each metal ion such as Cd^{2+} was corrected for background contributions by other metal ions present in the sample e.g. Cu^{2+} , when carrying out mixed species determinations, enabling multicomponent determinations to be carried out without prior separation as in FIA [26,69].

CHAPTER 2

COMPOSITION AND FUNCTION OF SYSTEM

2.1 Introduction

In the previous chapter, the background to electrochemical detection, and the development of multichannel amperometric arrays in flowing solution analysis was introduced. In this work, a computer controlled, multichannel potentiostat is required to independently control an array of working electrodes. The autonomy of each channel in the potentiostat was achieved by the utilisation of a dual channel DAC (AD7237) (Analog Devices) which is dedicated to electrode polarisation and background current offsetting. Electrochemical instrumentation is affected by developments in electronics, through their impact both on direct functions of measurement, and control, and on computer hardware. Control of the purpose built instrumentation was effected via a 486/33MHz personal computer and Analog Devices RTI cards which are responsible for hardware control functions and data acquisition via digital and analogue control lines. The analogue and digital circuits were designed to control system functions such as the I/E (current-to-voltage) converter, current offsets, analogue filtering and sensitivity selection. The instrumentation was used to evaluate the performance of both radial and linear thin layer flow cell configurations. Software for instrumentation control, data display (2 or 3-dimensional formats), on-line and post-run data processing and storage were developed using QuickBasic. The software approach taken incorporates many new features such as the utilisation of a "Windows style" environment for the user/computer interface, resulting in software which is comparable in both presentation and ease of use with commercially available software.

This chapter therefore describes the composition and function of a computer controlled multichannel potentiostat which can control an amperometric array for flowing solution analysis

2.2 Composition of Detection System

The basic schematic diagram of the detection system for applications with flowing solution analysis is shown in Figure 2.1. The detection system consists of

- a pump (ASC Model 351 isocratic pulse-free pump)
- an injection valve (Rheodyne 7125) with 20 and 50 μl sample loops,
- a multielectrode array and flow through cell,
- a multichannel potentiostat capable of controlling 4 working electrodes, 1 reference electrode (Ag/AgCl), and 1 auxiliary electrode,
- a computer interface RTI815 /RTI817 data acquisition cards (Analog Devices),
- a personal computer (Elonex 433/DX),
- software for control, data acquisition, and data processing (MS QBASIC 4.5 and an Assembly Language Toolbox)

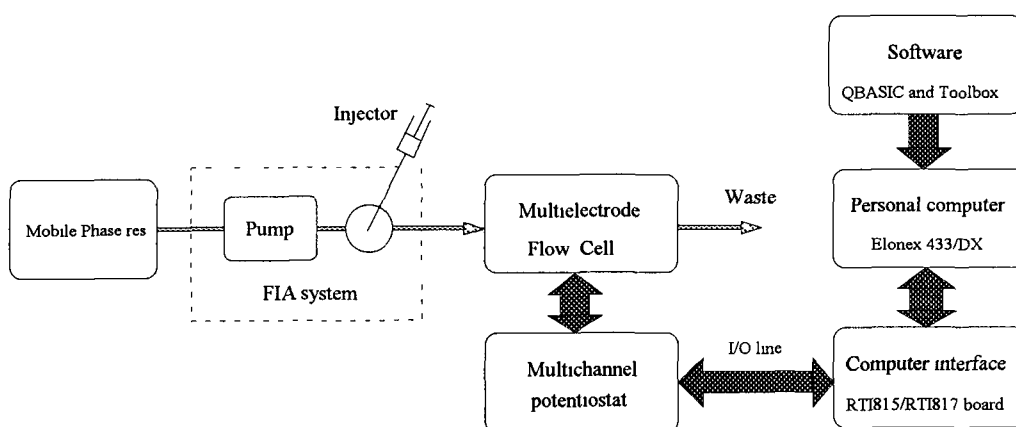


Figure 2.1 Basic layout of FIA system with multi-electrode array and computer controlled multichannel potentiostat

A block diagram of the detection system incorporating the computer controlled multichannel potentiostat is shown in Figure 2 2

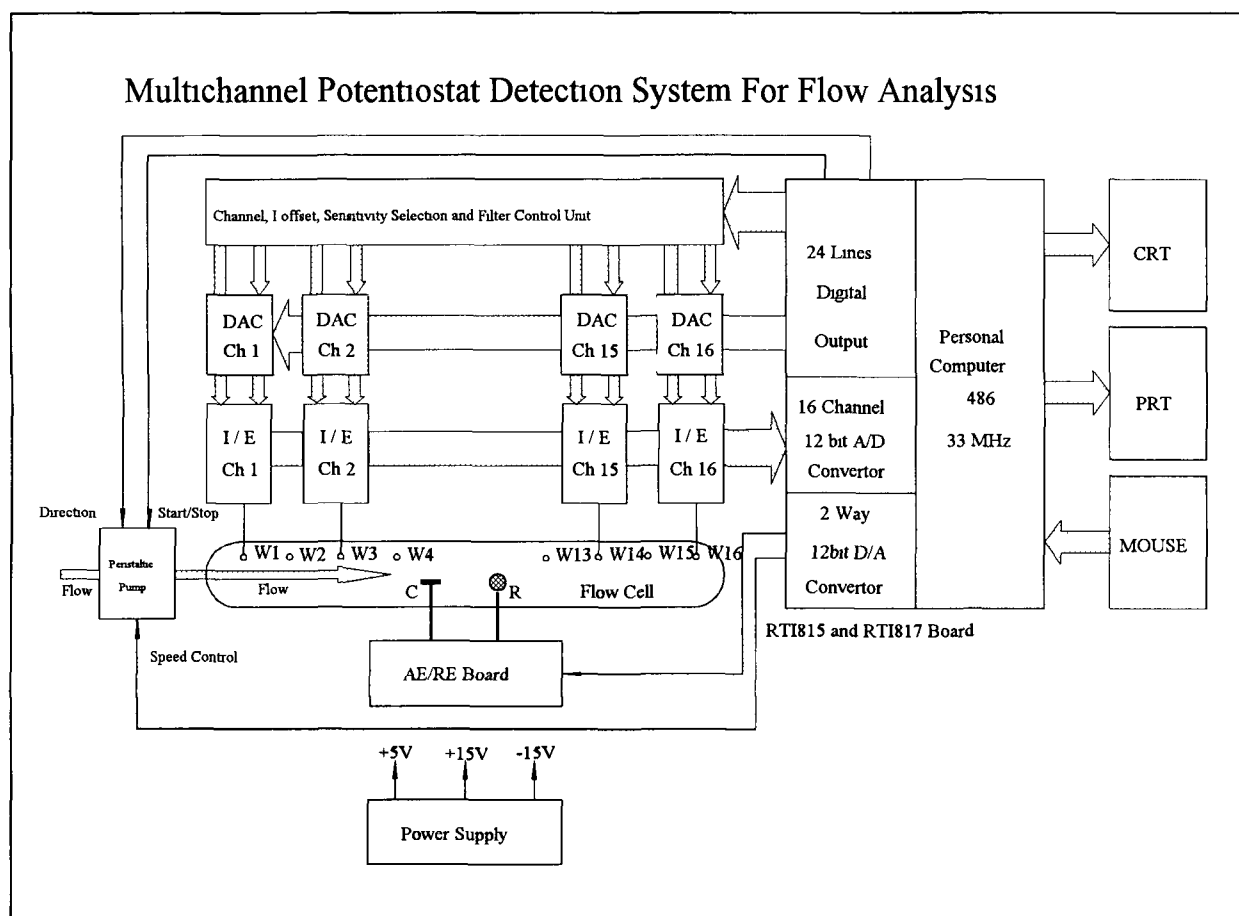


Figure 2 2 Block diagram of detection system of a computer controlled multichannel potentiostat for applications with flowing solution analysis

2.3 Technical Performance Criteria

In order to efficiently perform a variety of multiple electrode strategies, the potentiostat was designed to the following specifications

Electrode	Modular design capable of accommodating of up to 16 working electrodes		
	Common Counter and Reference Electrodes		
Potentiostat	Applied Potential Range	-2 000 V to +2 000 V	
	Applied Potential Resolution	1 mV	
Sensitivity	Current Range	10 pA to 1 mA, 9 decades	
	Current Resolution	1/4096 of full scale	
Current Offset Ranges	Range 1	-200 0 nA to +200 0 nA	Resolution 100 pA
	Range 2	-20 00 nA to +20 00 nA	Resolution 10 pA

2.4 System Functions

Operational Modes	Fixed potential DC voltammetry
	Linear sweep voltammetry
	Cyclic voltammetry
System Control Options	Graphical representation (two and three-dimensional plots)
	Baseline auto-offset and manual selection
	Sensitivity range
	Analog filtering
	Digital filtering options
	Working electrode calibration
	Potential step sequences
	Data file save for post-run data processing
	Working electrode electrochemical cleaning cycle
	Pump control (on\off, speed, direction)

CHAPTER 3

DESIGN OF MULTICHANNEL POTENTIOSTAT

3.1 Introduction

In chapter 2, the composition of the detection system of a computer controlled multichannel potentiostat for application with flowing solution was described. A multichannel potentiostat is required for setting independently each working electrode at a different potential and measuring the resulting currents individually. The design and development of the analogue and digital control circuit for a modular potentiostat capable of controlling up to 16 working electrodes with a common reference/counter electrode is discussed. The design utilised differs from the that used in conventional potentiostats, and incorporates many new hardware capabilities over work previously reported in the literature.

3.2 Composition of Multichannel Potentiostat

The computer controlled, modular potentiostat has been designed to control independently the potential of up to 16 working electrodes (WE), with common reference (RE) and counter electrodes (CE). The multichannel potentiostat consists of a power supply, a CE/RE unit, a channel selector, sensitivity selector, current offset extent selector, and analogue filter control unit, 16 I/E converter units, and 16 D/A converter units. The digital and analogue input/output signals are bussed through the back plane to interface boards (RTI815 and RTI817 cards) in the personal computer [71-72]. A block diagram of the multichannel potentiostat is shown in Figure 3.1.

Multichannel Amperometric Detection System For Flow Analysis

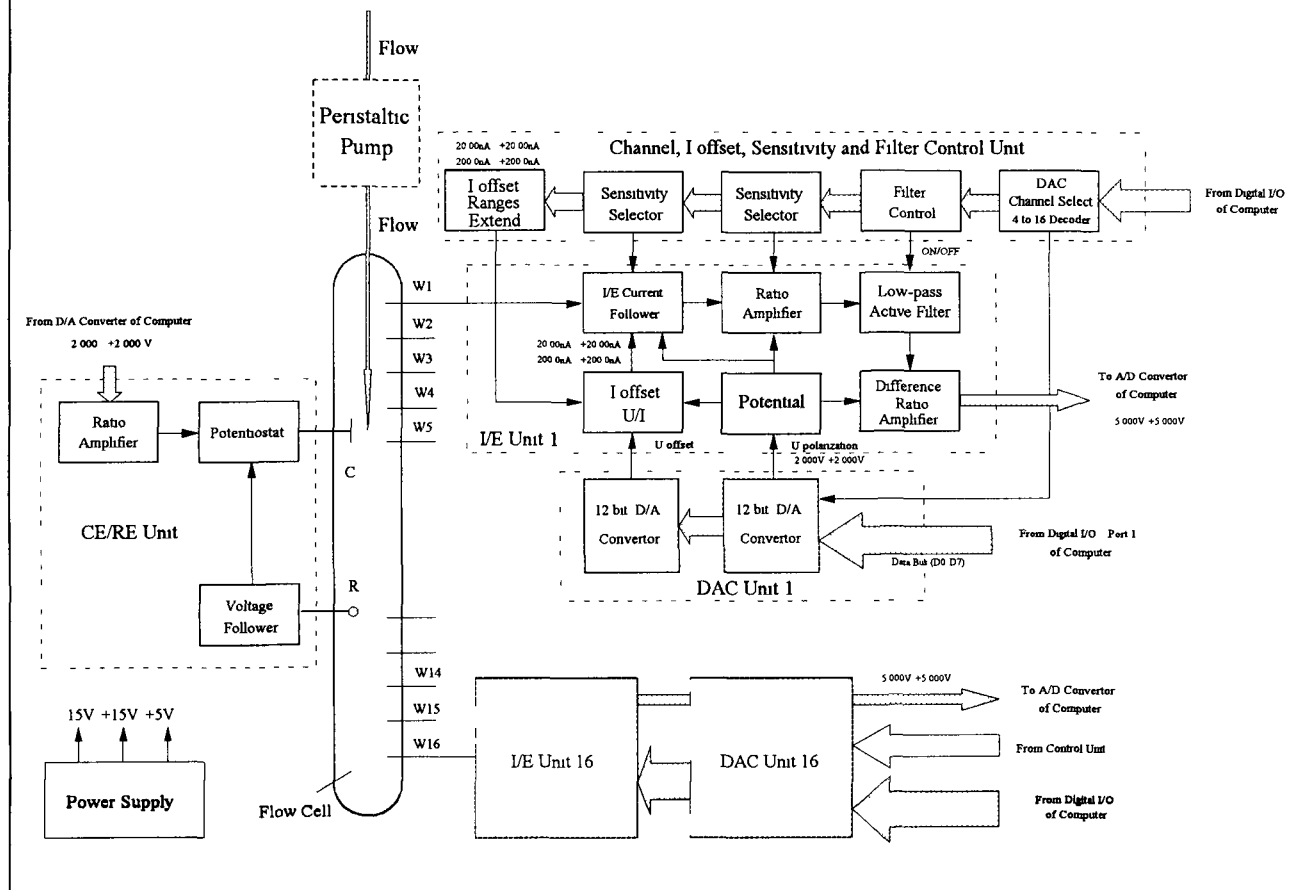


Figure 3 1 Block diagram of the multichannel potentiostat

3.3 Counter\Reference Electrode CE\RE Unit

The CE/RE unit consists of a ratio voltage amplifier, a potentiostat, voltage follower, and flow cell. A block diagram of the CE/RE unit is shown in Figure 3 2

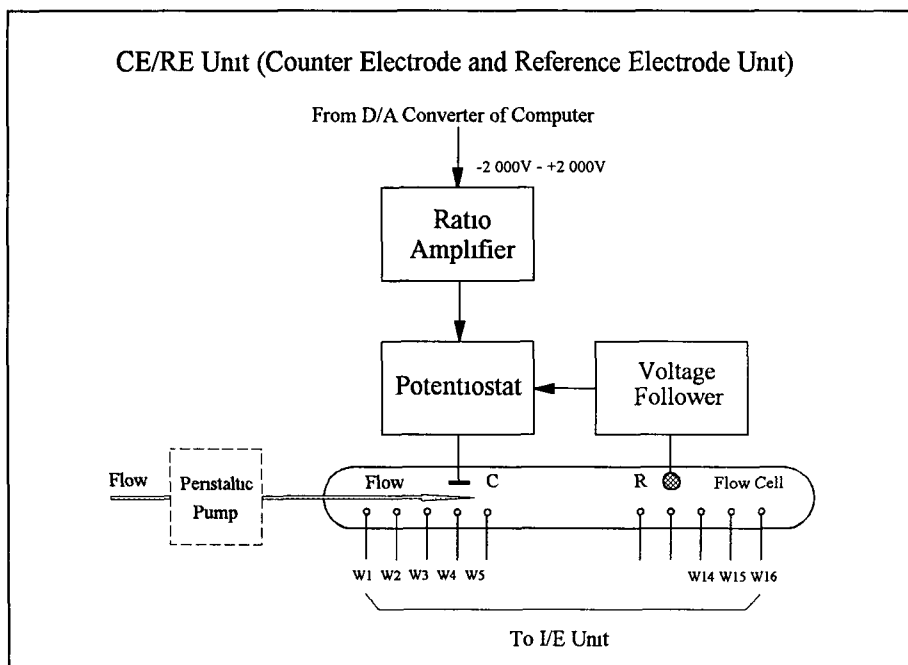


Figure 3 2 Block diagram of CE/RE unit

3.3.1 Feedback Circuit of CE\RE Unit

The potentiostat is a device for controlling the potential between the working electrode and the reference electrode at fixed and selected potentials. The potential of the working electrode (WE) is controlled versus the reference electrode (RE) using a feedback circuit. The operational amplifier is the key component of the potentiostat, and the feedback circuit drives the current between the working and counter electrode (CE) while ensuring that no current passes through the reference electrode circuit. In this way the contribution of the resistance of the electrolyte solution between the electrodes to the measured potential is minimised.

3.3.2 Counter Electrode\Reference Electrode Unit Circuit

The counter electrode/reference electrode (CE/RE) unit is the base circuit of the multichannel potentiostat. This circuit allows for setting a potential between the

reference electrode and the working electrode by driving current through the counter electrode sufficient to produce the desired potential difference between the working electrode and reference electrode for scan and cyclic voltage modes. The CE/RE unit was based on a quad op-amp (TL074)(SGS-Thompson Microelectronics). The circuit design utilised is shown in Figure 3.3. An input signal in the range $\pm 2.0\text{ V}$ (resolution 1 mV) which is controlled by a voltage ratio amplifier op-amp 1 via the DA converter of the RTI-815 card is applied to the potentiostat op-amp 2. The default setting is 0.0 V for normal mode operation. Op-amp 3 is a high impedance, unity gain, non-inverting voltage follower. The stable condition for the loop containing the op-amps 2 and 3 is when the output from op-amp 3 is equal in magnitude but opposite in polarity to the input voltage to op-amp 2. This means that the voltage at point (s), the summing junction, should always be at zero volts, however if a change occurs in the junction potential, the output of op-amp 2 will increase to maintain the summing junction at zero volts. The input potential therefore can be accurately maintained between the reference electrode and the working electrode.

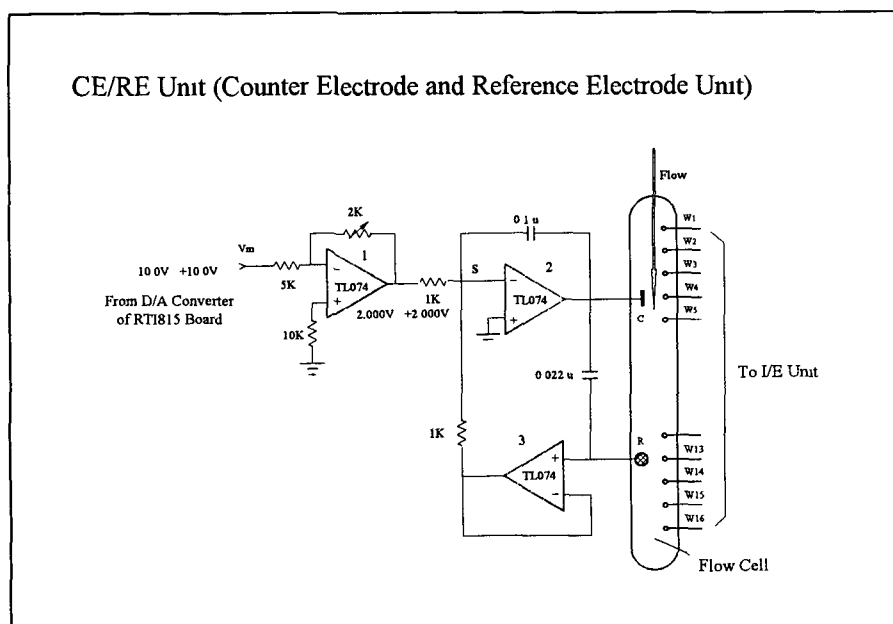


Figure 3.3 Circuit diagram for counter electrode/reference electrode unit

3.4 Current to Voltage (I/E) Converter Unit

A current to voltage unit consists of a current to voltage converter, 2 sensitivity selectors, an analogue filter, a current offset, and a differential amplifier. A block diagram of a current to voltage converter unit is shown in Figure 3.4.

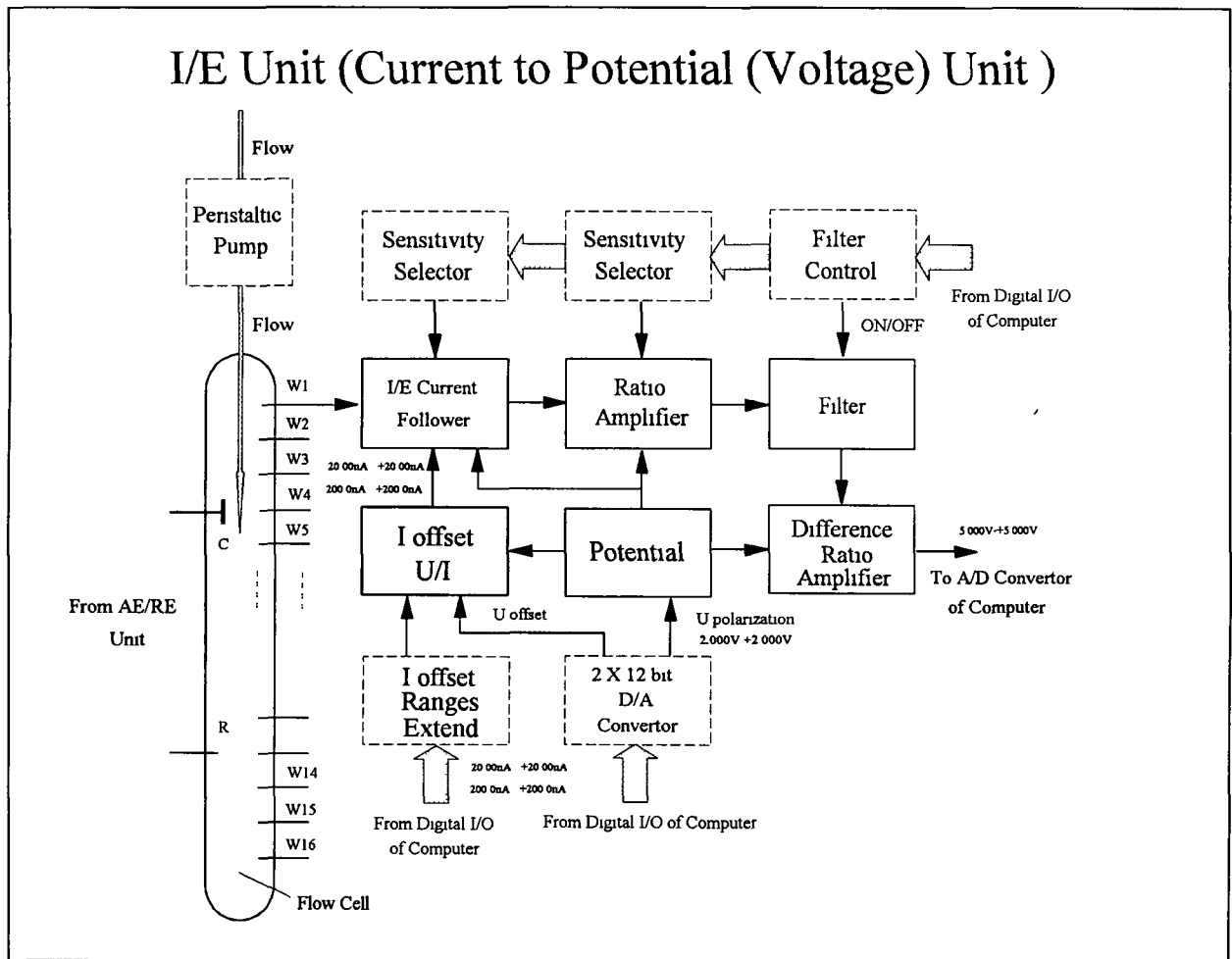


Figure 3.4 Block diagram of a current to voltage converter unit

3.4.1 Current to Voltage Converter

The current to voltage converter circuit is a current follower (Figure 3.5). The input is a current, I , that is obtained from the working electrode. The gain of the circuit is set by the value of the resistor R_f .

$$V_{out} = I \times R_f$$

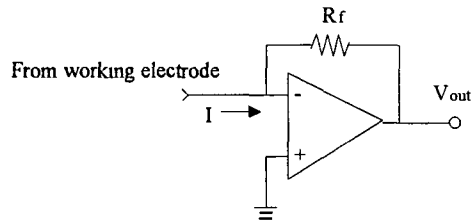


Figure 3.5 Schematic circuit for current to voltage converter

Since the two inputs of an ideal op-amp are always at virtually the same potential, it is intuitive that the non-inverting input (-) is a virtual ground. This feature is important because it allows currents to be converted to equivalent voltages while the current source is maintained at ground potential. This design was utilised when building the potentiostat.

3.4.2 Gain and Sensitivity Selection

Usually, the maximum close-loop gain of an op-amp is in the range of around 10^8 . The signal detected by the multichannel potentiostat discussed in this thesis is in the current range 10^{-11} - 10^{-3} A. If only one op-amp is used the gain is not enough for the required amplification. So we use a three op-amps design to achieve the desired amplification range. The total gain is

$$A = A_1 \times A_2 \times A_3$$

where A_1 is the gain of amplifier for current to voltage converter with gain in the range of 10^7 to 10^2 , A_2 is the gain of voltage ratio amplifier with gain in the range of 10^3 to 10^0 , and A_3 is the gain of difference amplifier with gain in the range of 10^1 .

The gain is selected by two analog switches for sensitivity selection which are controlled via a computer and Analog Devices RTI817 control cards, with sensitivity in the range of 1 mA to 10 pA (9 decades)

3.4.3 Current Offset

In order to set the background current baseline to zero and remove background noise that is produced by cell current, environmental sources and non-zero drift of the detection circuit, an input current offset has been used in each channel detector of the multichannel potentiostat. The baseline can be corrected automatically by the computer or manually set to zero (user defined offset). One DAC channel of the DAC unit is used to convert digital signals from the computer into an analogue voltage offset between -5 000V and +5 000V (resolution 2 441 mV). The V/I convertor circuit is used to transform the voltage offset signal into a current offset. An analogue switch is used to control and select the current offsetting facility in the V/I converter circuit. The ranges extend from -200 0nA to +200 0nA and -20 00nA to +20 00nA, with a resolution of ca 100 pA and 10 pA.

Design of Current Offset Circuit

The role of the current offset circuit is to convert the input voltages between -5 000 V and +5 000 V from the DAC unit into an output current in the ranges of -200 0 nA to +200 0 nA and -20 00 nA to +20 00 nA. Consider the basic circuit shown in Figure 3 6.

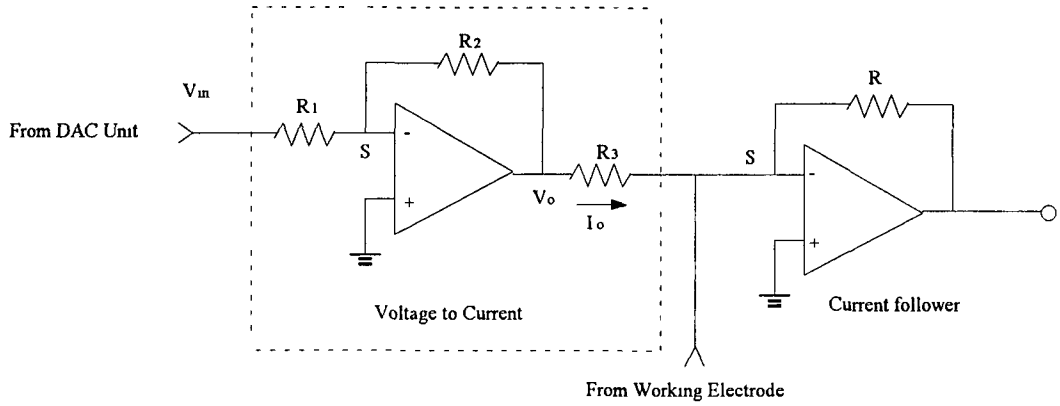


Figure 3 6 Schematic circuit for current offset of current to voltage converter unit

Since S is a virtual ground,

$$\text{From the circuit,} \quad V_{in} = -\frac{R_1}{R_2} V_o \quad (3.4.1)$$

$$V_o = I_o R_3 \quad (3.4.2)$$

where V_{in} is an input analog voltage from VB of the DAC unit, and I_o is an output current offset to the input of the current follower

Combining equations (3.4.1) and (3.4.2), one obtains

$$R_3 = -\frac{R_2 V_{in}}{R_1 I_o} \quad (3.4.3)$$

Current Offset in the Range of -200.0 nA to +200.0 nA

Selection, Resistance is $R_1 = 25 \text{ K}\Omega$, $R_2 = 10 \text{ K}\Omega$

When the current offset circuit input $V_{in} = +5.000 \text{ V}$, circuit output should be $I_o = -200.0 \text{ nA}$

From (3.4.3), Resistance is

$$R_3 = -\frac{R_2 V_{in}}{R_1 I_o} = -\frac{1 \times 10^4}{2.5 \times 10^4} \times \frac{5}{-2 \times 10^{-7}} = 10 \text{ M}\Omega$$

Current Offset in the Range of -20.00 nA to +20.00 nA

Selection, Resistor $R_2 = 10 \text{ K}\Omega$, $R_3 = 10 \text{ M}\Omega$

When current offset circuit input $V_m = +5\ 000\ \text{V}$, circuit output should be $I_o = -20\ 00\ \text{nA}$

From (3 4 3), Resistance is

$$R_1 = -\frac{R_2 V_m}{R_3 I_o} = -\frac{1 \times 10^4}{1 \times 10^7} \times \frac{5}{-2 \times 10^{-8}} = 250\ \text{K}\Omega$$

3.4.4 Analogue Filter

Low-pass Filter

A filter is a frequency-selective network that favours certain frequencies of input signals at the expense of others. Three very common types of filter are the *low-pass* filter, the *bandpass* filter, and the *high-pass* filter, although there are many more possibilities.

A low-pass filter passes all frequency components of a signal up to a certain maximum frequency. Frequencies above this cut-off frequency are rejected to a greater or lesser degree. Hi-fi treble controls and turntable scratch filters are typical low-pass filters.

Order

The order of a filter governs the strength of its falloff with frequency. For instance, a third-order low-pass filter falls off as the *cube* frequency for high frequencies, or at an 18-dB-peroctave rate. The number of energy-storage capacitors in most active filters determines their order. A fifth-order filter usually takes five capacitors, and so on. The higher the order of the filter, the better its performance, the more parts it will take, and the more critical the restrictions on component and amplifier variations.

Active Filters

Capacitors and inductors are inherently frequency-dependent devices. Capacitors more easily pass high frequencies and inductors better handle lower frequencies. Thus, most filters traditionally have been designed around combinations of inductors and capacitors. These are called *passive* filters.

Today, there is a new and often much better way to do filtering. Integrated circuitry, particularly the IC op-amp, can be combined with resistors and capacitors to accurately simulate the performance of traditional inductance-capacitance filters. Since this new approach usually has gain and needs some supply power, filters built this way are called *active filters*. While active filters as a concept have been around for quite some time, only recently have reliable, easy-to-use circuits and simple design processes emerged.

Why Use Active Filters ?

There are many advantages of active filters, compared with traditional passive filters

- Low Cost - component costs of active filter are usually far lower, particularly at very low frequencies, where inductors are large and expensive
- Isolation - most active filters have very high input impedance and very low output impedance. This makes their response essentially independent of source and load impedance and their changes
- Cascade ability - owing to the good isolation of active filters, complex filter problems are easily broken down into simple sections that combine to produce the desired final result
- Gain - active filters can provide gain or attenuation as needed to suit system or filter requirements. Current gain is almost always provided, voltage gain is an option
- Tuning - many active filters can be easily tuned over a wide range without changing their response shape. Tuning can be done electronically, manually, or by voltage control. Tuning ranges can go beyond 1000:1, much higher than is usually possible with passive circuits
- Small Size and Weight - this is particularly true at low frequencies, where inductors are bulky and heavy
- No Field sensitivity - shielding and coupling problems are essentially non-existent in active filters

Design of Analogue Filter for Detection System

For sensitive measurements such as these, noise reduction for enhancement of the signal to noise ratio is a vital aspect of the instrumentation function. As electrochemical signals of interest in our system were low frequency in nature, a third order unity gain analogue low-pass filter with a cut-off frequency of 1 Hz was used in the detection circuit for signal to noise ratio enhancement for all measurements. To prevent amplification by the low-pass filter, a third-order low-pass RC active filter of unity gain was used. The theory of analogue active filter design has been described by several workers [73-75]. Consider the base circuit shown in Figure 3.7.

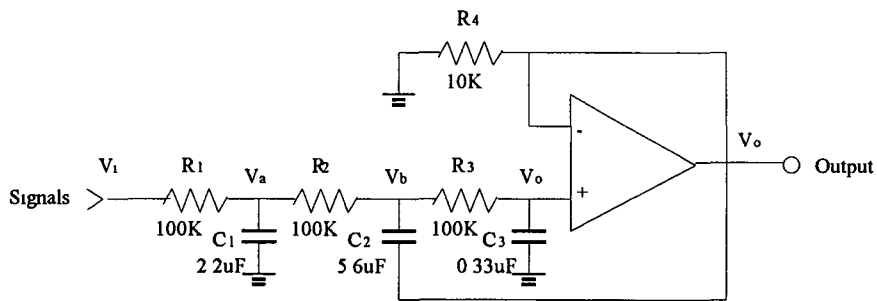


Figure 3.7 Schematic circuit for third-order unity gain low pass RC active filter

Kirchhoff's law of current provides that the sum of the currents into any node is zero. A nodal analysis of the unity-gain lowpass network yields equations (3.4.5.1) through (3.4.5.3)

$$\frac{V_i - V_a}{R_1} = \frac{V_a - V_b}{R_2} + \frac{V_a}{1/j\omega C_1} \quad (3.4.5.1)$$

$$\frac{V_a - V_b}{R_2} = \frac{V_b - V_o}{1/j\omega C_2} + \frac{V_b - V_o}{R_3} \quad (3.4.5.2)$$

$$\frac{V_b - V_o}{R_3} = \frac{V_o}{1/j\omega C_3} \quad (3.4.5.3)$$

where V_1 is the input voltage, V_o is the analog filter output voltage and $1/j\omega C_i$ is the capacitive reactance of each capacitor, C

Rearranging, these equations give

$$V_a = R_2 \left[\left(\frac{1}{R_2} + \frac{1}{R_3} + j\omega C_2 \right) (1 + R_3 j\omega C_3) - \left(\frac{1}{R_3} + j\omega C_2 \right) \right] V_o$$

$$V_b = (1 + R_3 j\omega C_3) V_o$$

$$\frac{V_o}{V_i} = \frac{1}{R_1 R_2 R_3 C_1 C_2 C_3 (j\omega)^3 + [(R_1 + R_2) R_3 C_2 C_3 + R_1 (R_2 + R_3) C_1 C_3] (j\omega)^2 + [R_1 C_1 + (R_1 + R_2 + R_3) C_3] (j\omega) + 1} \quad (3.4.5.4)$$

Letting $s = j\omega$,

a third-order function that realizes a low-pass active filter unity-gain characteristic is given by the following transfer function

$$H(s) = \frac{V_o}{V_i} = \frac{1}{R_1 R_2 R_3 C_1 C_2 C_3 s^3 + [(R_1 + R_2) R_3 C_2 C_3 + R_1 (R_2 + R_3) C_1 C_3] s^2 + [R_1 C_1 + (R_1 + R_2 + R_3) C_3] s + 1}$$

3.4.5 Differential Amplifier

In order to ensure that the I/E unit output is maintained at zero volts, when different potentials (working electrode potential $\neq 0$) are applied to the working electrode without any signal input ($V_s = 0$), a differential amplifier is used. Consider the base circuit shown in Figure 3.8. The difference amplifier was utilised to subtract the applied polarisation potential

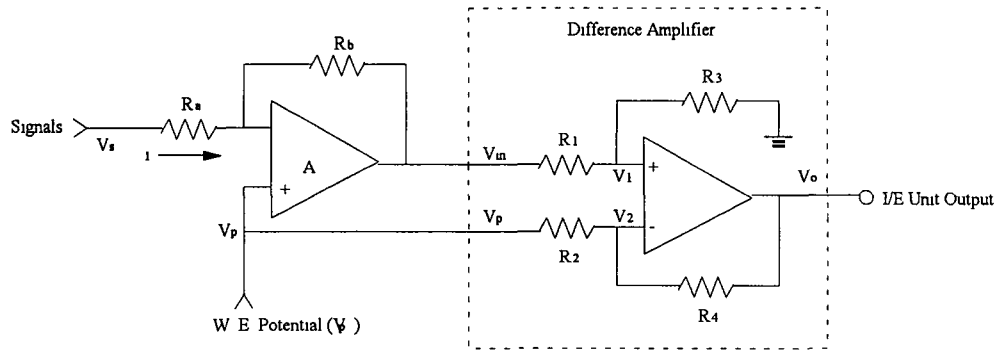


Figure 3 8 Schematic circuit for difference amplifier of current to voltage unit output part

From the circuit

$$V_1 = \frac{R_3}{R_1 + R_3} V_m \quad (3.4.4)$$

$$\frac{V_p - V_2}{R_2} = \frac{V_2 - V_o}{R_4} \quad (3.4.5)$$

where V_p is the working electrode potential, V_m is the output of the ratio amplifier, and V_o is the output of the difference amplifier

Since the two inputs of the op-amp are always at virtually the same potential, then $V_1 = V_2$

Combining equations (3.4.4) and (3.4.5), one obtains

$$\frac{V_p - \frac{R_3}{R_1 + R_3} V_m}{R_2} = \frac{\frac{R_3}{R_1 + R_3} V_m - V_o}{R_4} \quad (3.4.6)$$

Thus,

$$V_o = \frac{R_4}{R_2} \left[\frac{\frac{R_2/R_4 + 1}{R_1/R_3 + 1} V_m - V_p \right] \quad (3.4.7)$$

When the resistors are selected,

$$\frac{R_1}{R_3} = \frac{R_2}{R_4}$$

Thus,

$$V_o = \frac{R_3}{R_1} (V_m - V_p) \quad (3.4.8)$$

Since,

$$V_m = AV_s + V_p$$

where A is gain of the ratio amplifier and V_s is the signal input voltage,

and substitution into (3 4 8),

$$V_o = \frac{R_3}{R_1} AV_s \quad (3 4 9)$$

where the factor $\left(\frac{R_3}{R_1}\right)$ is the gain of the difference amplifier (normally $R_1=R_2$, $R_3=R_4$)

From (3 4 9), it is clear that I/E unit output V_o just depends on the input V_s , and is independent of the working electrode potential V_p

3.4.6 Current to Voltage Converter Unit Circuit

The current to voltage unit is a major unit of the multichannel potentiostat. It is used to convert current signal from the working electrode into a voltage signal which is then sent to the computer via the analogue to digital conversion interface of the Analog Devices RTI815 card. The output voltage of the I/E converter unit is $\pm 5V$ full scale. The circuit design utilised is shown in Figure 3 9. Each circuit of the I/E unit contains the following

- 1 a I/E converter with a low-noise and low bias current operational amplifier (OPA121) (Burr-Brown) acting as current follower,
- 2 a TL071(Texas Instruments) op-amp functioning as a voltage ratio amplifier,
- 3 a TL074(SGS-Thompson Microelectronics) quad op-amp utilised for analogue filtering, potential, current offsetting (V/I converter) and a difference ratio amplifier. The analogue low-pass (third-order Bessel) active filter has a cut-off frequency of 1 Hz, and can be switched on or off depending on the signal noise level,
- 4 sensitivity is controlled via an addressable array of relays which allow current measurements in the 0-1 mA to 0-10 μA range. Once selected, however, the chosen sensitivity is identical for each channel,

- 5 two multi-turn potentiometers are used in the current follower op-amp (A1) and ratio amplifier (A2) for zero-offset of the output,
- 6 incorporation of a calibration circuit with two multi-turn potentiometers into the current offset circuit (A) for accurate setting of the current offset ranges,
- 7 a multi-turn potentiometer is used in potential circuit (B) for accurate setting of the potential range

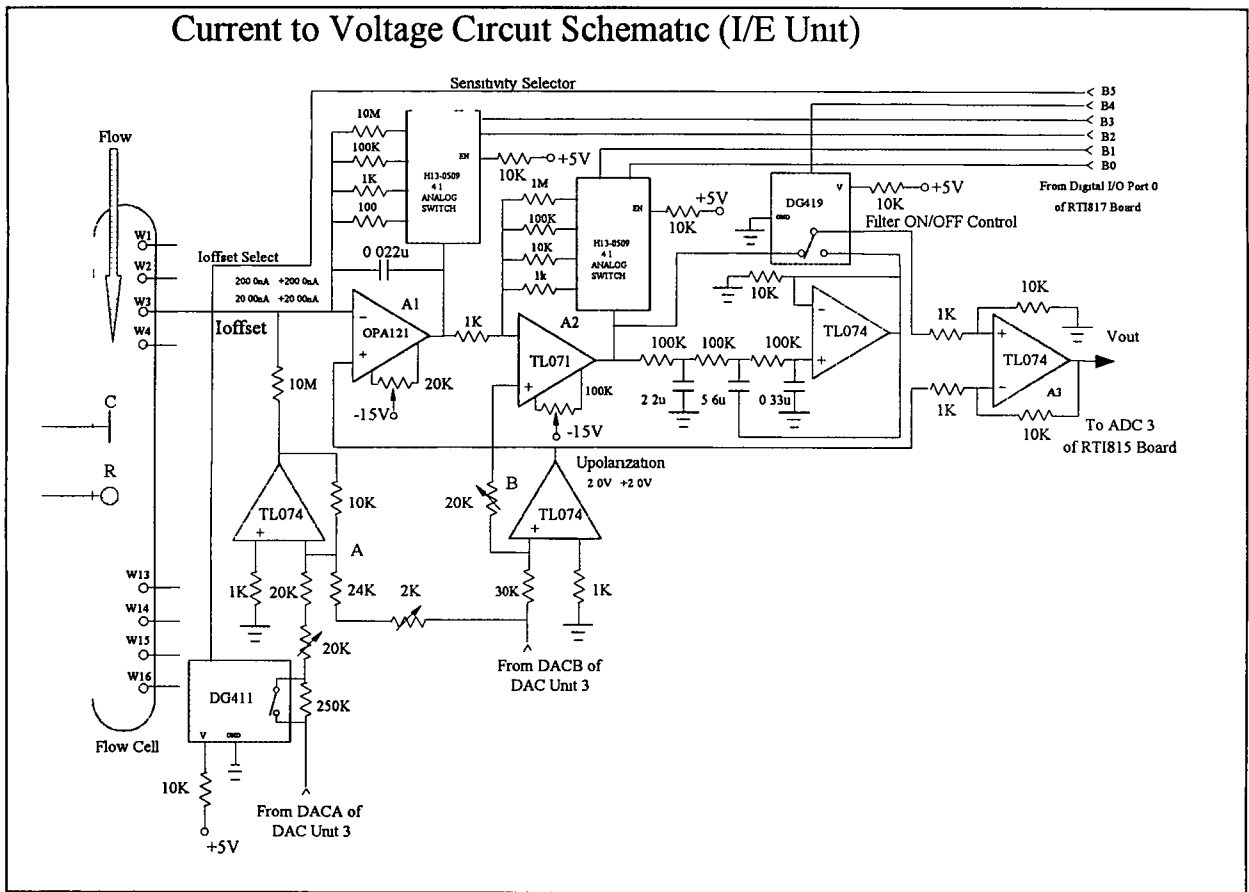


Figure 3 9 Circuit diagram for current to voltage unit

3.5 D/A Converter and Control Units

A fundamental feature of a multichannel potentiostat is that each working electrode in the array must function independently, with no electronic or chemical cross-talk between the channels. In this design, separate digital to analogue converters (DACs) are used to control each working electrode potential and background current offset. Each DAC unit was dual channel (2×12 bits, AD7237), one channel was used to convert digital signals from the computer into an analogue polarisation voltage (V_{pol}), the other DAC channel was used to control a current offset (I_{offset}). A block diagram of D/A converter and control unit is shown in Figure 3.10.

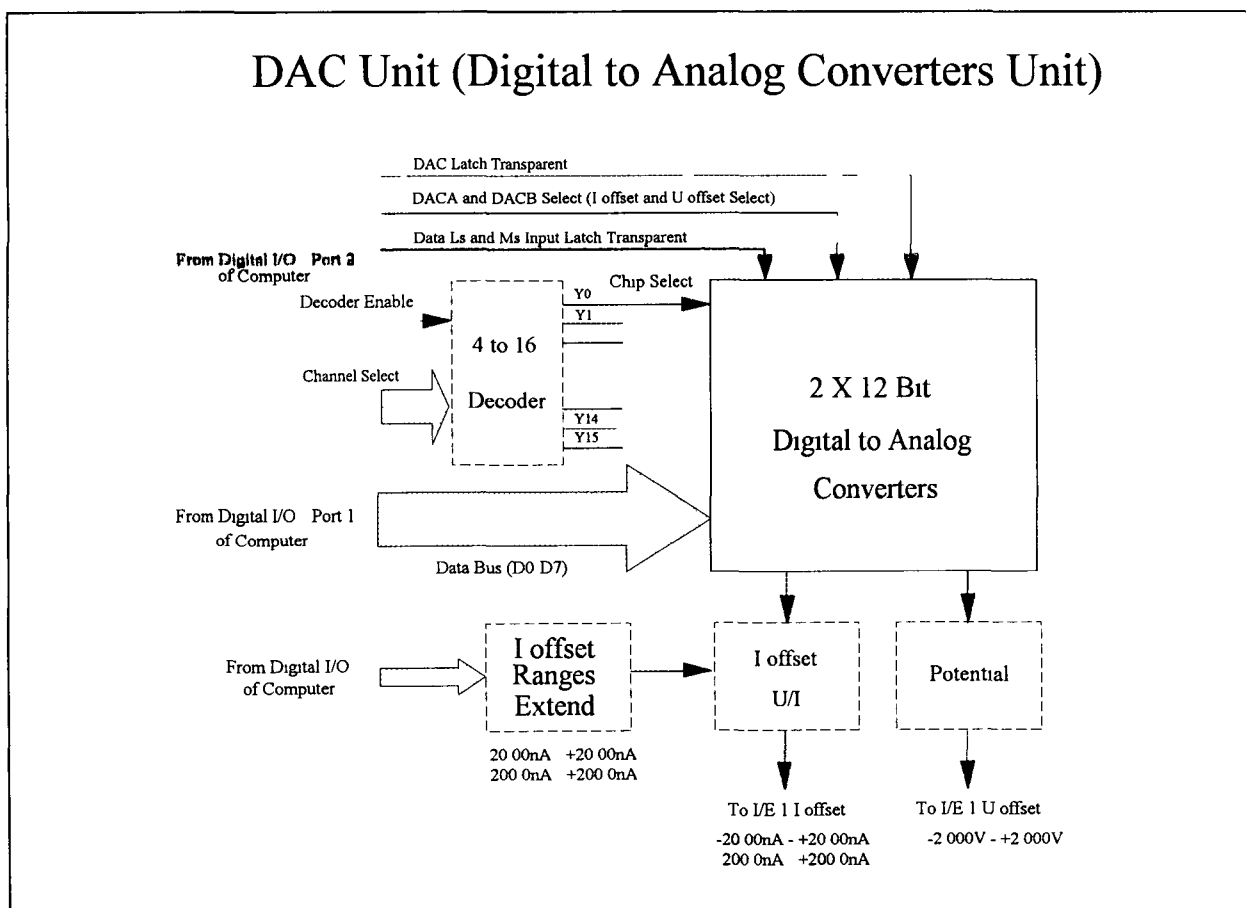


Figure 3.10 Block diagram of a digital to analog converter unit

3.5.1 AD7237 Introduction

The AD7237 is a complete, dual, 12-bit, voltage output digital-to-analog converter with output amplifiers and Zener voltage reference on a monolithic CMOS chip [76]. No external user trims are required to achieve full specified performance.

Both parts are microprocessor compatible, with high speed data latches and interface logic. The AD7237 has a double buffered interface structure and an 8-bit wide data bus with data loaded to the respective input latch in two write operations. An asynchronous \overline{LDAC} signal on the AD7237 updates the DAC latches and analog outputs.

A REF OUT/REF IN function is provided which allows either the on-chip 5 V reference or an external reference to be used as a reference voltage for the part. For unipolar supply operation, two output ranges of 0 to +5 V and 0 to +10 V are available, while these two ranges plus an additional ± 5 V range are available with bipolar supplies. The output amplifiers are capable of developing +10 V across a 2 k Ω load to GND.

A complete pin function description of the AD7237 is given in Table 3-1.

3.5.2 AD7237 - Digital I/O Port Interface

Table 3-1 AD7237 Pin Function Description

Pin	Mnemonic	Description
1	REF INA	Voltage Reference Input for DAC A. The reference voltage for DAC A is applied to this pin. It is internally buffered before being applied to the DAC. The nominal reference voltage for correct operation of the AD7237 is 5 V.
2	REF OUT	Voltage Reference Output. The internal 5 V analog reference is provided at this pin. To operate the part with internal reference, REF OUT should be connected to REF INA, REF INB.
3	REF INB	Voltage Reference Input for DAC B. The reference voltage for DAC B is applied to this pin. It is internally buffered before being applied to the DAC. The nominal reference voltage for correct operation of the AD7237 is 5 V.
4	ROFSB	Output Offset Resistor for DAC B. This input configures the output ranges for DAC B. It is connected to VOUTB for the +5 V range, to AGND for the +10 V range and to REF INB for the ± 5 V range.

5	VOUTB	Analog Output Voltage from DAC B This is the buffer amplifier output voltage Three different output voltage ranges can be chosen 0 to +5 V, 0 to +10 V and ± 5 V The amplifier is capable of developing +10 V across a 2 k Ω resistor to GND
6	AGND	Analog Ground Ground reference for DACs, reference and output buffer amplifiers
7	DB7	Data Bit 7
8-10	DB6-DB4	Data Bit 6 to Data Bit 4
11	DB3	Data Bit 3/Data Bit 11(MSB)
12	DGND	Digital Ground Ground reference for digital circuitry
13	DB2	Data Bit 2/Data Bit 10
14	DB1	Data Bit 1/Data Bit 9
15	DB0	Data Bit 0 (LSB)/Data Bit 8
16	A0	Address Input Least significant address input for input latches A0 and A1 select which of the four input latches data is written to (see Table 3 2)
17	A1	Address Input Most significant address input for input latches
18	\overline{CS}	Chip Select Active low logic input The device is selected when this input is active
19	\overline{WR}	Write Input \overline{WR} is an active low logic input which is used in conjunction with \overline{CS} , A0 and A1 to write data to the input latches
20	\overline{LDAC}	Load DAC Logic input A new word is loaded into the DAC latches from the respective input latches on the falling edge of this signal
21	VDD	Positive Supply, +15 V
22	VOUTA	Analog Output Voltage from DAC A This is the buffer amplifier output voltage Three different output voltage ranges can be chosen 0 to +5 V, 0 to +10 V and ± 5 V The amplifier is capable of developing +10 V across a 2 k Ω resistor to GND
23	VSS	Negative Supply, -15 V
24	ROFSA	Output Offset Resistor for DAC A This input configures the output ranges for DAC A It is connected to VOUTA for the +5 V range, to AGND for the +10 V range and to REF INA for the ± 5 V range

3.5.3 Interface Logic Information - AD7237

The input loading structure on the AD7237 is configured for interfacing to microprocessors with an 8-bit-wide data bus The part contains two 12-bit latches per DAC—an input latch and a DAC latch Each input latch is further subdivided into a least significant 8-bit latch and a most significant 4-bit latch Only the data held in the DAC latches determines the output from the part The input control logic for the AD7237 is shown in Fig 3 11, while the write cycle timing diagram is shown in Figure 3 12

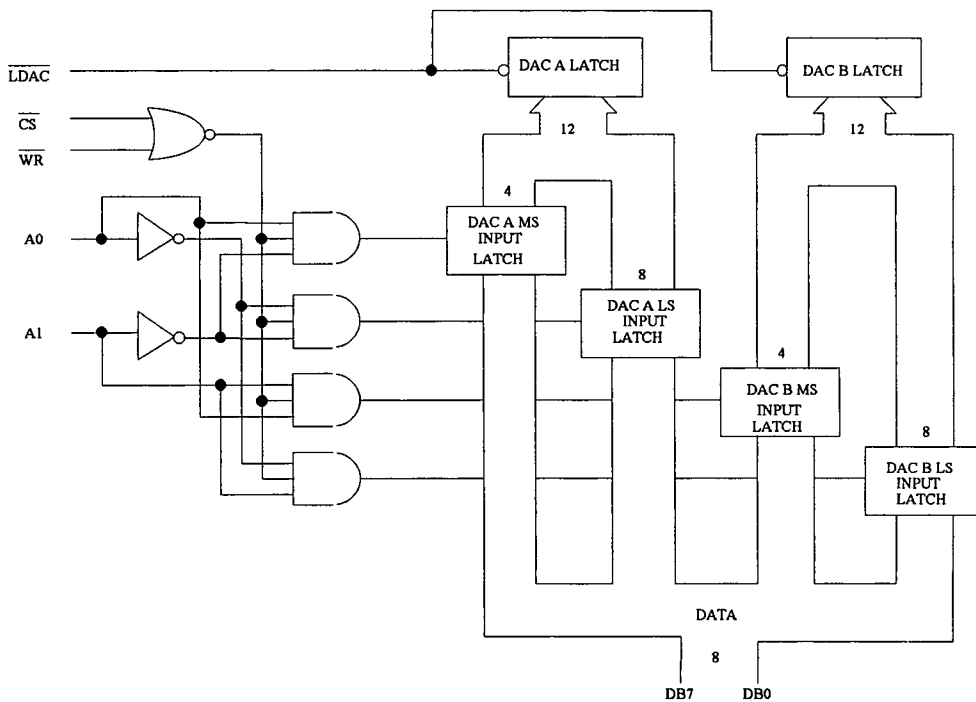


Figure 3 11 The input control logic diagram for the AD7237

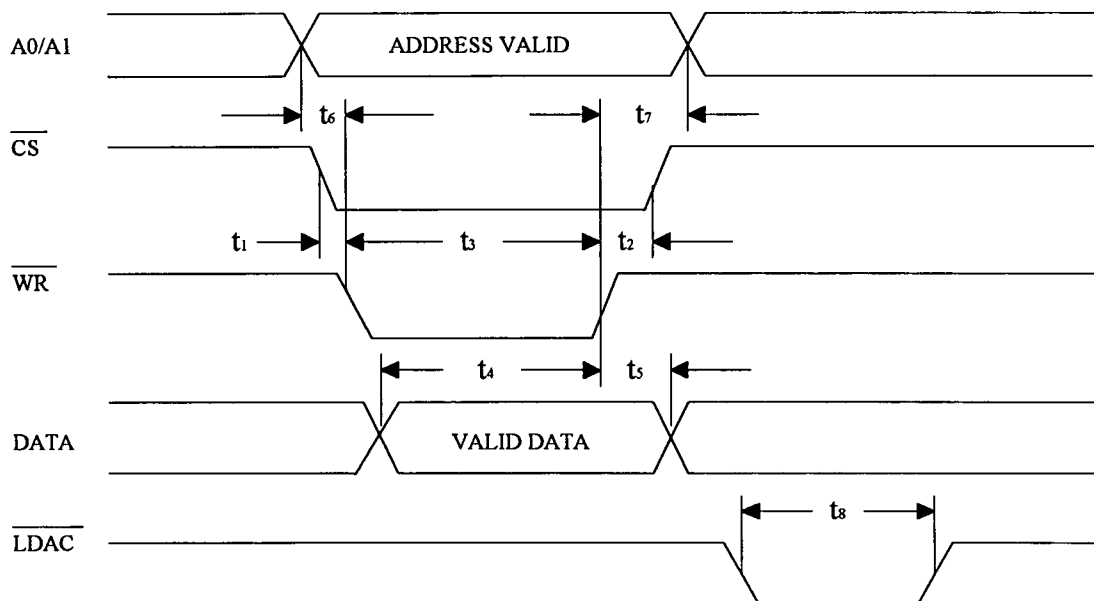


Figure 3 12 write cycle timing diagram for AD7237

\overline{CS} , \overline{WR} , A0 and A1 control the loading of data to the input latches. The eight data inputs accept right-justified data. Data can be loaded to the input latches in any sequence.

Provided that \overline{LDAC} is held high, there is no analog output change as a result of loading data to the input latches. Address lines A0 and A1 determine which latch data is loaded to when \overline{CS} and \overline{WR} are low. The selection of the input latches is shown in the truth table for AD7237 operation in Table 3.2.

Table 3.2 AD7237 Truth Table

\overline{CS}	\overline{WR}	A1	A0	\overline{LDAC}	Function
1	X	X	X	1	No Data Transfer
X	1	X	X	1	No Data Transfer
0	0	0	0	1	DAC A LS Input Latch Transparent
0	0	0	1	1	DAC A MS Input Latch Transparent
0	0	1	0	1	DAC B LS Input Latch Transparent
0	0	1	1	1	DAC B MS Input Latch Transparent
1	1	X	X	0	DACA and DACB DAC Latches Updated Simultaneously from the Respective Input Latches

X = status not significant

The \overline{LDAC} input controls the transfer of 12-bit data from the input latches to the DAC latches. Both DAC latches, and hence both analog outputs, are updated at the same time. The \overline{LDAC} signal is level triggered and data is latched into the DAC latch on the rising edge of \overline{LDAC} . The \overline{LDAC} input is asynchronous and independent of \overline{WR} . This is useful in many applications, especially in the simultaneous updating of multiple AD7237s. However, care must be taken while exercising \overline{LDAC} during a write cycle. If an \overline{LDAC} operation overlaps a \overline{CS} and \overline{WR} operation, there is a possibility of invalid data being latched to the output. To avoid this, \overline{LDAC} must remain low after \overline{CS} or \overline{WR} return high for a period equal to or greater than t_8 , the minimum \overline{LDAC} pulse width.

3.5.4 DAC Units to RTI 817 Digital I/O Map and Function

Digital I/O Map and Function

RTI 817 Port	Byte	DAC I/O	Status	Function Description
RTI 817 Port 1	BIT 0-7	D0-D7	X	DAC units and data bus are used together in the transfer of 12-bit digital data into an analog voltage signal of DAC units for the potential of the working electrodes and the input current offset The Digital-to-Analog Data Low and Digital-to-Analog Data High bytes are used together in the transfer of 12-bit digital data to a digital-to-analog converter Digital-to-Analog Data Low byte (Port 1 BIT 0-7) and Digital-to-Analog Data High byte (Port 1 BIT 0-3, BIT 4-7 don't cares) for DAC
RTI 817 Port 2	BIT 0-3	C0-C3	X	Decoder data input for DAC units channel selection Multichannel amperometric channel selection
			0	Decoder enable ($\overline{G1}$, $\overline{G2}$) DAC chip select, write input and data transfer
	BIT 4	C4	1	No decoder enable ($\overline{G1}$, $\overline{G2}$) No DAC chip select, no write input and no data transfer
			0	DAC A and DAC B DAC latches updated simultaneously from the respective input latches (\overline{LADC})
	BIT 5	C5	1	No data transparent (\overline{LADC})
			0	DAC A is selected DAC A data input latch transparent for Current offset
	BIT 6	C6	1	DAC B is selected DAC B data input latch transparent for potential of working electrodes
			0	DAC data low byte (LS) input latch transparent
BIT 7	C7	1	DAC data high byte (MS) input latch transparent	

Digital-to-Analog of DAC Units Data Low and High Bytes

✓ Digital Input Byte of DAC Units

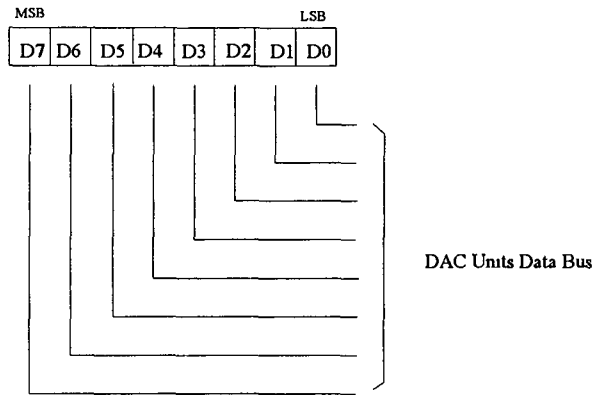


Figure 3 13 Digital to analog data byte for digital input byte of DAC units

Digital to Analog Data Low and High Bytes (for DAC Unit 1 to Unit 16)

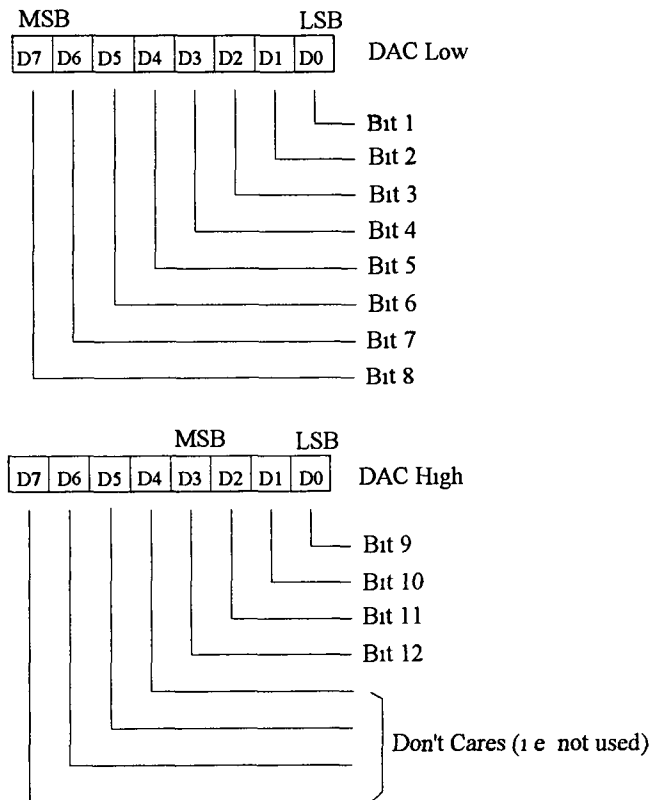


Figure 3 14 Digital to analog data low and high bytes for DAC units

The digital-to-analog data low byte (Port 1 BIT 0-7) and the digital-to-analog data high byte (Port 1 BIT 0-3, BIT 4-7 don't cares) are used together for the transfer of 12-bit digital data into an analog voltage signal for the potential of the working electrodes and the input current offset. Both are read-only bytes. Figure 3-13 shows an illustration of digital to analog data for digital input byte of DAC units. Figure 3-14 shows an illustration of digital-to-analog of DAC units data low and high bytes.

DAC Units Channel Select/Status Control Byte

The Channel Select/Status Control byte (C0-C7) is used to select the unit channel address of the DAC for the potential of the working electrodes and the input current offset, and to control the status control logic of the DAC units for the potential of the working electrodes and the input current offset. Figure 3-15 shows an illustration of the DAC units channel select/status control byte for digital input byte of DAC units.

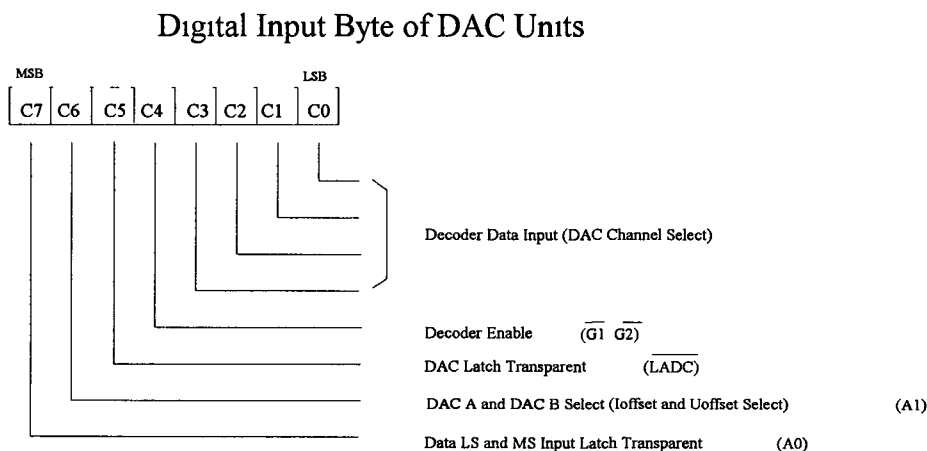


Figure 3-15 DAC unit channel selection/status control byte for digital input byte of DAC units

3.5.5 Control Flow Chart

According to the input control logic and the write timing of the AD7237, the data transfer, digital to analogue conversion and status control flow chart is shown Figure 3 16

Data Transfer, Digital to Analog Conversion and Status Control Flow Chart

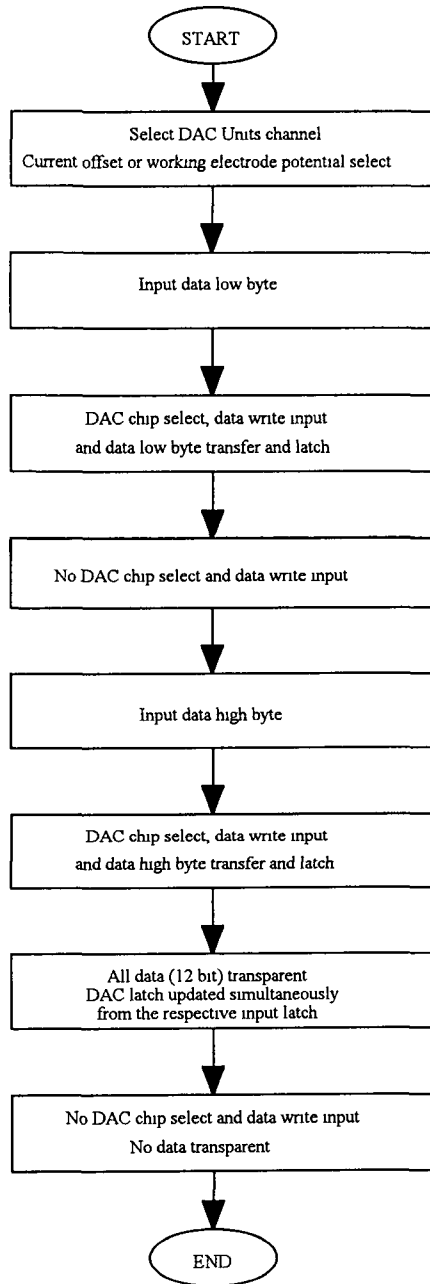


Figure 3-16 Data transfer digital to analog conversion and status control for AD7237 flow chart

3.5.6 DAC Unit Circuit

Each DAC (AD7237)(Analog Devices) unit is dual channel with 12-bit resolution (1 e 1 4095), with one channel being used to convert digital signals from the computer into an equivalent analogue voltage polarisation (V_{pol}) between $\pm 2.0V$ vs the reference potential electrode potential (resolution ca 1mV) and the other DAC channel being used to control a current offset

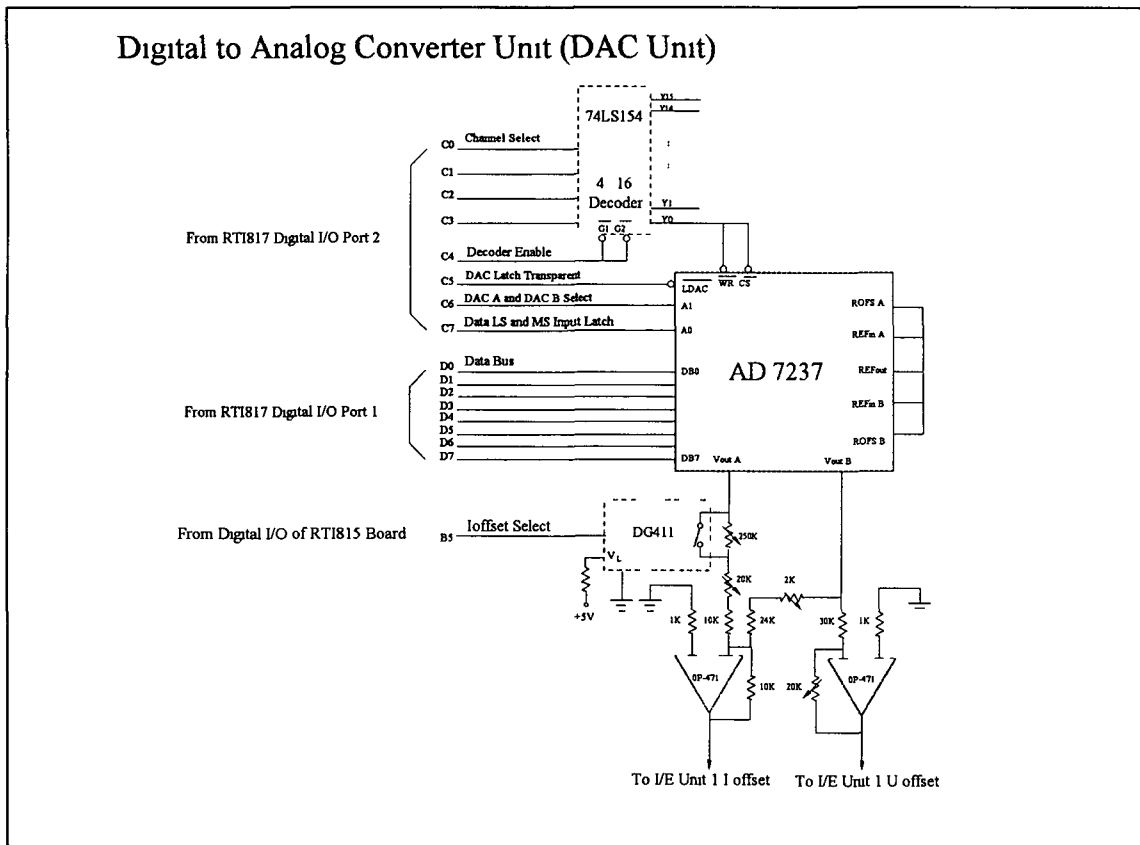


Figure 3 17 Circuit diagram for digital to analog converter unit

In order to allow the background current baseline to be set to zero an independent input current offset facility is used in each channel of the multichannel potentiostat. The baseline can be corrected automatically or manually set to zero (user defined offset) via the computer. One 12-bit D/A channel (1 e a in Figure 3 17) converts digital signals from

the computer into an analogue voltage offset between $\pm 2.0\text{V}$ (resolution $\approx 1\text{mV}$). This is passed to a V/I converter circuit which transforms the voltage offset signal into a current offset. An analogue switch controls and selects the current offsetting facility in the V/I converter circuit. The ranges extend from $\pm 200.0\text{nA}$ and $\pm 20.00\text{nA}$, and resolution from ca. 100pA and 10pA , respectively. The circuit design utilised is shown in figure 3.17.

3.6 Control Unit

A control unit contains a DAC channel selection, the sensitivity selection, the analogue filter control, a current offset extent control. A block diagram of control unit is shown in Figure 3.18.

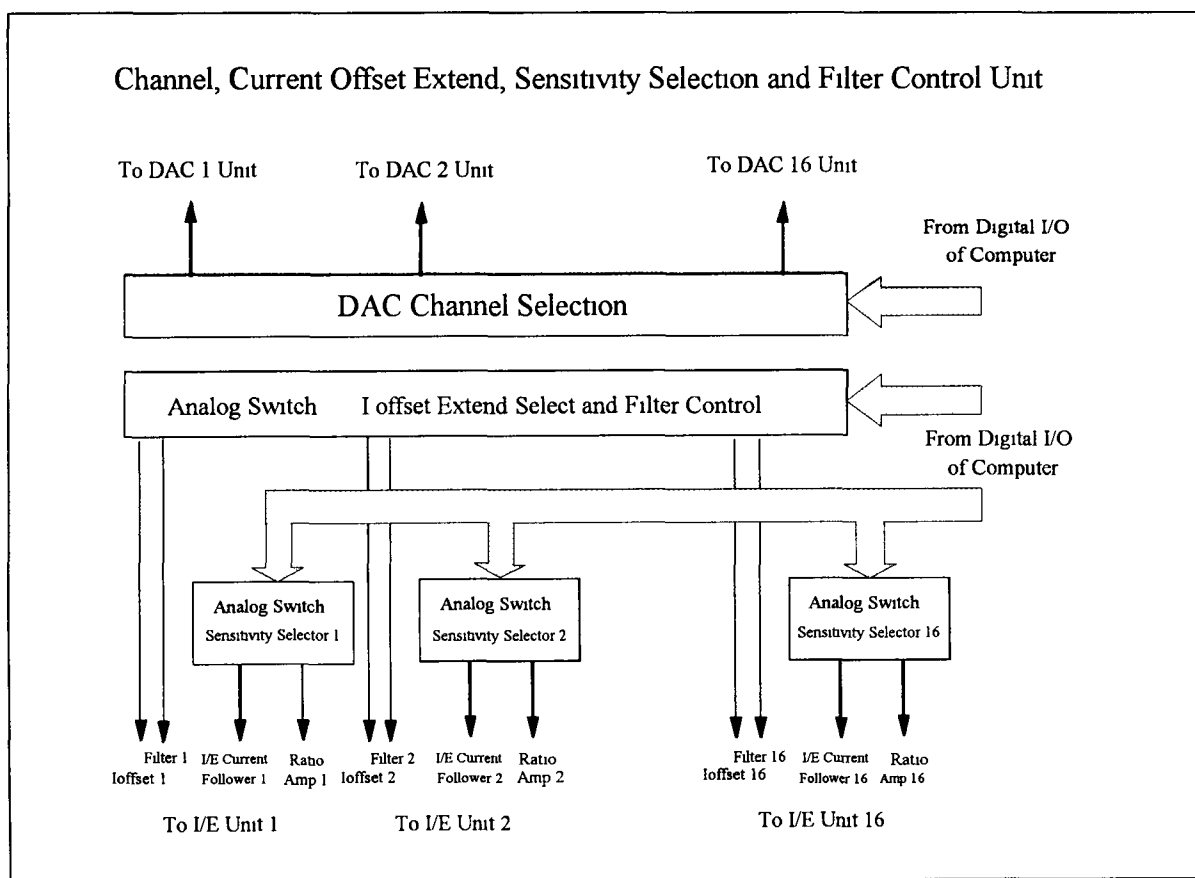


Figure 3.18 Block diagram for DAC unit channel selection/current offset extend/sensitivity selection/filter control unit

3.6.1 Analogue Switch (DC411, DG419 and H13-0509)

DG411

DG411 is a quad SPST CMOS analogue switch housed in a 16-pin PDIP plastic package

- ± 15 V input signal range
- Low RDS (ON) $< 25 \Omega$ typ
- $t_{ON} < 175$ ns
- $t_{OFF} < 147$ ns
- Ultra low power requirements $\leq 35 \mu W$
- Inputs logic 0 all switches ON
 logic 1 all switches OFF

DG419

DG419 is a precision SPDT CMOS analogue switch and ideally suited to battery powered or portable equipment applications

- DG419 features low power ($\leq 35 \mu W$)
- Low leakages and combines high-speed switching with low on resistance ($< 35 \Omega$)
- One SPDT switch per package
- Logic inputs as below

	Switch 1	Switch 2
Logic 0	ON	OFF
Logic 1	OFF	ON

H13-0509

H13-509 is a CMOS monolithic analogue multiplexers with dual 4 channels respectively. The H13-509 switches one of 4 differential inputs to a common differential output depending on the state of two binary addresses and an enable input

- TTL and 5 V CMOS logic compatible digital inputs
- The devices can comfortably operate anywhere in the 10.8 V to 16.5 V single or dual supply range

- Low leakage currents in the range of 20 pA make these multiplexers suitable for high precision circuits
- These multiplexers also feature high switching speeds and low RDS (ON) < 180 Ω typ
- Logic inputs as below

A1	A2	EN	ON SWITCH PAIR
X	X	0	NONE
0	0	1	1
0	1	1	2
1	0	1	3
1	1	1	4

3.6.2 Analogue Switch - Digital I/O Port Interface

The following is a functional description of all the analogue switch-digital I/O port 0 bits of RTI817 board interface contained within the sensitivity selection/control of the sensitivity selector 1 and 2, the status/control of the analog filter, and selection/status of the current offset ranges extend

RTI 817 Port	Byte	Unit I/O	Status	Function Description
RTI 817 Port 0	BIT 0-1	B0-1	X	Analog switches of sensitivity selector 2 channel select for sensitivity selection
	BIT 2-3	B2-3	X	Analog switches of sensitivity selector 1 channel select for sensitivity selection
	BIT 4	B4	0	Analog filter OFF
			1	Analog filter ON
	BIT 5	B5	0	Input current offset extend select -200 0 to +200 0 nA
			1	Input current offset extend select -20 00 to +20 00 nA

3.6.3 Sensitivity Select and Control Truth Table

The gain and sensitivity selection for the multichannel potentiostat was described previously. Through the value selection of the feedback resistors of the current follower A1 and the voltage ratio amplifier A2, the gain of the detection system is selected by two analog switches for sensitivity selection controlled via the computer and the RTI817 digital I/O control board. Table 3.3 lists the resistors and gain of the sensitivity selectors 1 and 2 truth table. Table 3.4 lists the sensitivity selection and control truth table, with sensitivity of the detection system in the range of 10 pA to 1 mA, 9 decades.

Table 3.3 Sensitivity Selector Truth Table

Sensitivity Selector 1				Sensitivity Selector 2			
Amplifier A1				Amplifier A2			
Resistor	A1 Gain	B3	B2	Resistor	A2 Gain	B1	B0
10 M	10^7	0	0	1 M	10^3	0	0
100 K	10^5	0	1	100 K	10^2	0	1
1 K	10^3	1	0	10 K	10^1	1	0
100	10^2	1	1	1K	10^0	1	1

Table 3.4 Sensitivity Select and Control Truth Table

Selector 1			Selector 2			A3	Sensitivity (A1·A2·A3)					
A1 Gain	B3	B2	A2 Gain	B1	B0	A3 Gain	A1A2A3	B3	B2	B1	B0	Range
10^7	0	0	10^3	0	0	10^1	10^{11}	0	0	0	0	10 pA
10^7	0	0	10^2	0	1	10^1	10^{10}	0	0	0	1	100 pA
10^5	0	1	10^3	0	0	10^1	10^9	0	1	0	0	1 nA
10^5	0	1	10^2	0	1	10^1	10^8	0	1	0	1	10 nA
10^5	0	1	10^1	1	0	10^1	10^7	0	1	1	0	100 nA
10^3	1	0	10^2	0	1	10^1	10^6	1	0	0	1	1 μ A
10^3	1	0	10^1	1	0	10^1	10^5	1	0	1	0	10 μ A
10^3	1	0	10^0	1	1	10^1	10^4	1	0	1	1	100 μ A
10^2	1	1	10^0	1	1	10^1	10^3	1	1	1	1	1 mA

3.6.4 Control Unit Circuit

The control unit circuit design utilised is shown in Figure 3 19 The DAC for each channel is selected via a 4-16 decoder (74LS154)(National Semiconductors) Two digitally controlled multiplexers (H13-0509)(Harris Semiconductors) are used for sensitivity selection for each I/E converter unit, and an analogue switch (DG411)(Silicomx) used for current offset range selection The analogue filter on each channel is switched to active\inactive mode via an analogue switch (DG419)(Siliconix)

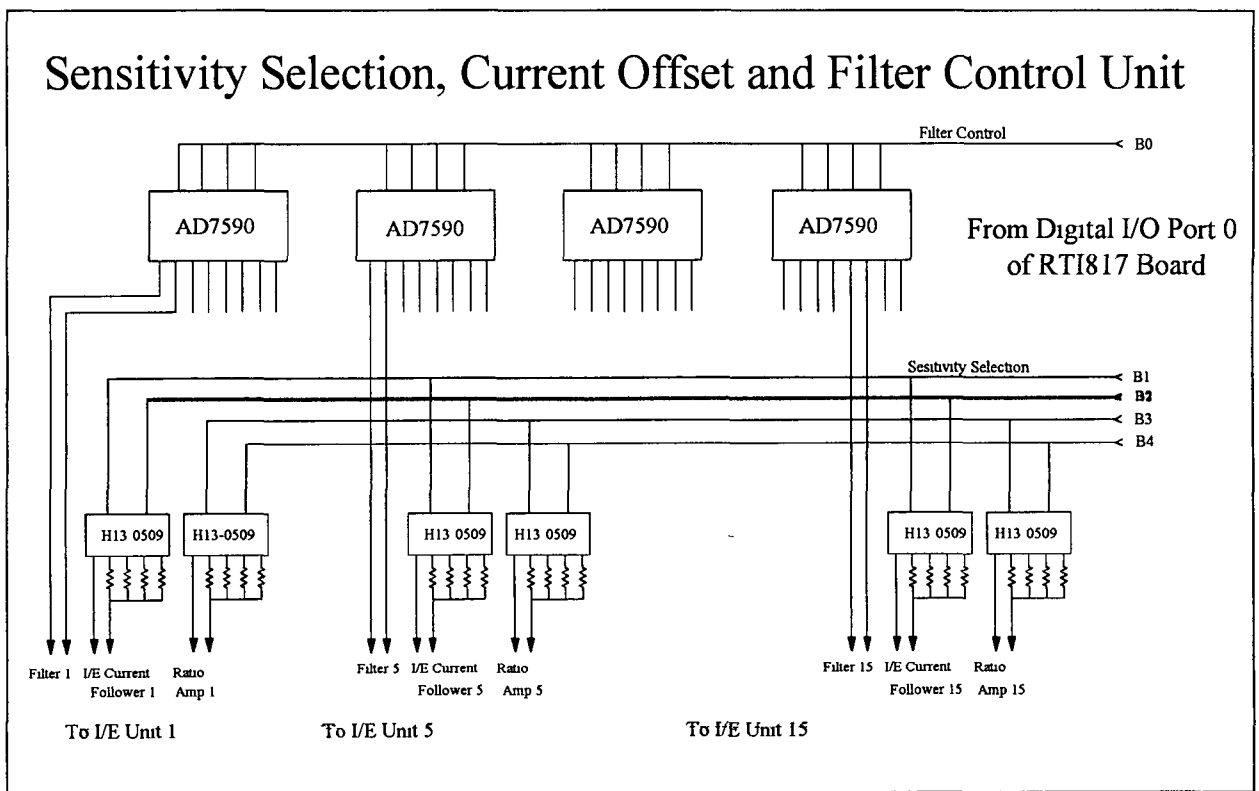


Figure 3 19 Circuit diagram for DAC unit channel selection/current offset extend/sensitivity selection/filter control unit

3.7 Power supply

A range of multi-output switch mode power supply is used for power supply of the multichannel potentiostat. The power supply general specifications as follows:

Input voltage	AC 50Hz, 176-264ac rms on 230V nominal
Output power	50W continuous (max)
Output voltage and current	DC -5V 1A, +5V 1A, -12V 1A, +12V 1A, +24V 1A
Line regulation	0.4% max. For 198 to 254V change at full proportional loading
Load regulation	Load on measured output varied 20% to 100% I _{max} typically 6% semi or quasi regulated outputs, 2% on regulated outputs
Ripple and Noise	All models 75mV pk-pk typical
Hold up time	After loss of input at full load typically 28ms at mains nominal 18ms at mains low

CHAPTER 4

COMPUTER AND INSTRUMENTATION INTERFACE

4.1 Computer and hardware configuration

- A PC compatible computer 486-33MHz with 16MB of RAM, and storage consisting of a single 250MB hard disk, and two floppy drives (3¹/₂", 5¹/₂") A microcomputer was selected for this research because the intent was to develop a PC-based multichannel computer controlled potentiostat for analysis in flowing streams. The selection of the computer hardware is very important for the ease of work, and the user can run more than one software package at the same time. For example, in this research, the user working with the multichannel amperometric detection system package can run other software like Microsoft EXCEL and return to Detection System at any time.
- A low radiation colour monitor with super VGA (1024×768) graphic display
- A mouse (X-30M) interaction with detection system menus
- A printer (Brother HL-10PS) for report printout

4.2 Interface card

For automated data-acquisition and control, the multichannel potentiostat has been interfaced to a computer. All control lines between the computer and the potentiostat are provided by the secondary input/output devices located on the I/O bus socket of the computer motherboard. The computer was equipped with Analog Devices RTI815 and RTI817 data acquisition/control cards [71-72]. The multiplexer analog inputs are used

for data-acquisition of 16 channel potentiostat. The analog outputs are used for the voltage of counter electrode output control and the pump speed control. Digital I/O is used for controlling the sensitivity selection, the potential of the working electrodes, the input current offset, the current offset extent selector, the analogue filter control, and the pump control. The software-selectable gain of the RTI-card allows for an expansion of the effective sensitivity range (over and above the that offered by the current gain circuitry described earlier) to 100 fA full scale. For synchronisation of data acquisition, potential scan-rate control, and working electrode cycles, the programmable interval counter and timer chip of the computer was used.

4.2.1 RTI 815 Board

The RTI 815 is a multifunction analog/digital input/output board that plugs into one of the available long expansion slots (16-Bit) in the IBM PC, PC/XT, PC/AT, or equivalent personal computer. The RTI 815 board has capabilities for analog input, analog output, digital input and output, and time-related digital I/O functions.

The RTI815 interface consists of

- 1 16 digital I/O lines (0 to +5V, TTL compatible)
- 2 32 single ended (16 differential) analogue input lines, 12-bit resolution, software selectable gain (1, 10, 100, 500), input voltage range ($\pm 5V$, $\pm 10V$, 0-10V) jumper selectable, conversion time 25 μ s, system throughput up to 31.2 kHz
- 3 2 analogue out lines (12-bit resolution), ranges 0 to +10V, $\pm 10 V @ 2 mA$

For effective data validity, measurements from each channel should be as small as possible to reduce the real time differential between the channels which increases with the number of channels. So, the A/D conversion time is 25 μ s and system throughput is 31.2 kHz for effective operation of the A/D converter (RTI 815).

Analog input and/or output connection are made to the RTI 815 through the 50-pin male connector J2 Digital I/O and counter/timer I/O are connected to the RTI 815 through the 34-pin male connector J1

4.2.2 RTI 817 Board

The RTI 817 is a 24-channel, TTL compatible (0 to +5V) digital I/O board that plugs into one of the available slots in the IBM PC, PC/XT, PC/AT, or equivalent personal computer. The RTI817 interface provides three 8-channel ports, ports 0, 1 and 2, for digital I/O operations. The channels/ports can be accessed through the J1 connector on the board. Depending on the application, One can address a single channel (bit) of a digital I/O port or all eight channels (byte) of a digital I/O port. Digital control signals can be sent out indicating the status of a control line or switch or, if the channels are configured as digital input channels, return a digital input value.

4.2.3 RTI 817 Digital I/O Port Byte

Each 8-bit port on the RTI 817 is controlled through its own Digital Data Output/Digital Data Input byte. Each byte is bi-directional and may be read from as well as written to. The digital I/O ports can be addressed on a bit-by-bit basis (channel-by-channel) or on a byte basis (an entire port). Configuration of an individual port as a digital input or digital output port is achieved by positioning jumpers on the RTI 817 board. In this research work, all RTI 817 digital I/O ports are configured as output ports.

Detection System Status/Control Byte

The Status/Control byte (BIT 0-7) for digital output port 0 (B0-B7) of the RTI817 board serves to control the sensitivity selection, the current offset range selector, the analogue

Digital Output Byte Port 1 of RTI817 Board

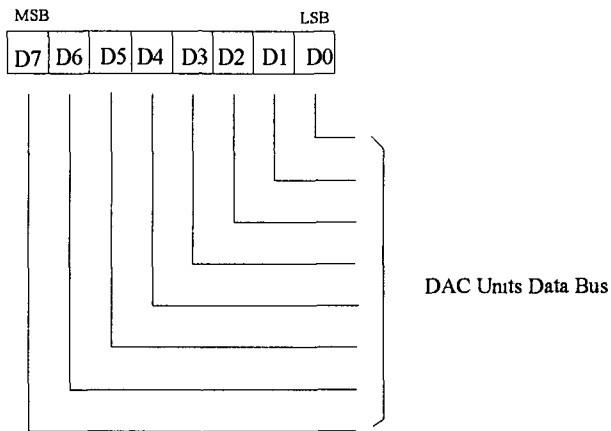


Figure 4 2 Data byte for digital output port 1 of RTI817 board

Digital to Analog Data Low and High Bytes (for DAC Unit 1 to Unit 16)

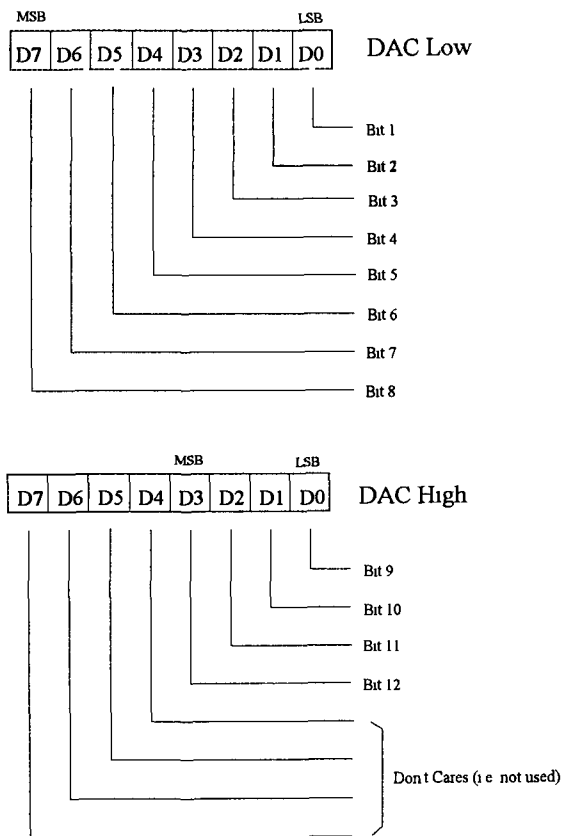


Figure 4 3 Digital to Analog data Low and High Bytes for digital output port 1 of RTI817 board

DAC Units Channel Select/Status Control Byte

The Channel Select/Status Control byte (BIT 0-7) for digital output port 2 (C0-C7) of the RTI 817 board is used to select the unit channel address of the DAC for the potential of the working electrodes and the input current offset, and to control the status control logic of DAC units for the potential of the working electrodes and the input current offset. Figure 4.4 shows an illustration of DAC units channel selection/status control byte for digital output port 2 of RTI817 board.

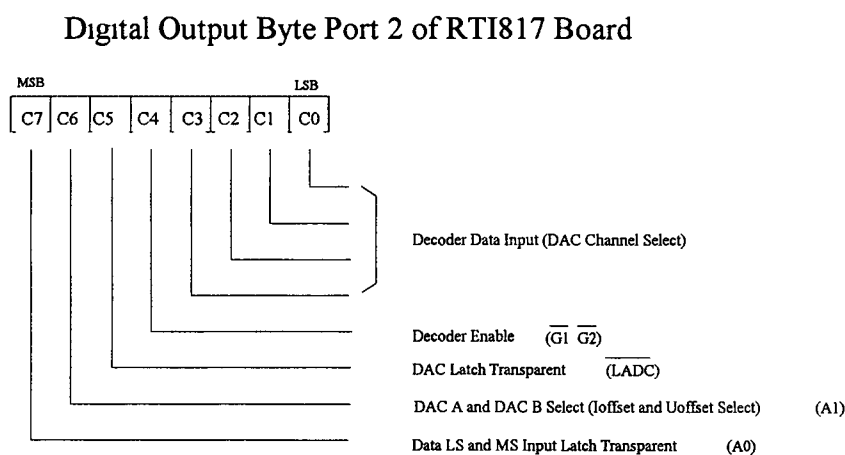


Figure 4.4 DAC units channel selection/status control byte for digital output port 2 of RTI817 board

Functional Description of all the Ports Byte

The following is a functional description of all the RTI 817 digital I/O ports bits contained within the Detection System Status/Control Byte, Digital-to-Analogue of ADC Units Data Low and High Bytes, and ADC Units Channel Select/Status Control Byte.

Port	Byte	Status	Function Description
Port 0	BIT 0-1	X	Analog switches of sensitivity selector 2 channel select for sensitivity selection
	BIT 2-3	X	Analog switches of sensitivity selector 1 channel select for sensitivity selection
	BIT 4	0	Analog filter OFF
		1	Analog filter ON
	BIT 5	0	Input current offset extend select -200 0 to +200 0 nA
		1	Input current offset extend select -20 00 to +20 00 nA
	BIT 6	0	Peristaltic pump STOP
		1	Peristaltic pump START
BIT 7	0	Peristaltic pump direction FORWARD	
	1	Peristaltic pump direction BACKWARD	
Port 1	BIT 0-7	X	DAC units and data bus are used together in the transfer of 12-bit digital data into an analog voltage signal of DAC units for the potential of the working electrodes and the input current offset The digital-to-analog data low and digital-to-analog data high bytes are used together in the transfer of 12-bit digital data to a digital-to-analog converter digital-to-analog data low byte (Port 1 BIT 0-7) and digital-to-analog data high byte (Port 1 BIT 0-3, BIT 4-7 don't cares) for DAC
Port 2	BIT 0-3	X	Decoder data input for DAC units channel selection Multichannel amperometric channel selection
	BIT 4	0	Decoder enable ($\overline{G1}$, $\overline{G2}$) DAC chip select, write input and data transfer
		1	No decoder enable ($\overline{G1}$, $\overline{G2}$) No DAC chip select, no write input and no data transfer
	BIT 5	0	DAC A and DAC B DAC latches updated simultaneously from the respective input latches (\overline{LADC})
		1	No data transparent (\overline{LADC})
	BIT 6	0	DAC A is selected DAC A data input latch transparent for Current offset
		1	DAC B is selected DAC B data input latch transparent for potential of working electrodes
	BIT 7	0	DAC data low byte (LS) input latch transparent
1		DAC data high byte (MS) input latch transparent	

4.2.4 Computer I/O Address Selection

The RTI 815 and RTI 817 cards are mapped into the computer I/O channel structure as a block of 16 consecutive bytes, addressable on any unoccupied 16-byte boundary from address 200H to 3FFH. The I/O address is specified by setting DIP switches.

In this research work, the I/O addresses are selected 350H to 35FH for RTI 815 and 300H to 30FH for RTI 817.

4.2.5 RTI 815 and RTI 817 Software Drivers

The RTI 800 Series Software Drivers provide a powerful and convenient software interface between the RTI 815, RTI 817 board and the IBM PC, PC/XT, PC/AT and 100% compatible computers. Included in this software package are system, configuration, I/O, and conversion routines that can be invoked from the host application program using a high-level language such as BASIC, C or Turbo Pascal.

CHAPTER 5

DEVELOPMENT FOR SOFTWARE OF SYSTEM

5.1 Introduction

Multichannel electrochemical detection is difficult to perform without computerised instrumentation. Therefore, both the control and data acquisition are fully computerised. The software support of the data-acquisition and hardware control have been developed "in-house".

The software used to control this system was written in QuickBASIC 4.5 (QBasic) with the initial system consisting of a set of system menus which were displayed on the screen. These menus allowed the user to set instrumental working parameters and perform functions such as running the system and plotting the information acquired. The problem with this system was that it was very cryptic and alienating for people who were not familiar with the operation of the system.

In an effort to overcome this problem it was decided to write software with a "Windows" style graphical environment. The new user-computer interface was written using an Assembly Language Toolbox which consisted of a collection of routines in a Quick Library and a stand alone library which could be used in the QBasic environment. Among these routines were ones which could produce vertical and horizontal menus on the screen from which the user could make selections using the mouse or the HotKey facility. HotKey facilities are characters, normally a letter or a number when pressed automatically executes that selection without the user having to press the return key afterwards. These HotKeys are easily recognisable in the menu as they appear highlighted. In the case of selections made using the mouse, this merely involves clicking on the selected choice to execute that particular selection.

The Assembly-Language Toolbox has the advantage that it can be used in both text and graphics mode. Also Assembly-Language is much faster than QuickBasic resulting in a program which is more compact thus requiring less CPU time.

5.2 Software Selection

The software for instrumental control, data acquisition, on-line display (2 or 3-dimensional formats), digital filtering and data storage were written in QuickBasic 4.5. The user interface utilises a Windows style display which was developed with an Assembly Language Toolbox. The Toolbox consists of a collection of routines in a Quick Library and a stand alone library which could be used in the QuickBasic environment.

The RTI-800 Series Software package provides a convenient and powerful software interface between the RTI 815 and RTI817 I/O boards and PC computer [76]. The RTI-800 Series software package consists of high-level language libraries, hardware library used to resolve references to any hardware libraries, utilities, and a sample program. Each language library consists of a language binding and the system routines. Bindings handle parameter passing between the detection system program and the hardware libraries. The hardware libraries are board specific (RTI 815 LIB, RTI 817 LIB), and contain the low-level subroutines that directly perform the I/O functions supported by the RTI-800 Series boards. System routines are hardware independent and include initialization, delaying program execution, and clearing logical channel definitions.

5.2.1 Assembly Language Toolbox Operation

The assembly language toolbox was designed to resemble standard QBasic *Sub Programs* and *Function* procedures. Routines which are required for the program are declared at the beginning of the program. A full set of these of these routines is provided with the toolbox from which the user can select the ones required for a particular application.

If for example it was required to output a large quantity of text to the screen at high speed, the following line would be placed at the beginning of the program

Declare Sub FastPrint (Row%, Col%, Text\$, Attr%)

Where

Row% is the row where printing is to start

Col% is the column where printing is to start

Text\$ is the string of text to be printed

Attr% is the video attribute given to the text

This routine allows text to be printed quickly in any position on the screen and is especially useful for printing inside Windows

Since in this case the program was being run in the QuickBasic environment, the Quick library was loaded into the QuickBasic directory using the following command

QB program_name.BAS/L.AltQuick.qlb

After the Quick library had been loaded it was possible to call the Assembly Language routines in a similar manner to QuickBasic sub programs

Example

FastPrint 25,20 "MultiChannel Amperometric Detection System",48

This will print 'Multichannel Amperometric Detection System' in the middle of the 25th row displaying it in black on a cyan background. Since a DECLARE statement was used it is not necessary to place parentheses around the argument list and even the call statement is unnecessary. When used in this way the toolbox routines become actual extensions to the QuickBasic language.

The same DECLARE statement can be used when the program is compiled from the DOS command line. In this case however, the compiled program must be linked to AltQuick Lib, the stand-alone library, with the following command

Link program_name,,,AltQuick.Lib;

The QuickBasic linker will only extract, from AltQuick Lib, those modules which are explicitly named by DECLARE statements in the source file. This ensures that the programs are not burdened with unnecessary code.

5.2.2 RTI Software Routines

I/O and system routines are used to access the functions of RTI 815 and RTI 817 boards. I/O routines are provided for analog I/O, digital I/O, frequency input, event counting, and pulse output when these functions are supported by the board. System functions are hardware independent and include initializing the system data, delaying program execution, and clearing logical channel definitions.

Each I/O routine has a setup routine associated with it, system routines do not. A setup routine defines a record in software, called a *logical channel*, which contains all the information necessary to perform the specified I/O function on a particular RTI board. Once the logical channel is defined, few parameters need to be specified for the I/O function itself. When operations use sequences of physical channels (such as AING), the setup routine also stores this information in a "channel sequence list" in memory.

The setup routine must be called before its associated I/O routine or an error will be reported. Up to 256 logical channels can be defined at one time. Once a logical channel is defined, it cannot be redefined unless it is first cleared using the system routine CLCHAN. If appropriate, CLCHAN also removes entries from the channel sequence list. These tasks are also accomplished when the system is initialized.

5.3 Software Design

The menu driven package includes routines which configure the system to the system setup required by the user, perform data analysis, archive data to and retrieve data from the hard disk, display data in either three dimensional (current vs time vs applied potential),

or two dimensional formats (current vs applied potential), or obtain a printout. The three dimensional display facility is also available in real time during data acquisition. Included in the main menu is a HELP option which allows the user to access help files on system functions and settings.

5.3.1 Structural Composition of Program

The program for data-acquisition and system control consists of the program and detection system initialisation, the system program main menu, the detection system main program, and display or print analysed results. A simplified structural layout for the multichannel potentiostat detection system software is shown in Figure 5.1.

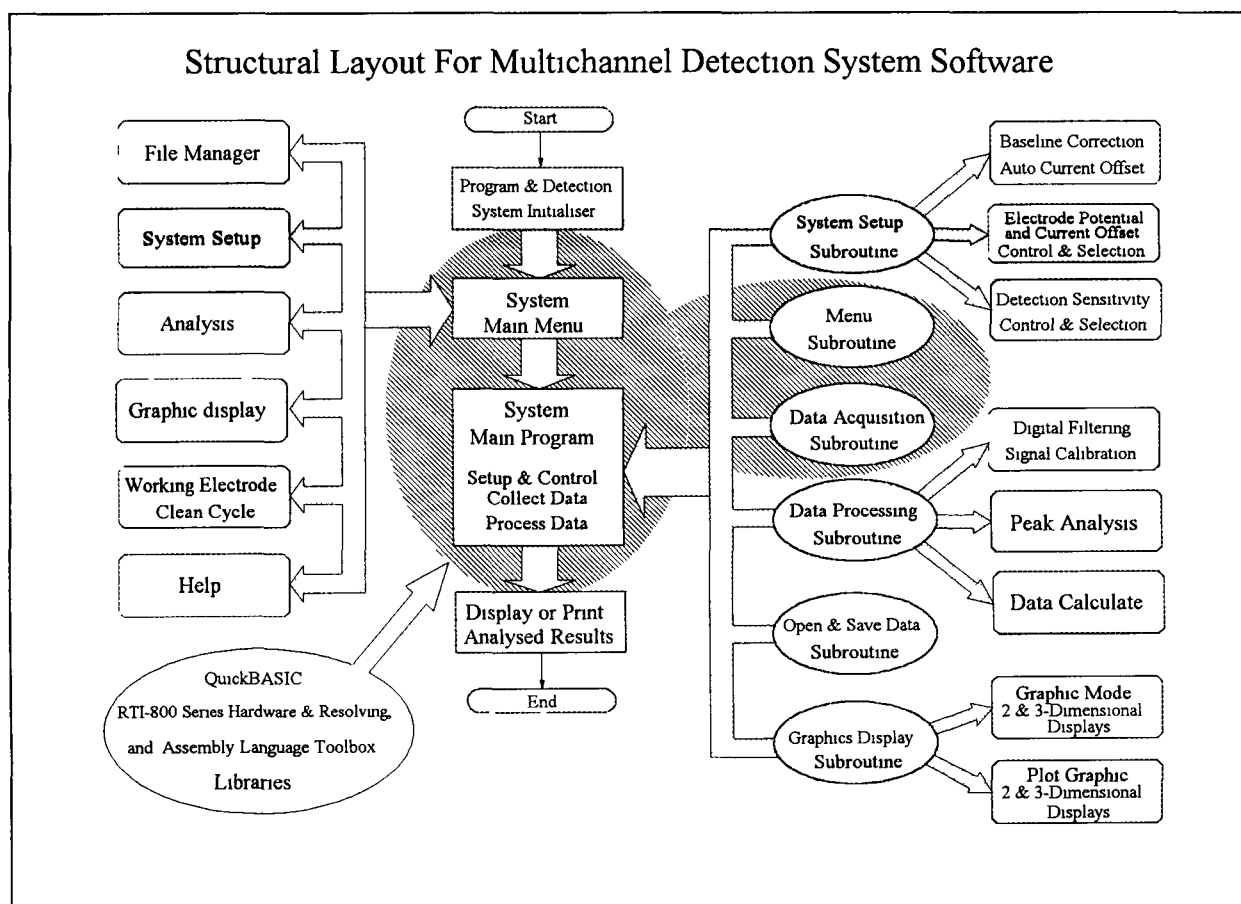


Figure 5.1 Structural layout for multichannel potentiostat detection system software

5.3.2 Program Flowchart

A multichannel potentiostat detection system control program flow chart are shown in Figure 5 2

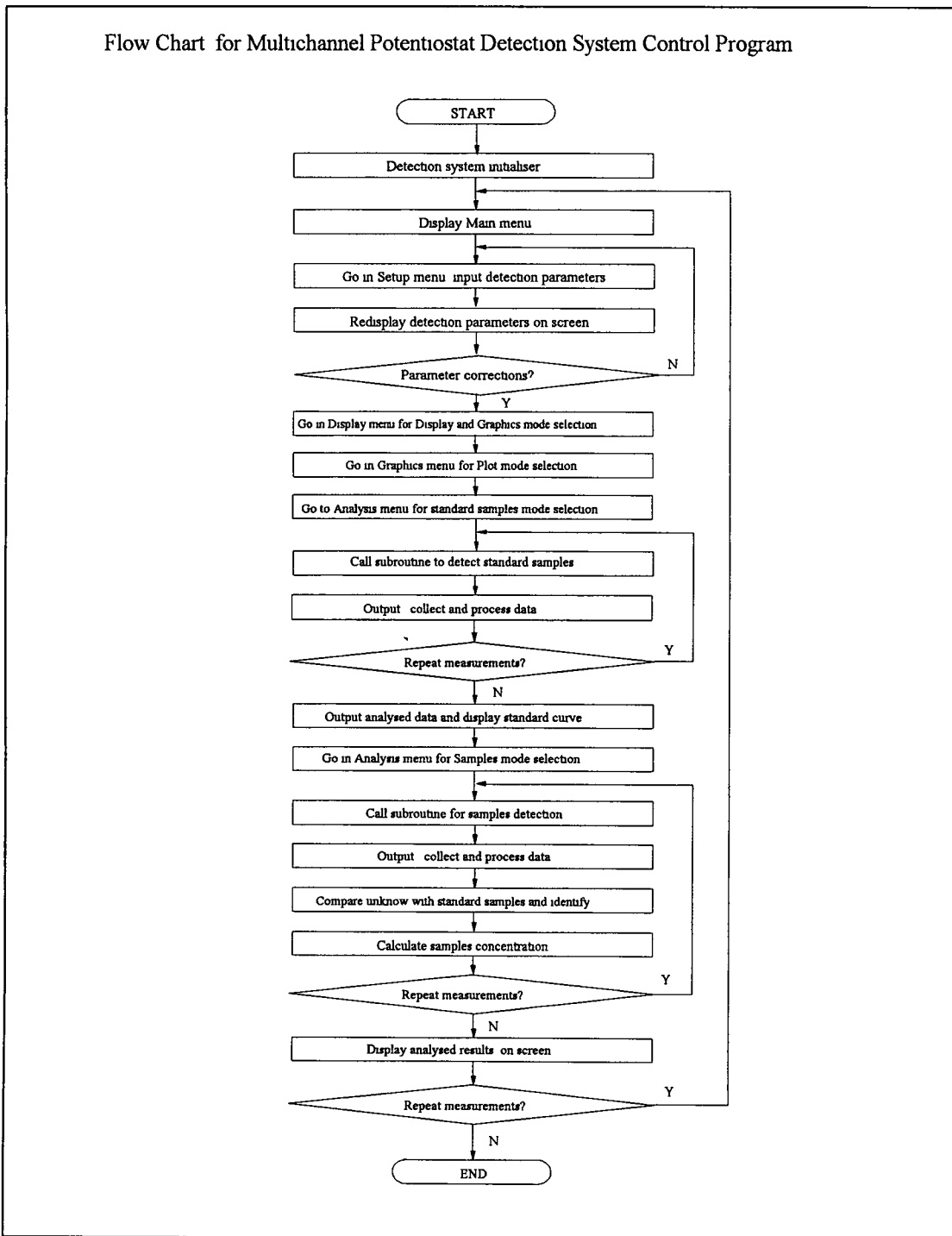


Figure 5-2 The multichannel potentiostat detection system control program flow chart

5.3.3 Initializing Routine

This routine consists of a Basic variable declaration, initialization and Basic setup routines for RTI routine and Assembly-Language Toolbox, system program initialization, and detection system hardware setup

5.3.4 Detection System Program Menu

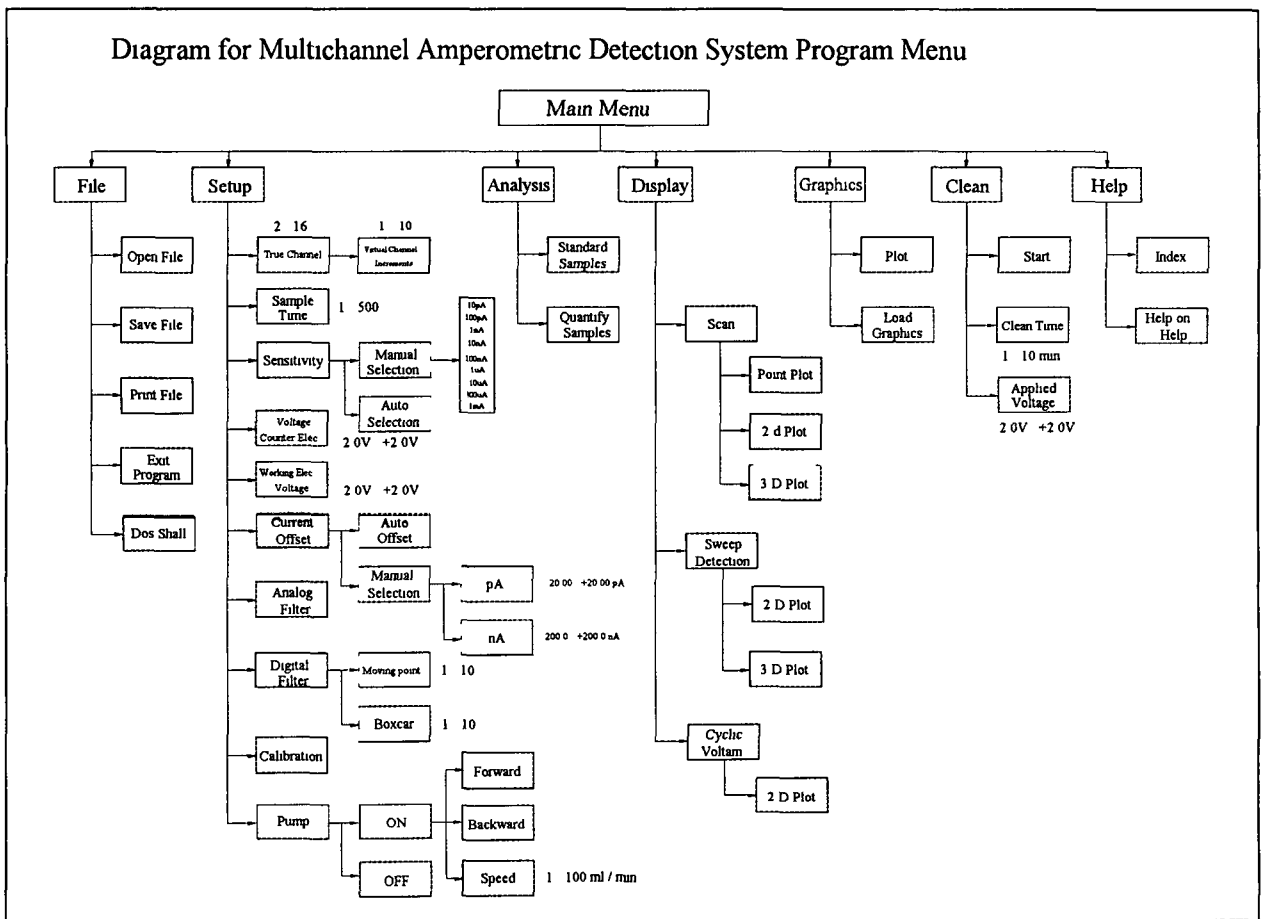


Figure 5 3 The diagram for multichannel amperometric detection system program menu

The diagram for multichannel amperometric detection system program menu is shown in Figure 5 3 As can be seen from the diagram there is a main menu oriented horizontally and from each item in this menu there are sub-menus oriented vertically The window menus were designed to follow this format in that the main menu was presented in a

horizontal format using a routine from the Assembly-Language Toolbox called Barmenu, while the vertical menus were presented in a vertical format using routines from the Toolbox known as VerMenus. The menu driven package includes routines which setup system, analysis samples, archive data to and retrieve data from diskette, display data graphically or in raw form to the screen or printer, and manage system parameters. Included in the main menu is a HELP option which allows the user to access help files on a particular topic. An effort was made to provide flexible, easy to use software requiring minimal training.

Detection System Main Menu

The multichannel Detection System program is the user interface which consists of seven pull-down menus.

File	Setup	Analysis	Display	Graphics	Clean	Help
------	-------	----------	---------	----------	-------	------

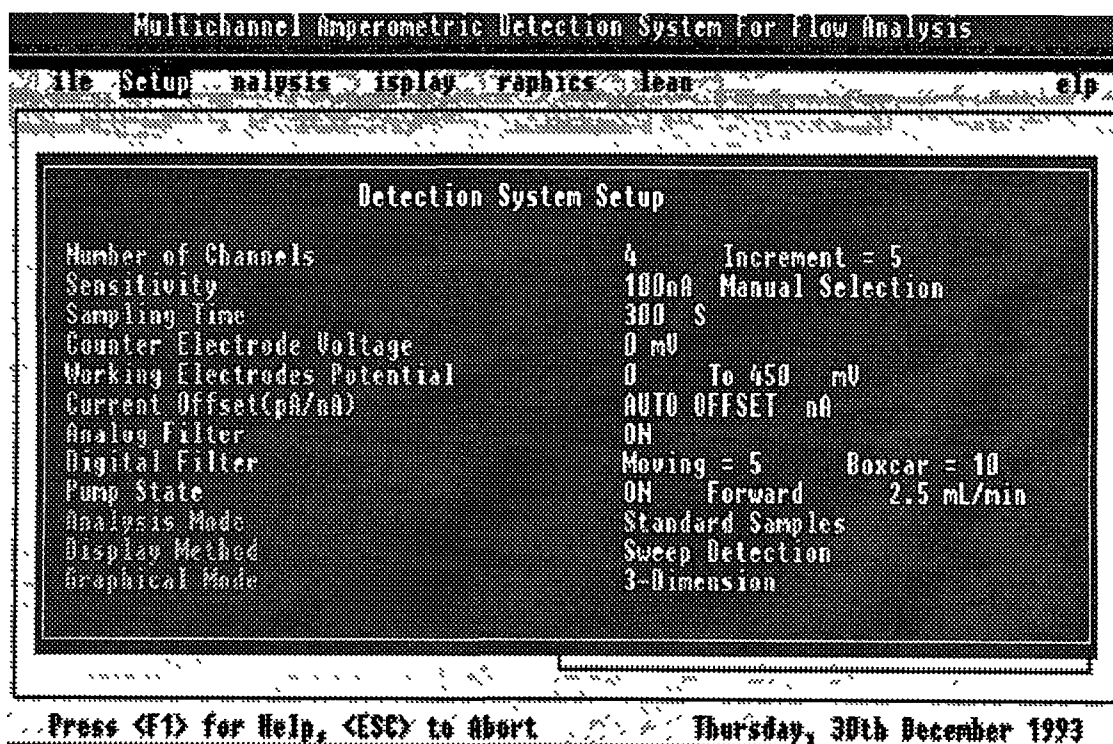


Figure 5.4 The main menu with a Windows style graphical environment on the screen

Figure 5 4 shows the main menu of the multichannel amperometric detection system with a Windows style graphical environment on the screen To activate the menu bar, one can use the Mouse or the HotKey to select the desired option

Detection System Submenu

The multichannel detection system submenu is consists of seven menu bar which contams a lot of different system option

Example

Detection System Setup Command

This command takes the user through a submenu which contains many setup and control of the detection system state to be selected by the user, this setup submenu has ten options, as follows

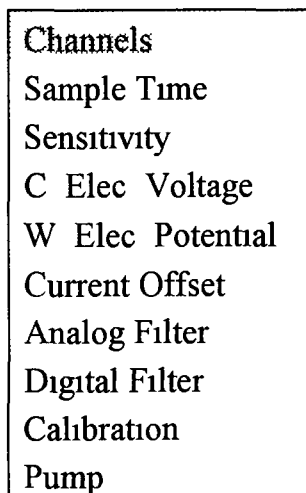


Figure 5 5 shows the **Setup** submenu of the multichannel amperometric detection system with a Windows style graphical environment on the screen

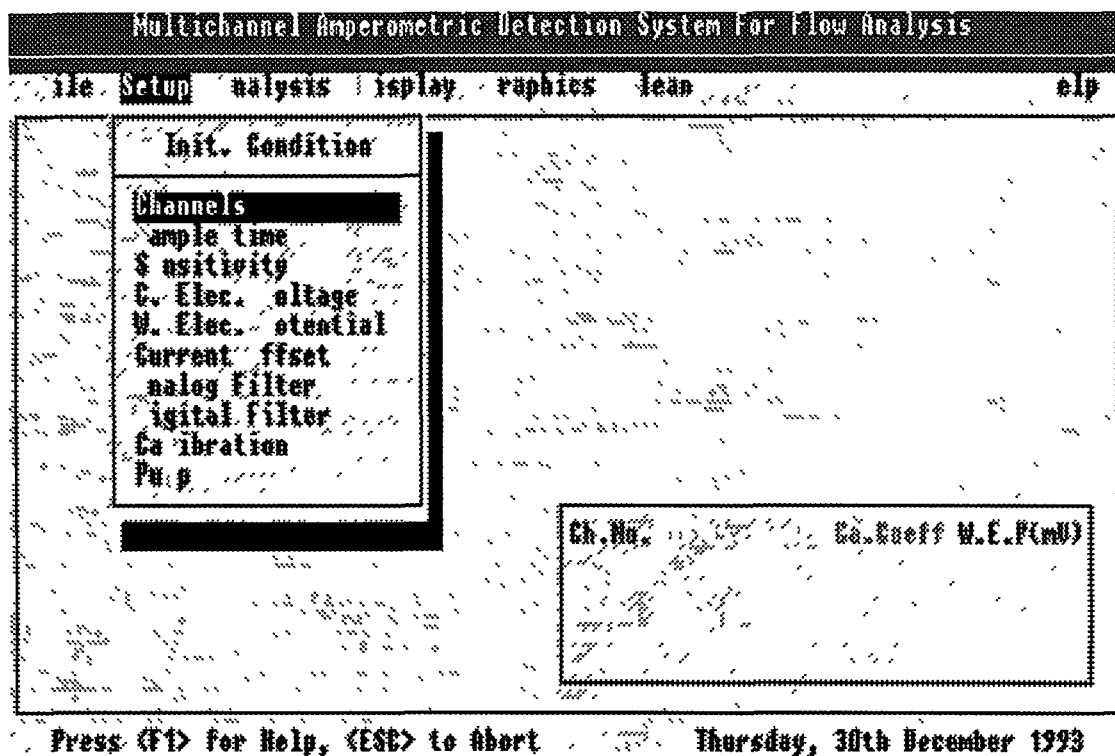


Figure 5.5 The Setup submenu with a windows style graphical environment on the screen

5.3.5 Graphical Display

The graphical representation includes two-dimensional plots of the currents of one or more selected channels vs time (chromatogram/FIA response) or vs potential (hydrodynamic voltammogram, three-dimensional plots of current vs time and potential)

Two-dimensional Graphical Display

For a 2 dimensional on-line display, the 4 electrodes are polarised between 200 mV and 500 mV at a $1\mu\text{A}$ sensitivity. Figure 5.6 shows an eight channel response. A 42.9 mV step is applied to each electrode to generate the 8 electrode response (4 real, 4 virtual channels). Each is represented by a different colour on the display to distinguish clearly between them.

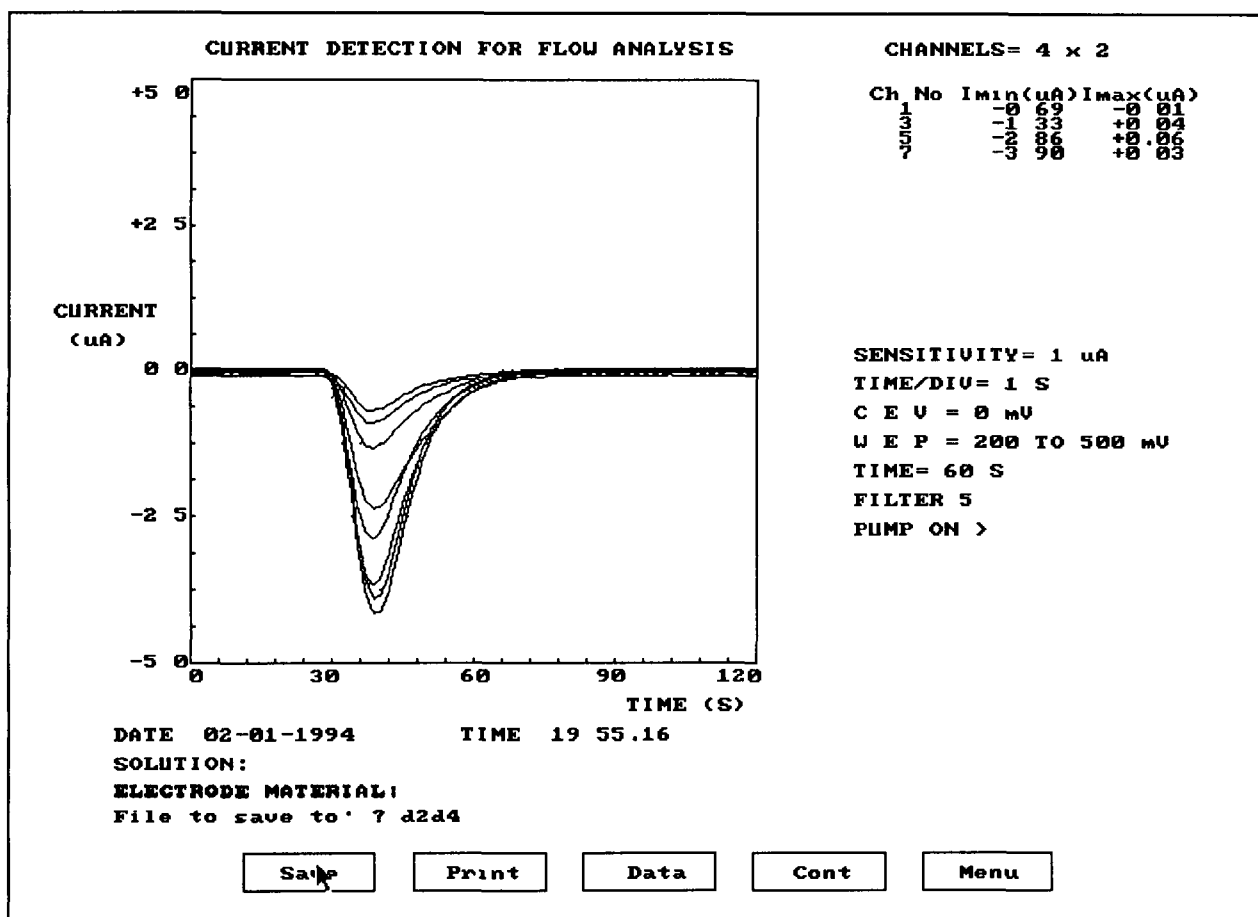


Figure 5.6 On-line display of an injection of uric acid ($2 \times 10^{-3} \text{M}$) in 0.05M phosphate buffer

Three-dimensional Graphical Display

Figure 5.7 shows the on-line display of 3-dimensional hydrodynamic voltammogram of hydroquinone (0.1M) in 0.05M phosphate buffer. Five sequential voltage steps of 15.8 mV are applied at the working electrode array which is polarised in the range -200 to 100 mV to generate a 20 working electrode (4 real, 16 virtual)

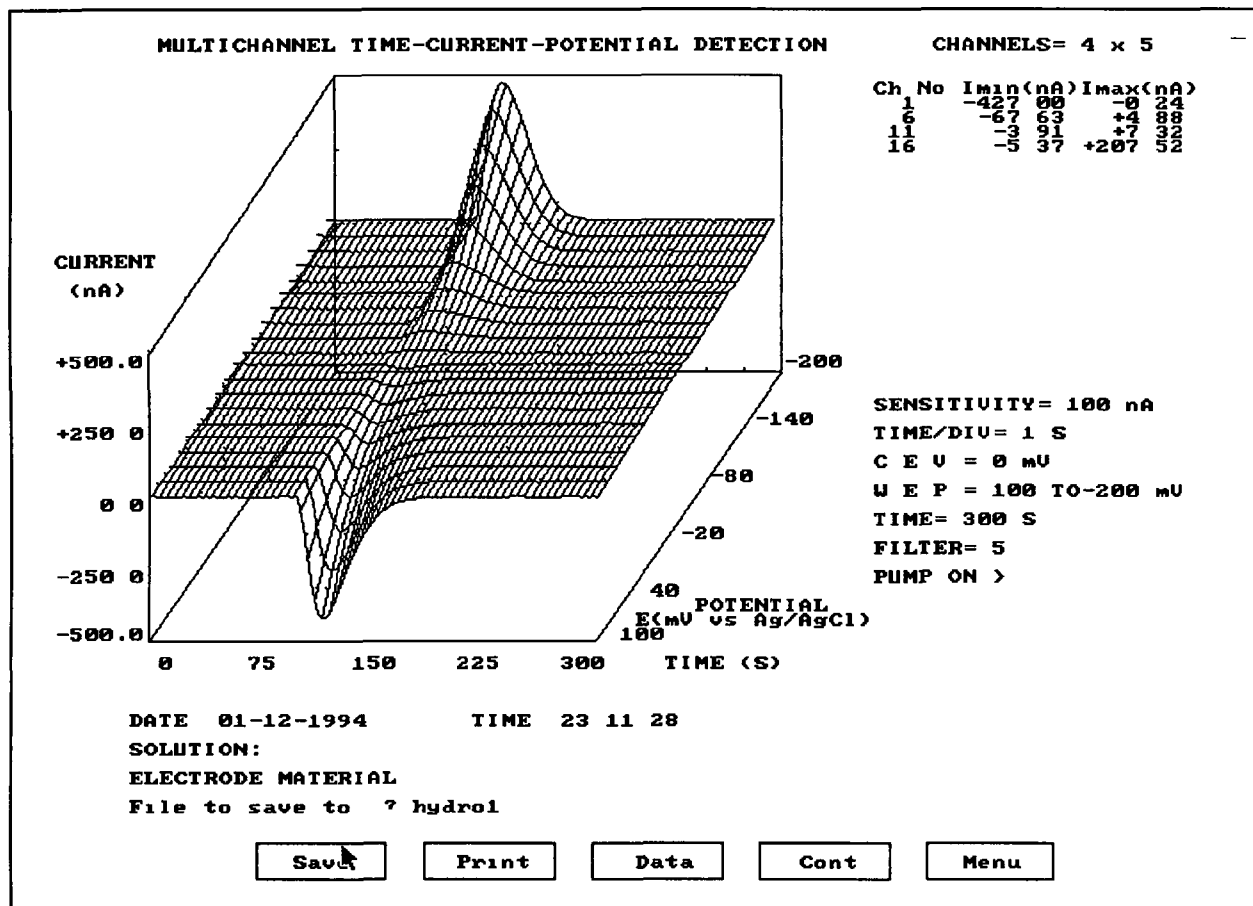


Figure 5 7 On-line display of a 3-dimensional hydrodynamic voltammogram of hydroquinone (0 1M) in 0 05M phosphate buffer Flow rate 0 5 mls/min

5.3.6 Data File Import and Export

In order to store the measured and sampled data for processing and analysis at a later stage, it is important that data files can be loaded, saved and printed In this program, the data files can be stored on a disk in ASCII format for post-run processing, the data file can be loaded on the screen, and the data and graphical results can be presented on a printer

Data File Save

This saves the sampled and processed data and the current document on the screen to a hard disk or a floppy disk. The DOS filenames can have up to eight characters plus an optional three-letter extension.

To save a file

- From the File menu of the detection system program, the user has to choose the SAVE command, then the SAVE dialogue box appears.
- In the FILE name box, the user has to type a name for the file. If the user wants to save the file on a different drive or directory, he has to type the path as part of the filename.

Data file save format

Data is stored in a spreadsheet compatible format (ASCII with "," column delimiter) to facilitate post-run processing with standard applications packages such as Microsoft Excel.

Data File Load

This retrieves a data document from the disk which represents a data file of any detection system measure and sample, and copies it on the screen for analysis. The user can load file by using the OPEN command on the File menu of detection system program.

To load a data file

- From the File menu, the user has to choose OPEN. Then the OPEN dialogue box appears.
- The user then has to type the filename required and press the Enter key. If the file of interest is not on the current drive or directory, the path must be typed as part of the filename.

Data and Graphical Results Print

To print the sampled and processed data and the current document, the user must have a printer connected to or the LPT1 parallel printer port.

5.3.7 Potential Step Sequences

To further improve the voltage resolution of the 3-D voltammogram, a series of potential steps (up to 5) can be applied at the working electrodes, thus generating a 20-channel response. A 150 ms delay time is utilised before the current is sampled to reduce charging current effects. All potential step sequences are software controlled. The software allows the selection of 1-5 potential steps at each working electrode.

5.4 Data Acquisition and I/O Control Routines

5.4.1 Data Acquisition

The purpose of an analogue interface is to convert voltage or other analogue output of an instrument or sensor to a binary form that can be handled by the digital computer. ADC's are characterised by their resolution, dynamic range, and maximum through-put. The resolution of an DAC is defined as the smallest change in an analog signal that can be observed at the digital output. Resolution (R) is determined by the number of bits in the digital signal. 12 bits, 1 part in 4096

$$R = V_{REF} / 2^n - 1 \quad (5.5.1)$$

where n = bit number of the DAC

Thus for an A/D converter with maximum range from -5V to +5V DC and 12 bits of output, the smallest change that can be detected in the digital output is

$$10V / (2^{12} - 1) = 2.442 \times 10^{-3} V$$

Sampling rates are an important consideration with ADC's. The sampling rate is determined by the experimental requirements and whether the ADC and the computer can

accept this rate. The sampling rate can depend both on how much information is required from the analog signal and on what kind of signal processing is planned for the collected data. For theoretical reasons it is necessary to sample a signal with a rate twice as high as the highest frequency component of the signal (Nyquist's Theorem).

The most important characteristics of ADC's are the speed and accuracy of conversion. These parameters are determined by the particular method used to convert the data which can be achieved by a number of methods. Successive approximation is used in analog to digital converter of RTI815 card. It has a fixed conversion time that is the same for any value of analog input.

5.4.2 Analog I/O Routine

The analog-to-digital data acquisition routines acquire the signals by reading from the 16 channel input ports of RTI 815 board. The Analog Input routine with Basic setup and Basic I/O routines are used to write convert command byte for data-acquisition from the 16 channel potentiostat. These routines are provided from the RTI-800 Series software package. The Basic setup routine is used for the QBasic calling order. The Basic I/O routine is used to control the RTI 815 analog I/O port. Before the AING routine is called, execute the appropriate AIN815 setup routine.

Basic Setup Routine	CALL AING815 (Lchan, Board, Chanarr(<i>n</i>), Count, Gam, Erstat%)
Basic I/O Routine	CALL AING (Lchan, Array(<i>n</i>), Erstat%)

where

Lchan is integer expression denoting the logical channel for the AING operation

Board is an integer value that is assigned to the RTI board during the configuration program

Chanarr(*n*) is the name of a user-defined integer array, where *n* is the element number of the array. The first element of this array specifies how many analog channels are in the array, the remaining elements in this array specify the actual channels to be read.

Count is an integer value that specifies the number of readings to be taken. The channel sequence is reiterated until the count is satisfied.

Gain allows you to amplify a low-level signal to a range that may be accurately measured. The following integer values for Gain may be selected: 1, 10, 100, or 500.

Array(*n*) is the name of a user-defined integer array in which the collected data will be stored, where *n* is an element in the array. Make sure that this array is large enough to store the data being collected.

Erstat% is an integer variable in which the error/status code is returned.

The digital-to-analog conversion routines of the RTI 815 board are used to convert twelve bits of digital data into an analog output voltage which is used to control the counter electrode voltage and the pump speed control. These routines are provided from the RTI-800 Series software package. The Basic I/O routine is used to control RTI 815 analog I/O port. Before the AOT routine is called, execute the appropriate AOT815 setup routine.

Basic Setup Routine CALL AOT815 (Lchan, Board, Pchan, Erstat%)

Basic I/O Routine CALL AOT (Lchan, Value, Erstat%)

where

Lchan is integer expression denoting the logical channel for the AOT operation.

Board is an integer value that is assigned to the RTI board during the configuration program.

Pchan identifies the physical (hardware) analog input channel to be sent.

Value is the integer variable in which the analog output value to be sent. The range for value is 0 to 4095 for straight binary coding.

Erstat% is an integer variable in which the error/status code is returned.

RTI 815 Analog Input Routine

This program fragment returns the analog input values from the 16 channel potentiostat using the sixteen analog input channels on the RTI 815 board. The control program is written as

```
Chanarr(0)=16  
Gain=1  
CALL AING815 ( 30, 1, Chanarr(16), 16, Gain, Erstat%)           ' Basic setup
```

```
CALL AING (30, Array(n), Erstat%)
```

Where, Lchan=30 Board=1 Gain=1 Count=16

The RTI 815 board is configured as board 1, and sixteen analog input channels, numbers 1 to 16 are read in the following order 1,2,3, ..., 15,16. AING 815 stores the specified setup information in logical channel 30. AING reads the channels and returns the analog input values in *data_array*.

RTI 815 Analog Output 1 Routine

This program converts a digital value to analog output voltage for setting the counter electrode potential and via channel 1 of analog output (DAC 1) on the RTI 815 board using the AOT routine. The control program is written as

```
CALL AOT815 ( 10, 1, 0, Erstat%)                               ' Basic setup
```

```
CALL AOT (10, Bitout, Erstat%)
```

Where, Lchan=10 Board=1 Pchan=0 Value=Bitout

AOT 815 stores the specified setup information for channel 1 of analog output (DAC 1) operation in logical channel 10. Bitout is the digital value required for obtaining the desired voltage for the counter electrode.

RTI 815 Analog Output 2 Routine

This program converts a digital number to an analog voltage which controlling the pump speed via channel 2 of analog output (DAC 2) on an RTI 815 board using the AOT routine. The control program is written as

```
CALL AOT815 ( 20, 1, 1, Erstat%)           ' Basic setup
```

```
CALL AOT (20, Bout, Erstat%)
```

where Lchan=20 Board=1 Pchan=1 Value=Bout

AOT 815 stores the specified setup information for the analog output 2 operation in logical channel 20. Bout is the digital number which sets the voltage for the pump speed control.

5.4.3 Digital I/O Control Routine

Digital I/O control routines with Basic setup and Basic I/O routines are used to write an 8-bit pattern to a digital output port of an RTI 817 board for controlling the sensitivity selection, the potential of the working electrodes, the input current offset, the current offset extent selector, the analogue filter control, and the pump control. These routines are provided from the RTI-800 Series Software package. Basic setup routine is used for setting the QBasic calling order. The Basic I/O routine is used to control the RTI 817 digital I/O port bytes. Before the DOT routine is called, execute the appropriate DOT817 setup routine.

```
Basic Setup Routine      CALL DOT817 ( Lchan, Board, Port, Erstat%)
```

```
Basic I/O Routine       CALL DOT (Lchan, Value, Erstat%)
```

where

Lchan is integer expression denoting the logical channel for the DOT operation

Board is an integer value that is assigned to the RTI board during the configuration program

Port identifies the 8-bit digital output port to which a value (0-2) will be sent

Value is the integer variable which contains the desired 8-bit output value (0-255) to be sent

Erstat% is an integer variable in which the error/status code is returned

RTI 817 I/O Port 0 Control Routine

This program fragment takes an integer value representing a bit pattern and sends it to digital output port 0 on an RTI 817 board using the DOT I/O routine. In this routine, the digital control byte (Port 0) is used for sensitivity selection, current offset extent ranges control, analog filter control, and the pump control. The control program is written as

```
CALL DOT817 ( 100, 2, 0, Erstat%)           ' Basic setup
```

```
CALL DOT (100, 255-PD-PS-CS-FL-SE, Erstat%)
```

where, Lchan=100 Board=2 Port=0 Value=255-PD-PS-CS-FS-FL-SE

DOT 817 stores the specified setup information for the digital output operation in logical channel 100. DOT sends the digital output specified in value to this channel. The Value is the integer variable which contains the desired 8-bit output value to be sent. This value should specify an integer from 0 to 255. It includes the values of sensitivity selection (SE), analog filter control (FL), current offset extent ranges selection (CS), pump START/STOP control (PS), and pump direction control (PD). The following is the functional description and all the values of the bits contained within the port 0 byte

Port	Byte	Statu	Value	Function Description
RTI 817 I/O Port 0	BIT 0-3	X	ES= 0-15	Analog switches of sensitivity selector 1,2 channel select for sensitivity selection
	BIT 4	0	FL= 0	Analog filter OFF
		1	FL=16	Analog filter ON
	BIT 5	0	CS=0	Input current offset extend select -200 0 to +200 0 nA
		1	CS=32	Input current offset extend select -20 00 to +20 00 nA
	BIT 6	0	FS=0	Peristaltic pump STOP
		1	FS=64	Peristaltic pump START
	BIT 7	0	FD=0	Peristaltic pump direction FORWARD
		1	FD=128	Peristaltic pump direction BACKWARD

RTI 817 I/O Port 1 Control Routine

This program fragment takes an integer value representing a bit pattern and sends it to digital output port 1 on an RTI 817 board using the DOT I/O routine. In this routine, the digital-to-analog data low and high bytes (Port 1) are used together in the conversion of 12-bit digital data into an analog voltage signal for setting the potential of the working electrodes and the input current offset. The digital data is sent to the specified digital-to-analog converter of the DAC unit by first writing the eight least significant data bits to the digital-to-analog data low byte, and then writing the four most significant data bits to the digital-to-analog data high byte. The program is written as

```
CALL DOT817 ( 150, 2, 0, Erstat%)           ' Basic setup

Ds= INT(DA1/2000*2048+2047)AND &HFF
CALL DOT (150, Ds, Erstat%)                 ' Transfer data low byte

Ds= INT((DA1/2000*2048+2047)/256) AND &HF
CALL DOT (150, Ds, Erstat%)                 ' Transfer data high byte
```

where, Lchan=150 Board=2 Port=1 Ds is the digital data low or high byte

DOT 817 stores the specified setup information for the digital output operation in logical channel 150 DOT sends the digital output specified in the variable to this channel Value is the integer variable (between 0 and 255) which contains the desired 8-bit output value to be sent The following is the functional description and all the values of the bits contained within the port 1 byte

Port	Byte	Statu	Value	Function Description
RTI 817 I/O Port 1	BIT 0-7	X	Ds=0-255	DAC units and data bus are used together in the transfer of 12-bit digital data into an analog voltage signal of DAC units for the potential of the working electrodes and the input current offset The digital-to-analog data low and digital-to-analog data high bytes are used together in the transfer of 12-bit digital data to a digital-to-analog converter digital-to-analog data low byte (Port 1 BIT 0-7) and digital-to-analog data high byte (Port 1 BIT 0-3, BIT 4-7 don't cares) for DAC

RTI 817 I/O Port 2 Control Routine

This program fragment takes an integer value representing a bit pattern and sends it to digital output port 2 on an RTI 817 board using the DOT I/O routine In this routine, the Channel Select/Status Control byte (Port 2) is used to select the unit channel address of DAC for the potential of the working electrodes and the input current offset, and to control the status control logic of DAC units for the potential of the working electrodes and the input current offset The control program is written as

```
CALL DOT817 ( 200, 2, 2, Erstat%)           ' Basic setup
CALL DOT817 ( 150, 2, 0, Erstat%)         ' Basic setup

Ds= INT(DA/2000*2048+2047)AND &HFF
CALL DOT (150, Ds, Erstat%)                ' Transfer data low byte
CALL DOT (200, 255-IU-32-CH, Erstat%)      ' Data write input and latch
```

CALL DOT (200, 255-IU-32-16-CH, Erstat%) ' No data transparent
Ds= INT((DA/2000*2048+2047)/256) AND &HF
CALL DOT (150, Ds, Erstat%) ' Transfer data high byte
CALL DOT (200, 255-128-IU-32-CH, Erstat%) ' Data write input and latch
CALL DOT (200, 255-128-IU-32-16-CH, Erstat%) ' Data (12 bit) transparent
CALL DOT (200, 255-IU-32-16-CH, Erstat%) ' No data transparent

where, Lchan=200 Board=2 Port=2 Value=255-LH-IU-LD-WR-CH

DOT 817 stores the specified setup information for the digital output operation in logical channel 200 DOT sends the digital output specified in the variable to this channel Value is the integer variable (between 0 and 255) which contains the desired 8-bit output value to be sent It include the values of DAC units channel selection (CH), DAC chip select and write input (WR), current offset extent ranges selection (CS), DAC units data transparent (LD), and current offset and Potential of the working electrode (IU) The following is the functional description and all the values of the bits contained within the port 2 byte

Port	Byte	Statu	Value	Function Description
RTI 817 I/O Port 2	BIT 0-3	X	CH=0-15	Decoder data input for DAC units channel selection Multichannel amperometric channel selection
	BIT 4	0	WR=0	Decoder enable ($\overline{G1}$, $\overline{G2}$) DAC chip select , write input and data transfer
		1	WR=16	No decoder enable ($\overline{G1}$, $\overline{G2}$) No DAC chip select, no write input and no data transfer
	BIT 5	0	LD=0	DAC A and DAC B DAC latches updated simultaneously from the respective input latches (\overline{LADC})
		1	LD=32	No data transparent (\overline{LADC})
	BIT 6	0	IU=0	DAC A is selected DAC A data input latch transparent for Current offset
		1	IU=64	DAC B is selected DAC B data input latch transparent for potential of working electrodes
	BIT 7	0	LH=0	DAC data low byte (LS) input latch transparent
		1	LH=128	DAC data high byte (MS) input latch transparent

5.5 Data Processing

The objective of data processing is to maximise the information content of an experimental signal. The data processing and representation program has been designed to provide for digital filtering, baseline correction, calibration of the electrode responses, and peak analysis [78-87]. A number of digital filters were used and evaluated in terms of their noise reduction capabilities, and their effect on signal attenuation. The filters investigated included boxcar averaging and moving point averaging.

5.5.1 Baseline Correction

Due to background noise levels that are produced by inherent cell currents and non-zero drift by components of the detection circuit, the resultant baseline is non-zero in nature and subsequently produces deviations in the background signal. If the deviation of the baseline is substantial it results in both detection and display overloads. In order to solve this problem an input current offset facility has been incorporated into each channel. Before the signal is passed to the measurement circuit, the baseline of each channel is corrected by the instrumentation control program. The deviation value of the baseline and the required current offset are computed and the desired current offset for each channel is automatically applied via the DAC unit for that channel.

5.5.2 Digital Filter

The increasing use of computerised instruments has correspondingly increased the importance of software techniques for data acquisition and signal to noise enhancement. Operations such as filtering, linearization and attenuation, formerly accomplished by hardware devices, are now achieved by software resident in the microcomputer component of the instrument. Software operations offer the advantages of flexibility and diversity. For example, a variety of software filters can be implemented by changing computer algorithms, whereas considerable effort may be required to change hardware.

filters. Nevertheless, in situations where the computer cannot execute the required function at a satisfactory rate, implementation with hardware components is necessary.

The minimum hardware units required for software signal-processing functions consists of analogue signal conditioning circuits, analogue-to-digital converter, as well as the microcomputer chips. The rates of sampling the analogue data and of the analogue-to-digital conversions must be fast enough to provide an adequate frequency range to cover the analogue signal and thus ensure minimum loss of information. Although the conversion frequency increases with the sampling rate, the upper frequency limit is determined by the speed of the computer and the memory available for data storage. The minimum frequency required for accurate sampling, known as the "Nyquist frequency", should be twice that of the highest frequency component found in the data set. Each data point requires two co-ordinates, frequency and amplitude. If the sampling occurs at a rate less than the minimum, it is not clear which frequencies correspond to a given amplitude. If the sampling frequency significantly exceeds this minimum frequency, no additional information is transferred and the noise may increase because of the larger frequency bandwidth associated with faster sampling rates. Sampling rates corresponding to the fundamentals and harmonics of known environmental noise frequencies should be avoided.

Once the data is in digital form, a variety of software enhancement techniques may be used to increase the signal-to-noise ratio. Although these software techniques are readily available and widely used, caution should be exercised in their applications. The chemist should understand the advantages of each technique as well as potential problems such as undersampling, oversmoothing, and the time required to apply the technique to a set of data points.

Noise is a central problem in data acquisition and is often difficult to handle. Any electronic system contains (and produces) many types of noise. There are a number of software techniques for the enhancement of the signal to noise ratio. Three of the most commonly used software signal enhancement techniques are boxcar averaging, ensemble averaging, and weighted digital filtering.

5 5 2 1 BOXCAR AVERAGING

In this method a group of closely spaced digital data points depicting a slowly changing analog signal is replaced by a single point representing the average of the group. Since this technique is well suited for applications in which the analogue signal changes slowly with time, boxcar averaging can often be implemented in real time (averaging occurs simultaneously with the acquisition of the data). In this mode of operation, one group (boxcar) of points can be acquired and averaged before the next boxcar of data arrives. The maximum possible enhancement of the S/N ratio is calculated by the following equation

$$S/N = \sqrt{n}(S/N)_0 \quad (5 5 2)$$

where $(S/N)_0$ is the signal to noise ratio of the untreated data and n is the number of points averaged in each boxcar.

5 5 2 2 ENSEMBLE AVERAGING

The technique complements the boxcar method because it can be applied to signals that are changing rapidly. The results of n repeated series of measurements of the same phenomenon are added and the sum is divided by n to obtain an average scan. If each set of measurements is recorded in the same way, the data contained in the measurements will sum coherently, whereas the random noise should average to a value smaller than the enhanced signal. To the extent that n represents a normal statistical distribution, the resulting S/N will be increased by a factor of n over that of a signal scan.

5 5 2 3 SMOOTHING (WEIGHTED DIGITAL FILTERING)

In digital filtering each of the data points to be averaged contributes equally to the calculation of the average. Assigning different weights to points as a function of their

position relative to the central point can produce more realistic filtering. The values of the filtering parameters depends on the mathematical smoothing functions employed, the number of points and their positions relative to the central point in the moving average, and the number of times the data are processed by the smoothing function. Although this signal enhancement technique offers optimum flexibility in the choice of filter algorithms, the possibility of signal distortion is also great. The amount of time involved in weighted digital filtering usually requires that the method be applied after all the data have been acquired, in other words, extensive software digital filtering is not usually performed in real time.

5.5.2.4 DIGITAL FILTER DESIGN FOR DETECTION SYSTEM

A number of digital filters were used for noise reduction both on-line and off-line. Boxcar averaging, and moving point averaging, a combination of both with variable window sizes were available in real time.

The boxcar averaging is defined by the formula

$$S_n = \frac{1}{n} \sum_{k=1}^n D_k \quad (5.5.3)$$

where, S_n is boxcar averaging values, D_k are input data of one group (boxcar), and the n is the number of points averaged in each boxcar.

The moving point averaging is defined by the formula

$$Y_n = \sum_{k=-n}^n C_k U_{n-k} \quad (5.5.4)$$

where, the coefficient C_k are the constants of the filter, the U_{n-k} are the input data, and the Y_n are the outputs that are moving point averaging.

The output Y_n is the sum of all the products $C_k U_{n-k}$. Having computed one value, one strip, say the coefficient strip, is moved one space down, and the new set of products is computed to give the new output Y_{n+1} . Each output is the result of adding all the products formed after displacement of the two zero-subscripted terms.

Seven point Savitzky-Golay moving point averaging was available for post-run application in Excel if required. All filtering regimes were carefully selected to minimise any signal attenuation.

5.5.3 Normalisation of the Signals

One of the problems arising with these arrays was that all the electrodes give a slightly different response under the same conditions, hence it was required to normalise every electrode before starting an analysis. The method used to achieve this was to prepare solutions of known concentration, to inject them, and to assess the response in terms of peak height.

Normalisation of the electrode response involves multiplying the response of each channel by a weighting factor to compensate for inherent differences in the working electrode surfaces. The weighting factor is calculated with respect to the channel with the best average response. The software is programmed to normalise the array with respect to the array average. Each data point is then multiplied by this factor before it is displayed on screen.

The software is designed to normalise the array by multiplying the individual electrode responses with a weighting factor which is calculated using the following equation:

$$W_{F(n)} = 1 + \frac{R_{AV} - R_{E(n)}}{R_{E(n)}} \quad (5.5.4)$$

where, $W_{F(n)}$ = weighting factor for each channel, $R_{(av)}$ = averaged array response, and $R_{E(n)}$ = individual electrode response.

5.5.4 Peak Analysis

The peak analysis section of the software calculates either the maximum or minimum peak current values, retention time, peak heights, and peak areas if required when performing quantitative work

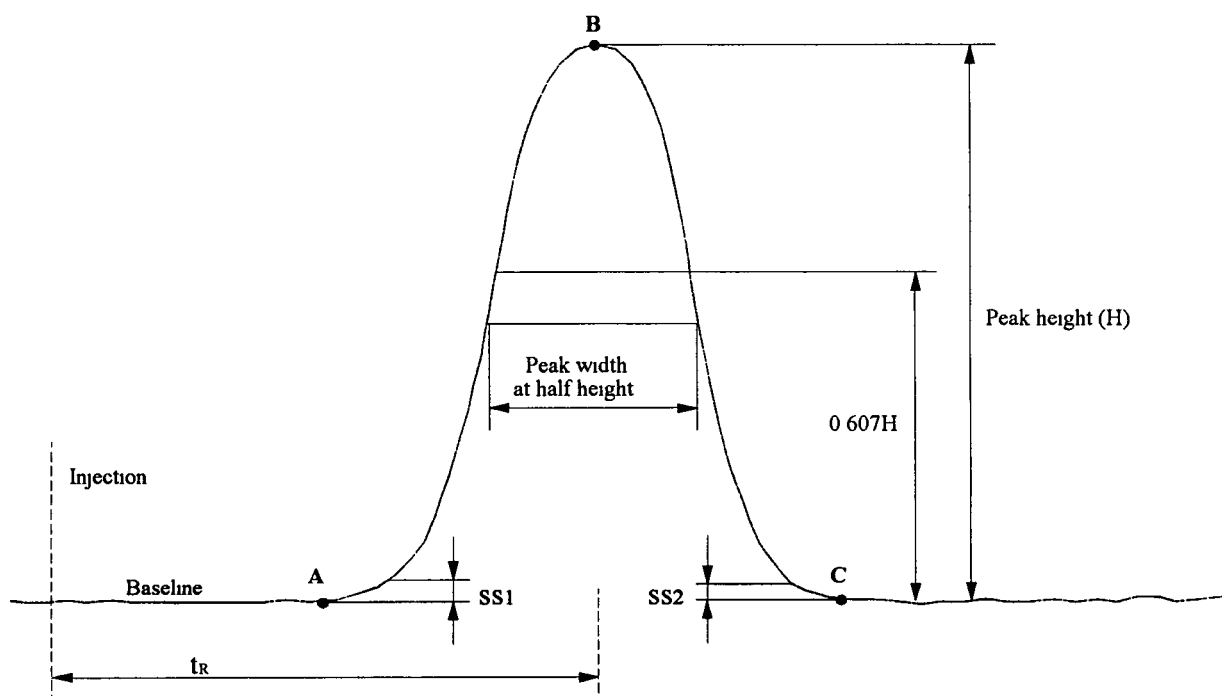


Figure 5 8 Evaluation of a peak t_R is retention time SS1 and SS2 are threshold value for peak determination

Peak Determination

The peak determination is important and essential in the peak analysis The peak determination flow chart is shown in Figure 5 9 The steps involved in peak determination are as follows

- Front valley determination (point A) (Figure 5 8),
- Summit determination (point B),
- Behind valley determination (point C)

Peak Determination Flow Chart

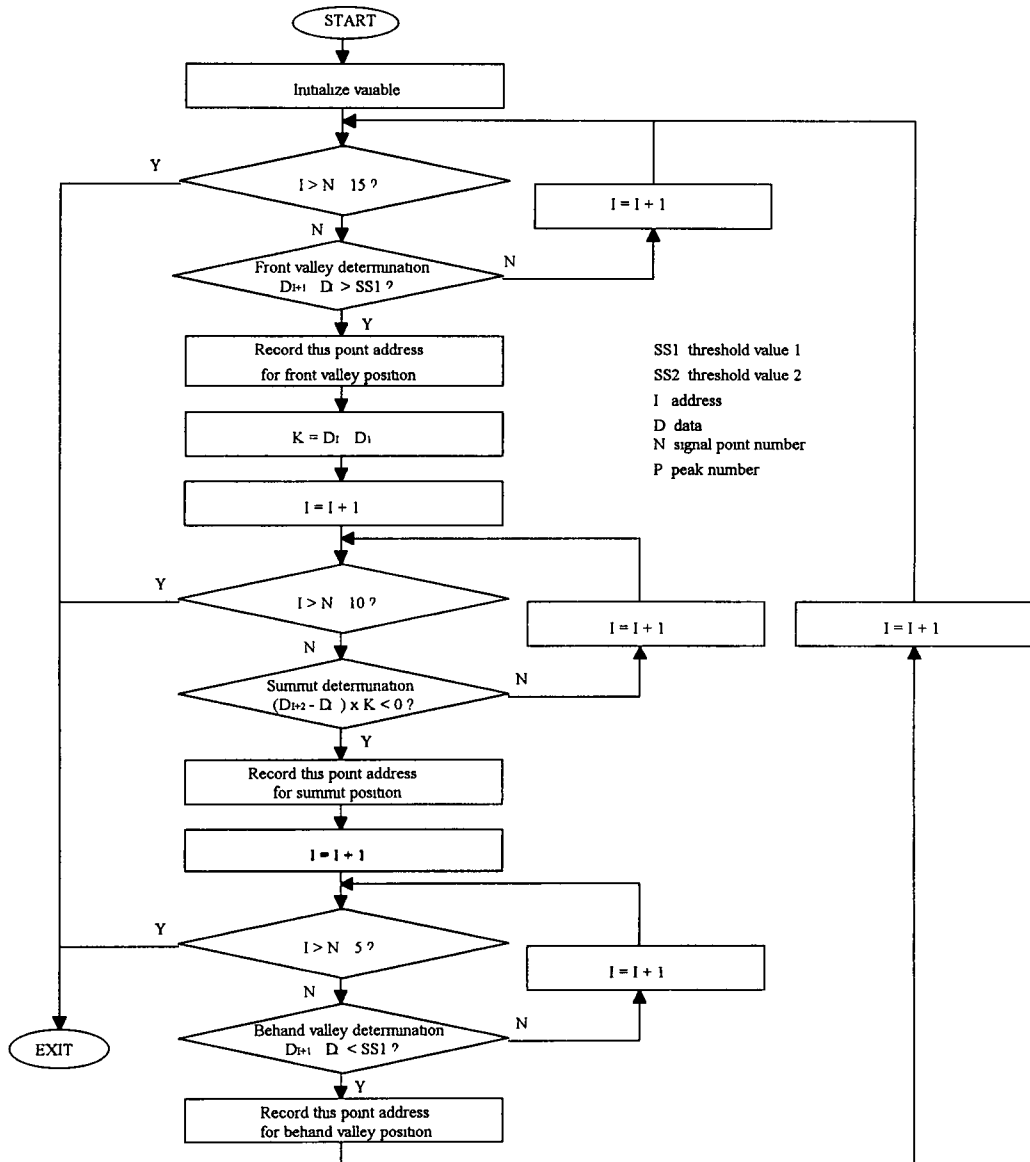


Figure 5 9 The flow chart for peak determination

Computing Peak Height

The point at the maximum concentration of any FIA peak is known as the peak maximum and the distance between this peak maximum and a line joining the base of the peak by extrapolation of the baseline is the peak height (H) (Figure 5 8)

CHAPTER 6

DESIGN OF FLOW CELL AND MULTI-ELECTRODE ARRAYS

6.1 Introduction

For optimal amperometric detection, several flow cell parameters are important such as the cell resistance and capacitance. These are critical to good potential control at any particular electrode and the degree of cross-talk between the working electrodes is important at low analyte concentrations. The flow rate dependent delay in linear flow cells between the working electrodes due to the spatial separation must be known in order to relate the downstream current to the upstream potential.

When designing and using electrochemical detectors, three principal problems must be solved

- 1 The working electrode material must function in a suitable potential range with any residual current and noise being low and constant. The kinetic parameters of the analyte electrode reaction should be favourable and free of interferences from adsorption effects.
- 2 The measuring cell must be constructed with hydrodynamic conditions permitting sensitive and reproducible measurements.
- 3 A suitable measuring technique must be chosen from the point of view of sensitivity of measurement, accuracy and reproducibility, selectivity, and ease of signal handling.

The design and evaluation of the flow cell utilising an array of independently controlled electrodes in conjunction with amperometry, has been investigated for application to flowing solution analysis. Two basic flow cell bodies were used in this work

- A linear flow cell
- A radial flow cell

6.2 Design and Fabrication of Flow Cell

A schematic of the linear flow cell is shown in Figure 6.1. It consists of four main components:

- the cell base (containing the planar electrode array),
- the stainless-steel cell body (counter electrode),
- a thin flow directing spacer,
- the reference electrode holder

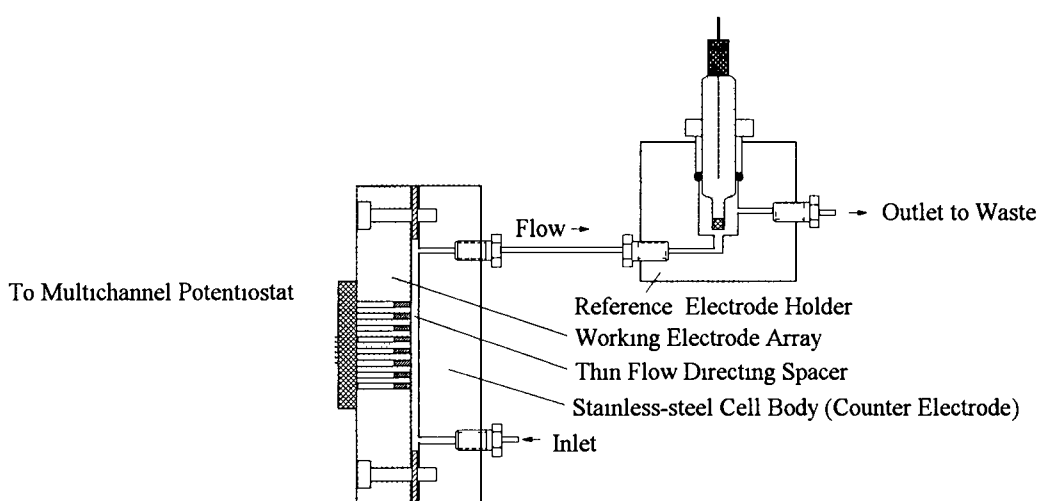


Figure 6.1 Schematic diagram for main components of flow cell

6.2.1 Multi-electrode array

The working electrode array was constructed from glassy carbon rods 5 mm in length (ϕ 1 mm) which were sealed into 1 mm diameter holes in a perspex holder of suitable dimensions. The glassy carbon electrodes were sealed in position with silver loaded epoxy (RS). An 8 pin chip holder with the legs positioned in the correct spatial arrangement was embedded in the epoxy to act as a connector for signal wires. The joints were checked with a multimeter to ensure that electrical contact had been established.

The analogue input lines from the I/E units of the detection system were connected to the chip holder for electrode polarisation and signal measurement

6.2.2 Flow Cell body (Counter electrode)

The main body of each flow cell was fabricated from stainless steel. For the linear flow cell (Figure 6.2), inlet and outlet holes (ϕ 1 mm) were drilled into the stainless steel block with a spatial distance between them slightly larger than the maximum separation of the array. The inlet and outlet holes were drilled 3.4 mm and tapped with an M5 tap compatible with standard HPLC connections. All surfaces were ground with a horizontal grinder to obtain a high precision finish. Finally the stainless-steel body was polished with silicon carbide grade 1200 to a final mirror finish. The flow cell surface was checked to ensure planar continuity without which laminar flow conditions may be disrupted.

6.2.3 Thin Flow Directing Spacer

A spacer shaped from an acetate sheet was placed between the array and the stainless steel body. The flow cell assembly was together with 4 hexagonal stainless steel screws ensuring correct positioning of the spacer. The stainless steel body of the flow cell acted as the counter electrode and was electrically isolated from the working electrode array by the spacer.

6.2.4 Reference Electrode Holder

The outlet from the cell was connected to the reference (Ag/AgCl) holder via stainless steel tubing from which the sample stream flowed to waste.

A commercial Ag/AgCl reference supplied from EG&G (Princeton Applied Research) was utilised for all experimental procedures. A holder for the electrode was constructed using a flow controller valve from a pump. The assembly was connected downstream to the flow cell. One inlet was utilised with the linear flow while two were used with the radial flow cell. The outlet of the assembly was connected to the waste collection vessel with Teflon tubing.

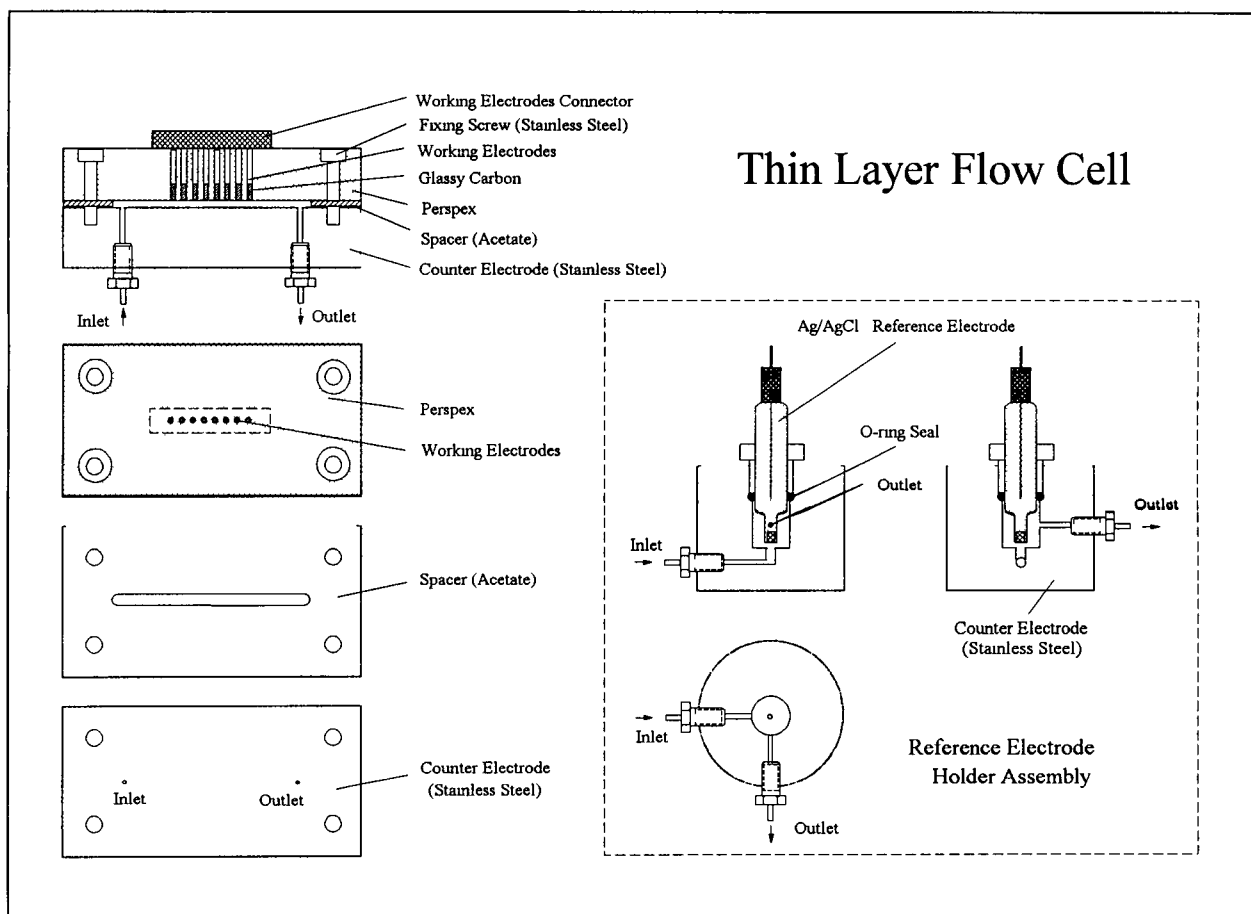


Figure 6 2 Expanded linear flow cell schematic

6.3 Design and Fabrication of Radial Flow Cell

6.3.1 Design and Construction of Radial Flow Cell

Design and construction of radial flow cell is shown Figure 6 3

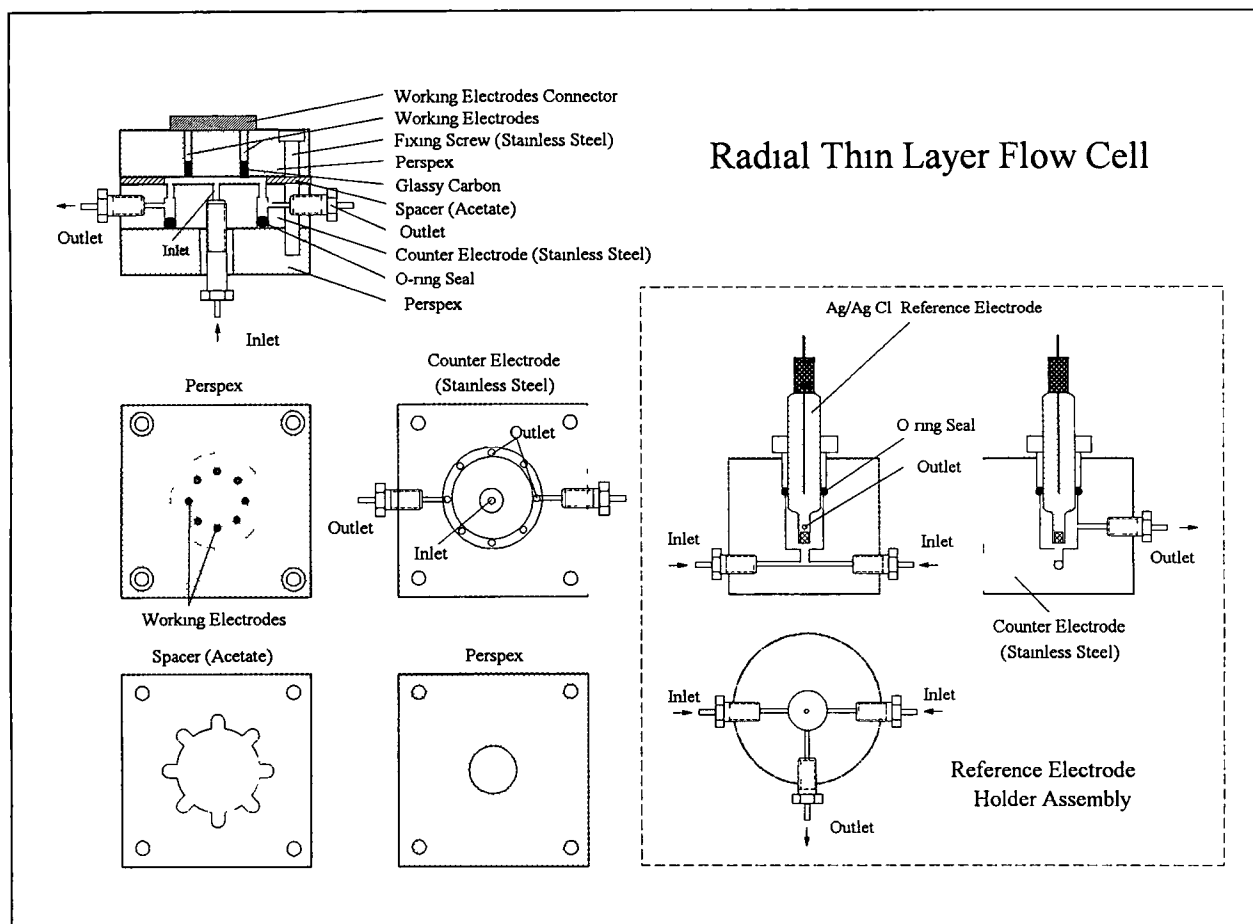


Figure 6 3 Expanded radial flow cell configuration

6.3.2 Production and Assembly

The same method of fabrication as described for the linear flow cell was utilised in the construction of the radial flow cell. The electrodes were placed in a circular configuration of diameter 9 mm. A central inlet of diameter 1 mm was drilled in the stainless steel

body On the reverse side, a trench of outside diameter 17 mm, inside diameter 13 mm and depth 4 mm was machined Two holes of diameter 1mm were drilled horizontally into the trench to which the outlets were connected They in turn were connected to the reference holder assembly Outlet holes (total 16) were drilled in a circular fashion into the trench, this allowed provision for a 16 working electrode array where each electrode would have its own outlet This approach was adopted in an effort to ensure that similar laminar flow conditions were achieved at each working electrode An O-ring seal was pressed into the trench creating a water tight seal and a cavity for fluid collection of suitable dimensions The assembly was held together as previously described The cells were placed in a Faraday cage to reduce the effect of noise pick-up from environmental sources

CHAPTER 7

FLOWING SOLUTION ANALYSIS

7.1 Experimental

7.1.1 Chemicals

All chemical used were of analytical grade. Deionised water for the preparation of aqueous solutions was obtained by passing distilled water through a Milli-Q water purification system (Millipore). Ascorbic acid was obtained from BDH Chemicals. Potassium ferricyanide was obtained from May and Baker Ltd, dipotassium hydrogen phosphate from Riedel-de Haen and potassium dihydrogen orthophosphate from BDH Chemicals. Hydroquinone was purchased from the Aldrich Chemical Co. All electroactive solutions were freshly prepared each day and degassed for 10 minutes with nitrogen prior to use.

7.1.2 Flow-Injection Analysis System

The FIA system was composed of an ACS Model 351 isocratic pulse-free pump, an injector port with a 20 μ l fixed sample loop (Rheodyne 7125), PTFE tubing (200 mm x 0.25 mm id) and stainless tubing (0.009" mm id). The carrier stream was 0.05M phosphate buffer, pH 7.4. Flow rates in the range 0.5-1.0 ml min⁻¹ were used for the flow injection studies.

7.1.3 Working Electrode Preparation

Newly constructed glassy carbon arrays were initially prepared by polishing with 1200 grade silicon carbide paper. The array was then polished with 6 μ m alumina (Metrohm), followed by diamond paste (Kemet) on polishing pads for 3 minutes respectively, before being sonicated in deionised water for 3 minutes to remove any particulate matter. The array was then assembled in the flow cell, and software controlled pre-treatment potentials applied. The conditioning program consisted of the application of both ± 1 0V (vs Ag/AgCl) potentials for 3 minute periods. The array was electrochemically cleaned on a daily basis before commencing work. The array was only polished when a significant reduction in sensitivity was observed.

7.2 Results and Discussion

7.2.1 Linearity

The linearity of the amperometric array was evaluated by injection of standard solutions of potassium ferricyanide in the concentration range 10^{-1} - 10^{-7} M. The injections were repeated 5 times at each concentration. Samples were injected using both flow cell designs. Table 7.2 shows data calibration of log-log concentration vs current peak height for linear and radial flow cells. The radial flow cell yielded a plot with a slope of 0.998 and a correlation coefficient of 0.9992. A slope of 0.997 and a correlation coefficient of 0.9985 were obtained for the linear flow cell. The limit of detection was calculated to be 2×10^{-7} M (4 pmoles injected) (S/N=3). At concentrations of 10^{-1} M and greater the error or deviation in the response signal increases significantly as the electrode surface approaches saturation. Best operating conditions were achieved between 10^{-2} - 10^{-4} M. Plots of log-log concentration vs current peak height for linear and radial flow cells are shown in Figure 7.1.

RADIAL FLOW CELL					LINEAR FLOW CELL				
Concentration (M)		Current (A)			Concentration (M)		Current (A)		
	Log	Av	Log	SD		Log	Av	Log	SD
10^{-7}	-7	2.476×10^{-11}	-10 606	0.313×10^{-11}	10^{-7}	-7	1.501×10^{-11}	-10 824	0.256×10^{-11}
10^{-6}	-6	2.400×10^{-10}	-9 620	0.167×10^{-10}	10^{-6}	-6	1.544×10^{-10}	-9 811	0.169×10^{-10}
10^{-5}	-5	2.423×10^{-9}	-8 616	0.246×10^{-9}	10^{-5}	-5	1.184×10^{-9}	-8 927	0.140×10^{-9}
10^{-4}	-4	2.048×10^{-8}	-7 689	0.060×10^{-8}	10^{-4}	-4	0.885×10^{-8}	-8 053	0.036×10^{-8}
10^{-3}	-3	2.204×10^{-7}	-6 657	0.068×10^{-7}	10^{-3}	-3	0.801×10^{-7}	-7 096	0.012×10^{-7}
10^{-2}	-2	2.348×10^{-6}	-5 629	0.050×10^{-6}	10^{-2}	-2	0.689×10^{-6}	-6 162	0.052×10^{-6}
10^{-1}	-1	1.267×10^{-5}	-4 897	0.106×10^{-5}	10^{-1}	-1	0.272×10^{-5}	-5 565	0.046×10^{-5}

Table 7 2 1 Linearity of the amperometric array are evaluated by injection of standard solutions of potassium ferricyanide in the concentration range 10^{-1} - 10^{-7} M for linear and radial flow cells

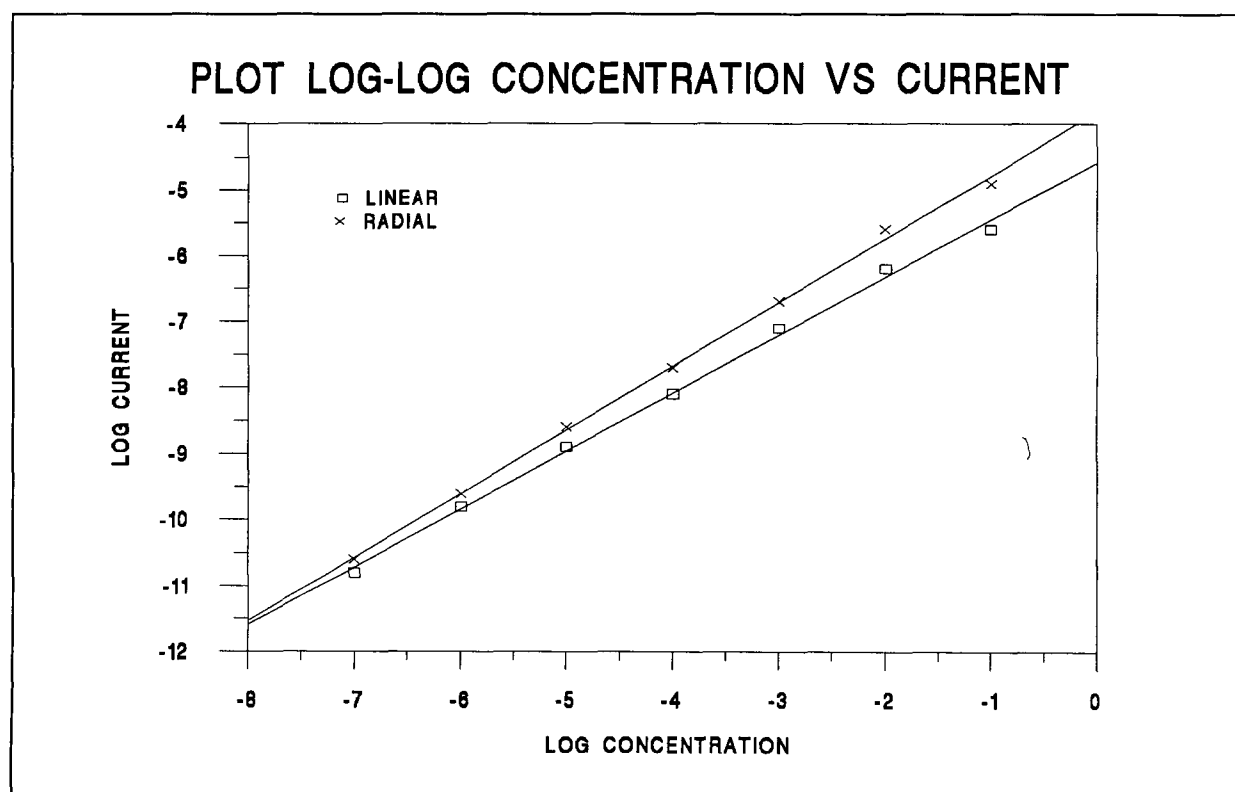


Figure 7 1 Plot of log-log concentration vs current for linear and radial flow cells Flow rate 0.4ml/min, carrier stream 0.05M phosphate buffer (pH 7.4), working electrode potential 0.0 mV vs Ag/AgCl

7.2.2 Filters

The effect of analogue and digital filtering on the signal were investigated to evaluate their respective merits and performances. Boxcar averaging and moving point averaging digital filters were utilised in conjunction with an analogue third order low pass Bessel filter which was used on-line. The results obtained are summarised in Table 7.2.2

Filter type (no analogue filter)	Relative Standard Deviation	Theoretical Prediction	Filter type (analogue filter)	Relative Standard Deviation	Theoretical Prediction
no digital filters	15.6	-	no digital filters	6.4	-
Boxcar averaging	5.9	4.8	Boxcar Averaging	4.5	2.0
Moving Point Av	7.3	7.0	Moving Point Av	5.7	2.9
Boxcar Av & Moving Point Av	5.4	2.2	Boxcar Av & Moving Point Av	2.9	0.9

Table 7.2.2 Radial flow cell, Flow rate 0.4 ml/min, Carrier stream 0.05M phosphate buffer
Concentration 4×10^{-6} M potassium ferricyanide. The effects up of various filters
on the electrode responses are presented with the theoretically predicated values

where,

$$\text{Theoretical Prediction} = \sqrt{n} \left(\frac{s}{n} \right)_0$$

$$= \sqrt{n_1} \sqrt{n_2} \left(\frac{n}{s} \right)_0$$

$$\text{Relative Standard Deviation} = \frac{\overline{SD}}{\overline{X}} \times 100\%$$

The most satisfactory results were obtained with a combination of analogue filtering and digital both filters (2.9% RSD). The major problem associated with digital filtering on-line is that of signal attenuation. The effects of the various digital filters are presented in Table 7.2.3. A combination of boxcar averaging and moving point averaging results in a signal attenuation of 22.4% but conversely results in a 55% reduction in the noise. The improvements in the S/N ratio are not as large as predicted theoretically and therefore would indicate that the noise level in the system has a large random characteristic which is difficult to filter out completely. The value of good hardware filtering is also demonstrated. Activation of the hardware filter results in a 59% reduction in the noise level observed in the response signal.

Digital Filter Type	% Attenuation (Array Average)
Boxcar Averaging [10]	5.1
Moving Point Averaging [5]	8.1
Boxcar[10] + Moving Point Av [5]	22.4

[] number of data points in each window

Table 7.2.3 The effect of two digital filters and their additive effect on signal attenuation is outlined

7.2.3 Electrode Response Weighting

To compensate for differences in the planar electrode surfaces a software normalisation routine was utilised. Table 7.2.4 shows a comparison between data (radial flow cell) which was digitally filtered using moving point averaging (window size 5) without any normalisation. The second set of data was filtered as before but the response of each electrode weighted to reduce the deviation of the responses.

The benefit of normalisation is clearly evident from the major improvement obtained

Conc. (M) Potassium ferricyanide	Unweighted Average % Error	Weighted Average % Error
10 ⁻⁷	13.3	6.3
10 ⁻⁶	18.6	5.6
10 ⁻⁵	18.5	2.9
10 ⁻⁴	17.4	2.3
10 ⁻³	19.1	1.2
10 ⁻²	19.7	1.7
10 ⁻¹	16.1	0.7

Table 7.2.4 Radial flow cell, Flow rate 0.4mls/min, Carrier stream 0.05M phosphate buffer

7.2.4 Array Normalisation Procedure Evaluation

The array was statistically investigated to evaluate both the necessity and effect of an on-line array normalisation procedure. Standard solutions of potassium ferricyanide in the concentration range 10⁻⁷-10⁻¹M were injected 4 times and the resulting data was statistically analysed. A sample data analysis tables are shown in Table 7.2.5 and Table 7.2.6. The plots of log-log concentration vs current for electrode array of radial flow cell front responses with and without normalisation are shown in Figure 7.2(a) and Figure 7.2(b). This standard format was adopted for all statistical analysis thus allowing clear comparison between the data sets. Both the inter-electrode and inter-injection RSD's were compared for array responses with and without normalisation. The results for the unnormalised radial flow cell data are presented in Figure 7.3. The results indicate that

- the RSD between the electrodes is independent of concentration
- the RSD between the electrodes is at least 3-4 times that of the RSD for a single electrode with multiple injections

NO NORMALISATION				RADIAL FLOW CELL			
CONCENTRATION 1E-7M				CURRENTx 1E-12A			
INJECTION NO	1	2	3	4	MEAN	STDEV	RSD
	17 93	23 14	22 43	16 96	20 115	3 121864	15 52008
	16 87	25 64	20 23	17 81	20 1375	3 931915	19 52534
	19 91	21 36	18 97	19 76	20	0 996025	4 980127
	19 01	22 98	18 99	17 95	19 7325	2 220876	11 25492
MEAN	18 43	23 28	20 155	19 99625			
STDEV	1 141315	1 530163	1 40914	1 320649			
RSD	7 150717	7 589693	8 073106	6 498877			
CONCENTRATION 1E-6M				CURRENTx 1E-12A			
INJECTION NO	E1	E2	E3	E4	MEAN	STDEV	RSD
	185	253	191	186	203 75	32 93807	16 16593
	194	276	187	168	206 25	47 77988	23 166
	183	247	175	189	198 5	32 83799	16 54307
	181	261	180	176	199 5	41 05687	20 57989
MEAN	185 75	259 25	183 25	179 75			
STDEV	5 737305	12 55322	7 135592	9 604686			
RSD	3 088724	4 842129	3 893911	5 343358			
CONCENTRATION 1E-5M				CURRENT x 1E-9A			
INJECTION NO	E1	E2	E3	E4	MEAN	STDEV	RSD
	1 83	2 66	1 86	1 77	2 03	0 421663	20 77159
	1 89	2 49	1 95	1 82	2 0375	0 306309	15 03355
	1 78	2 58	1 83	1 79	1 995	0 390598	19 57884
	1 76	2 62	1 84	1 76	1 995	0 41837	20 97092
MEAN	1 808982	1 808982	1 808982	1 808982			
STDEV	0 058023	0 072744	0 054772	0 026458			
RSD	3 196859	2 811356	2 928998	1 482214			
CONCENTRATION 1E-4M				CURRENT x 1E-9A			
INJECTION NO	E1	E2	E3	E4	MEAN	STDEV	RSD
	19 58	25 91	18 83	17 75	20 5175	3 672632	17 9
	18 62	24 32	18 04	17 27	19 5625	3 219507	16 45754
	18 11	25 22	17 92	17 31	19 64	3 735621	19 02048
	18 91	25 45	17 98	17 56	19 975	3 693332	18 48977
MEAN	18 805	25 225	18 1925	17 4725	19 92375		
STDEV	0 531249	0 578554	0 370498	0 194984			
RSD	3 262074	2 648392	2 351597	1 288585			

CONCENTRATION 1E-3M		CURRENT x 1E-9A						
INJECTION NO	E1	E2	E3	E4	MEAN	STDEV	RSD	
1	193 82	284 77	211 84	208 1	224 6325	40 83667	18 17932	
2	189 45	283 74	203 28	201 1	219 3925	43 32583	19 74809	
3	196 3	293 95	213 15	209 97	228 3425	44 34496	19 42037	
4	191 8	285 54	207 12	204 3	222 19	42 75485	19 24247	
MEAN	192 8425	287	208 8475	205 8675				
STDEV	2 9158	4 691645	4 525773	3 958142				
RSD	1 512011	1 63472	2 167023	1 922665				

CONCENTRATION 1E-2M		CURRENT x 1E-6A						
INJECTION NO	E1	E2	E3	E4	MEAN	STDEV	RSD	
1	1 96	3 05	2 32	2 15	2 37	0 476585	20 10907	
2	1 98	3 04	2 35	2 17	2 385	0 462061	19 37361	
3	1 96	3 01	2 35	2 11	2 3575	0 463708	19 66948	
4	1 99	3 06	2 31	2 13	2 3725	0 476681	20 09194	
MEAN	1 9725	3 04	2 3325	2 14				
STDEV	0 015	0 021602	0 020616	0 02582				
RSD	0 760456	0 710608	0 883838	1 206537				

CONCENTRATION 1E-1M		CURRENT x 1E-6A						
INJECTION NO	E1	E2	E3	E4	MEAN	STDEV	RSD	
1	8 86	12 82	10 89	9 93	10 625	4 804557	15 82977	
2	8 67	12 68	10 67	9 89	10 4775	4 997375	16 06565	
3	8 84	12 79	10 96	9 72	10 5775	5 201824	16 18792	
4	8 72	12 75	10 88	9 86	10 5525	5 314574	16 20615	
MEAN	8 7725	12 76	10 85	9 85				
STDEV	0 09215	0 060553	0 125167	0 091287				
RSD	1 050444	0 474553	1 153609	0 926773				

Table 7 2 5 Statistical analysis of electrode array responses for 4 repetitive injections of potassium ferricyanide Both the inter-electrode and the individual electrode RSD's are calculated The data is presented here without normalisation

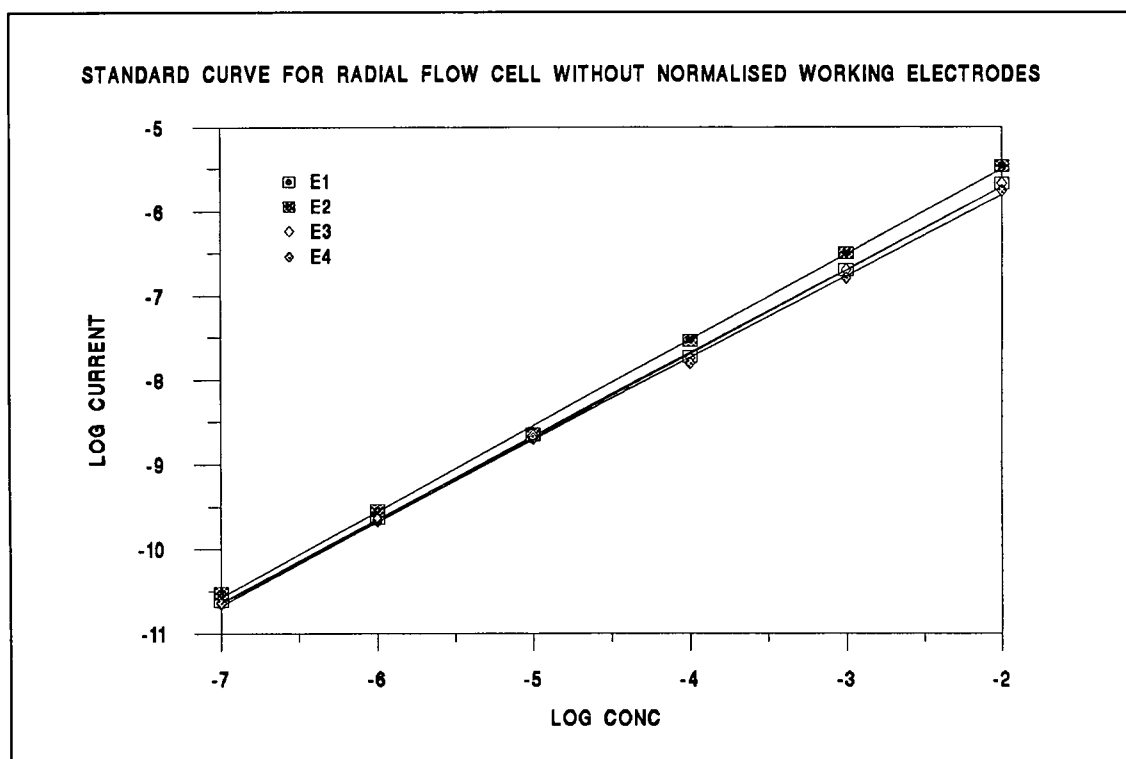


Figure 7 2(a) Plot of log-log concentration vs current for electrode array of radial flow cell responses without normalisation

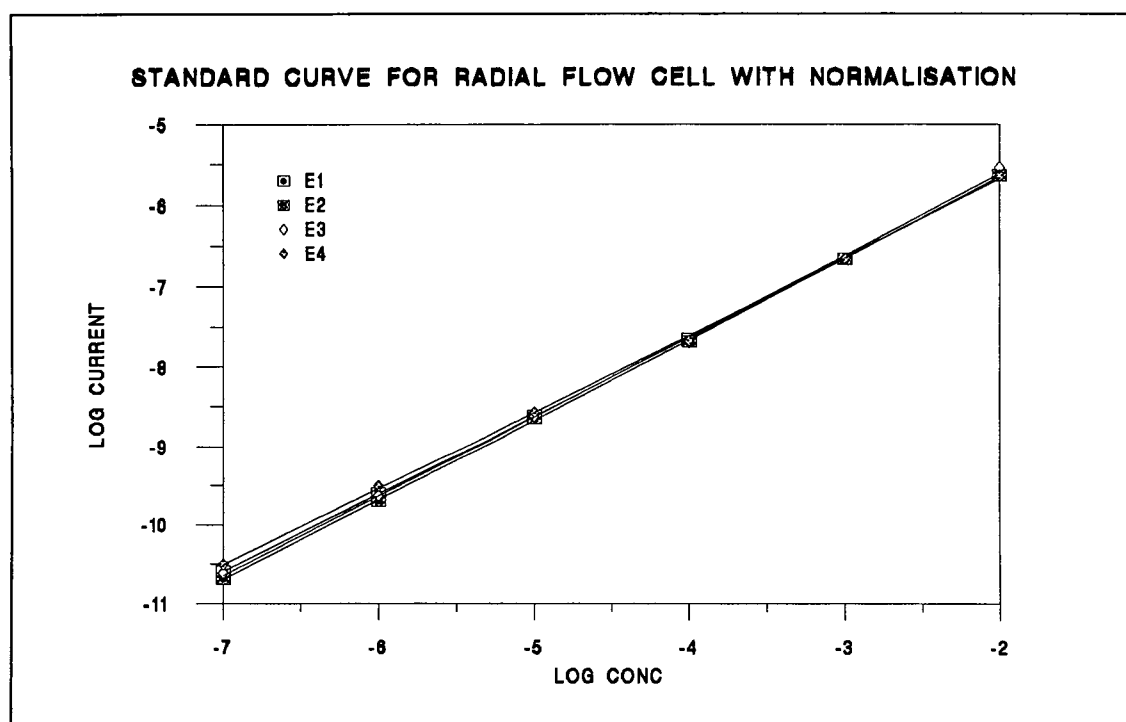


Figure 7 2 (b) Plot of log-log concentration vs current for electrode array of radial flow cell responses with normalisation

NORMALISED		RADIAL FLOW CELL						
CONCENTRATION 1E-7M		CURRENT x1E-12A						
INJECTION NO	E1	E2	E3	E4	MEAN	STDEV	RSD	
	1	18 98	20 5	21 19	19 27	19 985	1 03899	5 198849
	2	19 87	23 2	19 81	21 63	21 1275	1 619143	7 663677
	3	20 11	21 96	20 16	18 72	20 2375	1 328166	6 562896
	4	19 46	20 89	20 19	21 17	20 4275	0 765436	3 747084
MEAN		19 605	21 6375	20 3375	20 1975			
STDEV		0 495614	1 210795	0 593935	1 419046			
		2 527998	5 595818	2 920391	7 02585			
CONCENTRATION 1E-6M		CURRENT x1E-12A						
INJECTION NO	E1	E2	E3	E4	MEAN	STDEV	RSD	
	1	184	196	193	182	188 75	6 800735	3 603039
	2	178	209	186	193	191 5	13 17826	6 8816
	3	187	214	206	188	198 75	13 40087	6 742576
	4	180	197	191	191	189 75	7 088723	3 735823
MEAN		182 25	204	194	188 5			
STDEV		4 031129	8 906926	8 524475	4 795832			
		2 211868	4 36614	4 394059	2 544208			
CONCENTRATION 1E-5M		CURRENT x 1E-9						
INJECTION NO	E1	E2	E3	E4	MEAN	STDEV	RSD	
	1	1 97	2 02	1 93	1 84	1 94	0 076158	3 925656
	2	1 99	2 01	1 97	1 98	1 9875	0 017078	0 859283
	3	1 91	2 04	1 96	1 89	1 95	0 066833	3 42734
	4	1 92	2 05	1 91	2 01	1 9725	0 068496	3 472534
MEAN		1 9475	2 03	1 9425	1 93			
STDEV		0 038622	0 018257	0 027538	0 07874			
RSD		1 983163	0 89938	1 41765	4 079797			
CONCENTRATION 1E-4M		CURRENT x 1E-9A						
INJECTION NO	E1	E2	E3	E4	MEAN	STDEV	RSD	
	1	21 68	22 1	21 89	21 61	21 82	0 221359	1 01448
	2	19 84	21 02	19 94	20 03	20 2075	0 547197	2 707893
	3	20 32	20 96	19 54	19 76	20 145	0 634849	3 151398
	4	20 29	21 16	19 62	21 96	20 7575	1 019882	4 913316
MEAN		20 5325	21 31	20 2475	20 84			
STDEV		0 79588	0 533292	1 108554	1 106014			
RSD		3 876196	2 502542	5 475016	5 307168			

CONCENTRATION 1E-3M		CURRENT x 1E-9A						
INJECTION NO	E1	E2	E3	E4	MEAN	STDEV	RSD	
1	232 78	239 59	240 72	238	237 7725	3 51036	1 476352	
2	222 06	230 54	226 03	228 09	226 68	3 58955	1 583532	
3	226 34	227 42	228 73	227 84	227 5825	0 992182	0 435966	
4	227 45	231 67	236 87	228 74	231 1825	4 18261	1 809224	
MEAN	227 1575	232 305	233 0875	230 6675				
STDEV	4 410248	5 178574	6 864364	4 903029				
RSD	1 941494	2 229214	2 944973	2 125583				

CONCENTRATION 1E-2M		CURRENT x 1E-6A						
INJECTION NO	E1	E2	E3	E4	MEAN	STDEV	RSD	
1	2 37	2 41	2 41	2 38	2 3925	0 020616	0 861673	
2	2 46	2 5	2 51	2 47	2 485	0 023805	0 957938	
3	2 24	2 38	2 38	2 25	2 3125	0 078049	3 375098	
4	2 41	2 45	2 52	2 34	2 43	0 075277	3 09783	
MEAN	2 37	2 435	2 455	2 36				
STDEV	0 094163	0 051962	0 070475	0 091287				
RSD	3 973121	2 133944	2 870655	3 868097				

CONCENTRATION 1E-1M		CURRENT x 1E-6						
INJECTION NO	E1	E2	E3	E4	MEAN	STDEV	RSD	
1	10 57	10 64	10 58	10 81	10 65	0 111056	1 042775	
2	10 54	10 64	10 6	10 68	10 615	0 059722	0 562615	
3	10 54	10 61	10 58	10 65	10 595	0 046547	0 439334	
4	10 55	10 65	10 56	10 69	10 6125	0 068496	0 645425	
MEAN	10 55	10 635	10 58	10 7075				
STDEV	0 014142	0 017321	0 01633	0 070415				
RSD	0 134049	0 162863	0 154347	0 657627				

Table 7 2 6 Statistical analysis of electrode array responses for 4 repetitive injections of potassium ferricyanide Both the inter-electrode and the individual electrode RSD's are calculated The data is presented here have been normalised

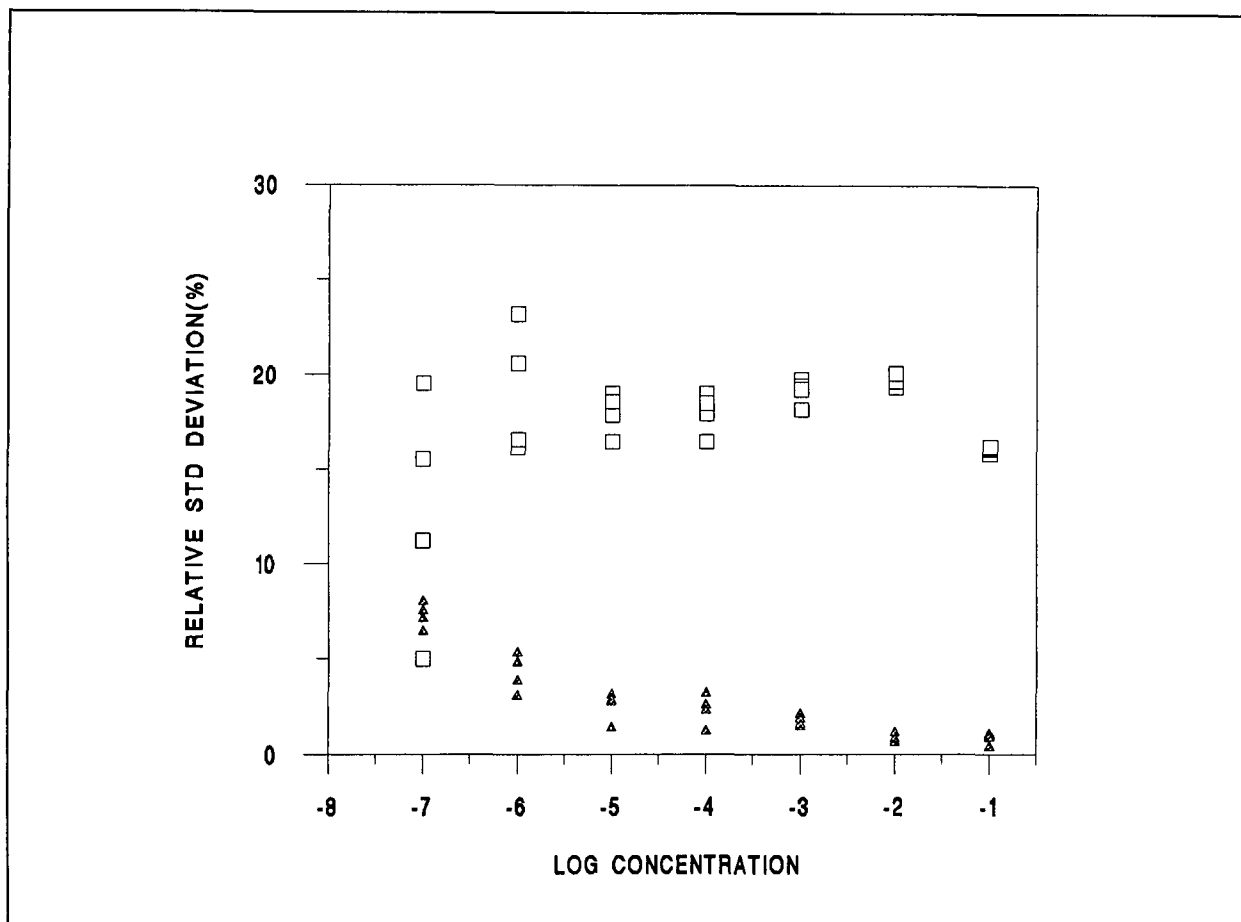


Figure 7.3 Plot of relative standard deviation between the electrodes (□) and at the individual electrodes (Δ) vs \log_{10} concentration for 4 repetitive injections of potassium ferricyanide. The radial electrode responses are presented here without normalisation.

The normalised responses are shown in Figure 7.4(a) and 7.4(b). The RSD between the electrodes is considerably reduced and is comparable to the RSD for a single electrode with multiple injections. These results demonstrate the averaging of that array response without normalisation will introduce significant imprecision and error into the results, thus demonstrating the necessity of applying a normalisation procedure. Further analysis of the data by two factor ANOVA demonstrates that all the inter electrode variances differ substantially from the inter-injection variances without normalisation. All F-tests for the inter-electrode variances were significant, while the inter-injection F-tests were

found to be non-significant. Application of the normalisation procedure results in a decrease of inter-electrode variance to a level which is comparable to the inter-injection variance. The resultant F-tests are either non-significant or marginally significant. The inter-injection variance remains of the same order of magnitude as the unnormalised data. The ANOVA results are reinforced by the trends exhibited in Figures 7.3, 7.4(a) and 7.4(b). Further refinement of the normalisation procedure is necessary however to achieve a situation where none of the F-tests are significant, i.e. no significant difference exists between the of both the inter-electrode and the inter-injection variances.

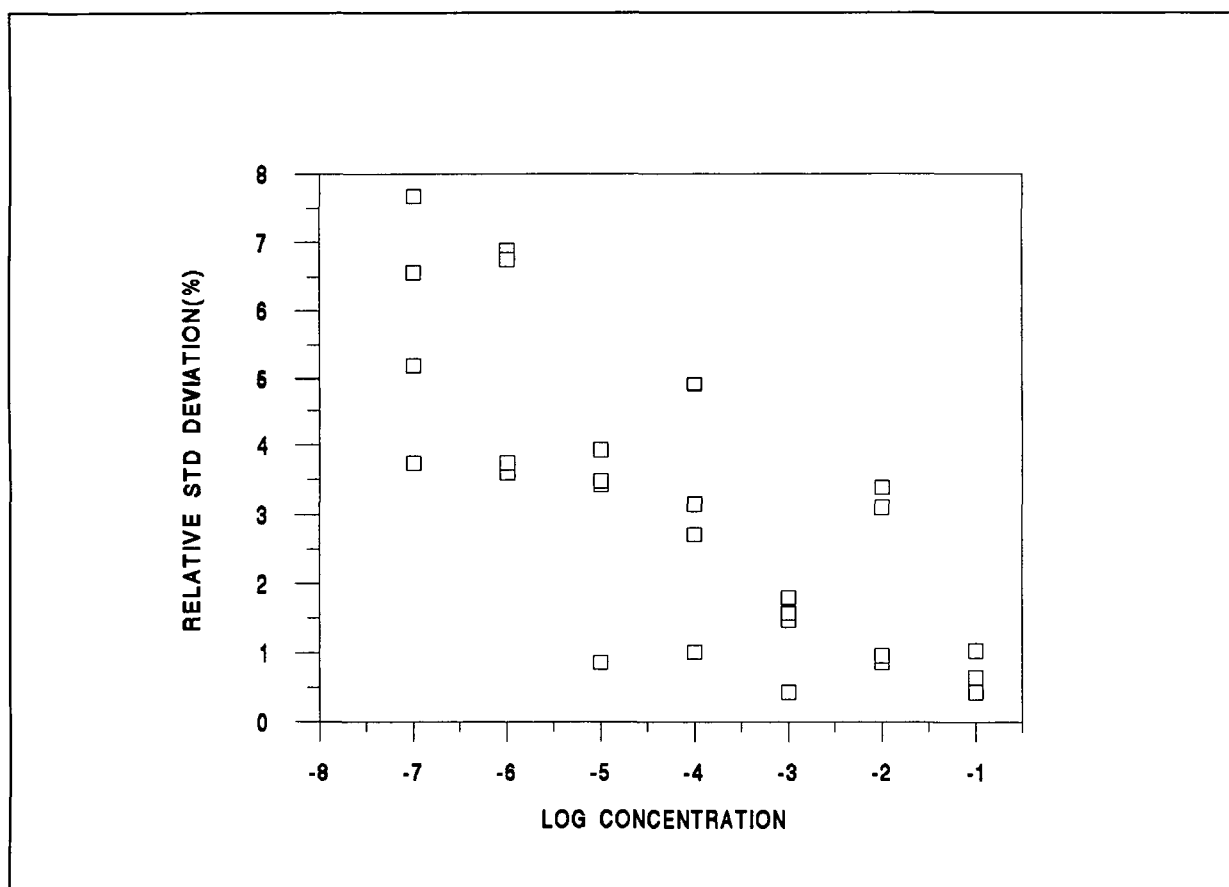


Figure 7.4(a) Plot of the inter-electrode relative standard deviation (\square) vs \log_{10} concentration potassium ferricyanide for 4 repetitive injections. The radial flow cell responses have been normalised.

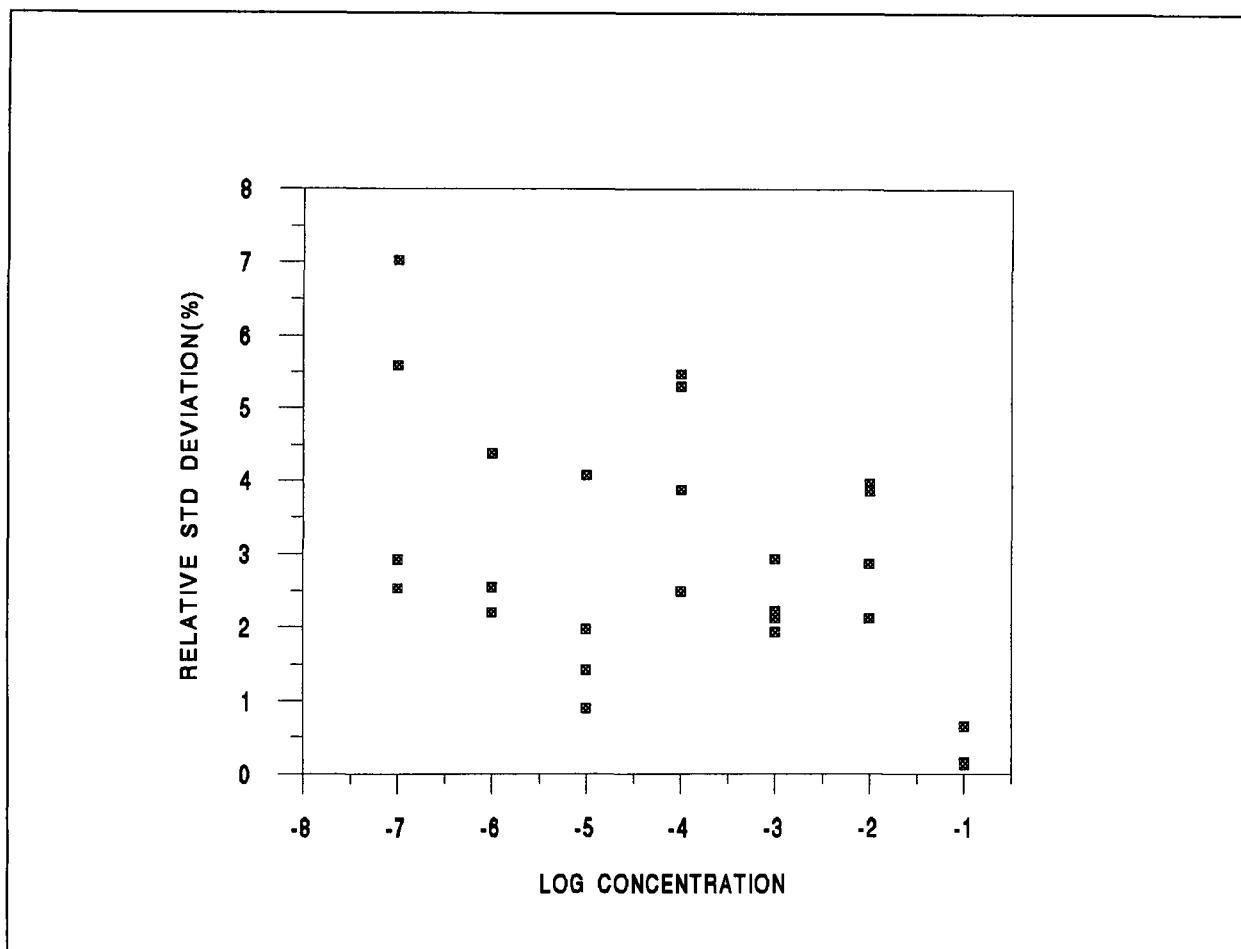


Figure 7.4(b) Plot of relative standard deviation (■) at each individual electrode electrode vs \log_{10} concentration potassium ferricyanide for 4 repetitive injections. The radial array responses have been normalised.

7.2.5 Three-Dimensional Results

Use of multielectrode arrays enables a 3-dimensional plot of the electrochemical response to be obtained, thus enabling features which would normally be hidden in a standard two dimensional display to be identified. This has important applications in chromatography, where the problem of two components eluting at the same time can be difficult to detect. An array approach offers a possible solution to this problem in a manner similar to that of

spectrophotometric diode-array peak purity elucidation It is also applicable in FIA for simultaneous multicomponent determination without prior separation may be possible

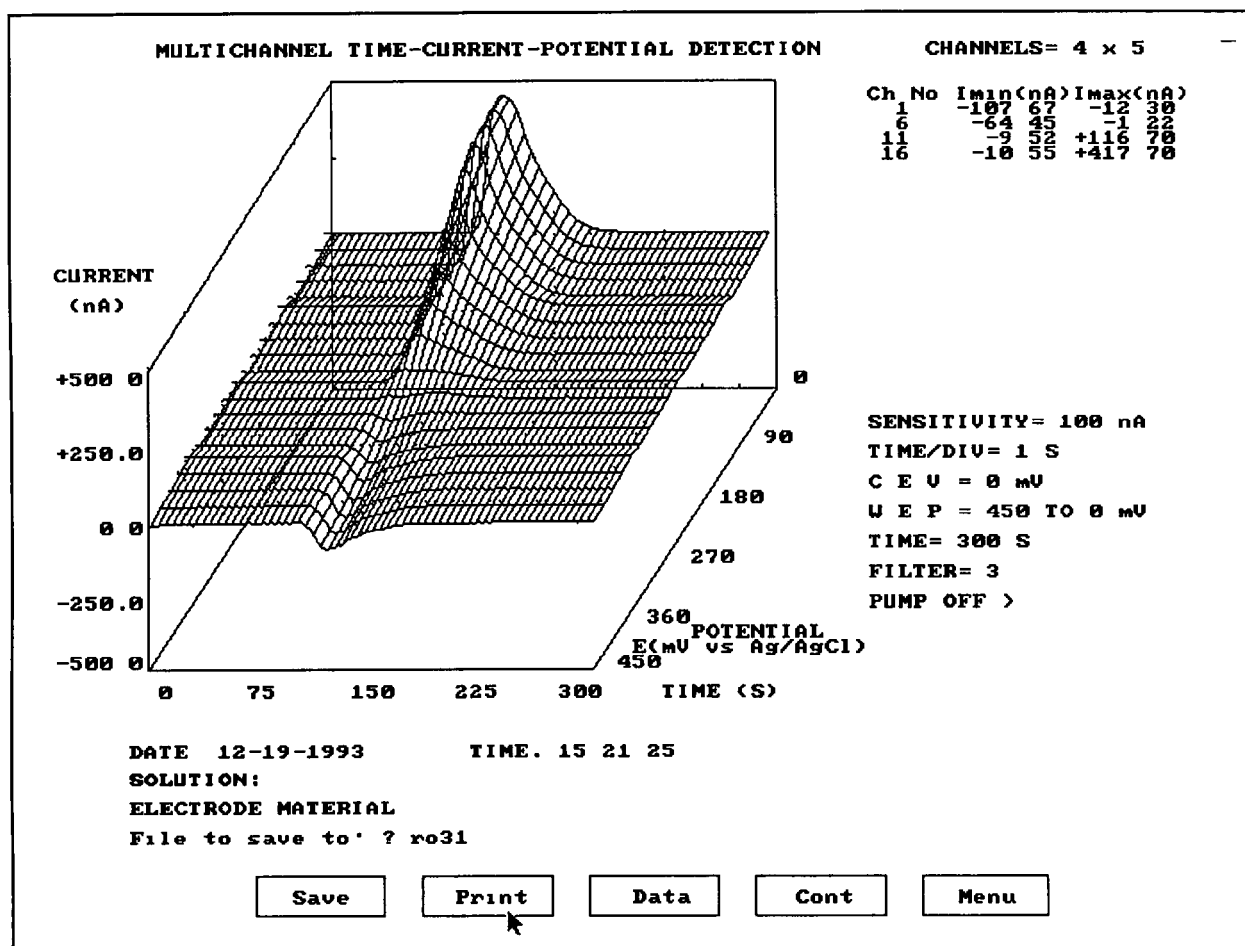


Figure 7.5 On-line display of 3-D voltammogram of potassium ferricyanide ($1 \times 10^{-3} \text{M}$) Five sequential voltage steps of 23.68 mV are applied at the working electrode array which is polarised in the range 0 to 450 mV to generate a 20 working electrode result using the linear flow cell configuration

Figure 7.5 shows the real-time 3-d display generated by the FIA electrochemical array detector (FIA-EA) to an injection of 10^{-4}M potassium ferricyanide (20 channels i.e. 0-450 mV ca. 23.68 mV resolution) Both the oxidation and reduction peaks can be clearly

seen demonstrating the quasi-reversible nature of the compound. The data is stored in ASCII format which facilitates post-run with spreadsheets and other commercial software packages for post-run processing (e.g. removal of charging current distortions) and 3-dimensional display in line or surface formats. This approach enables the user to take advantage of the powerful but flexible data processing and display options offered by statistics packages and/or spreadsheets such as EXCEL (vs 4.0). This facility is useful for the investigation of charging current effects or electrode base line linearity. Easy access to the tabulated data within the spreadsheet enables 2-dimensional hydrodynamic voltammogram to be obtained at any desired time during the analysis run (i.e. t slices).

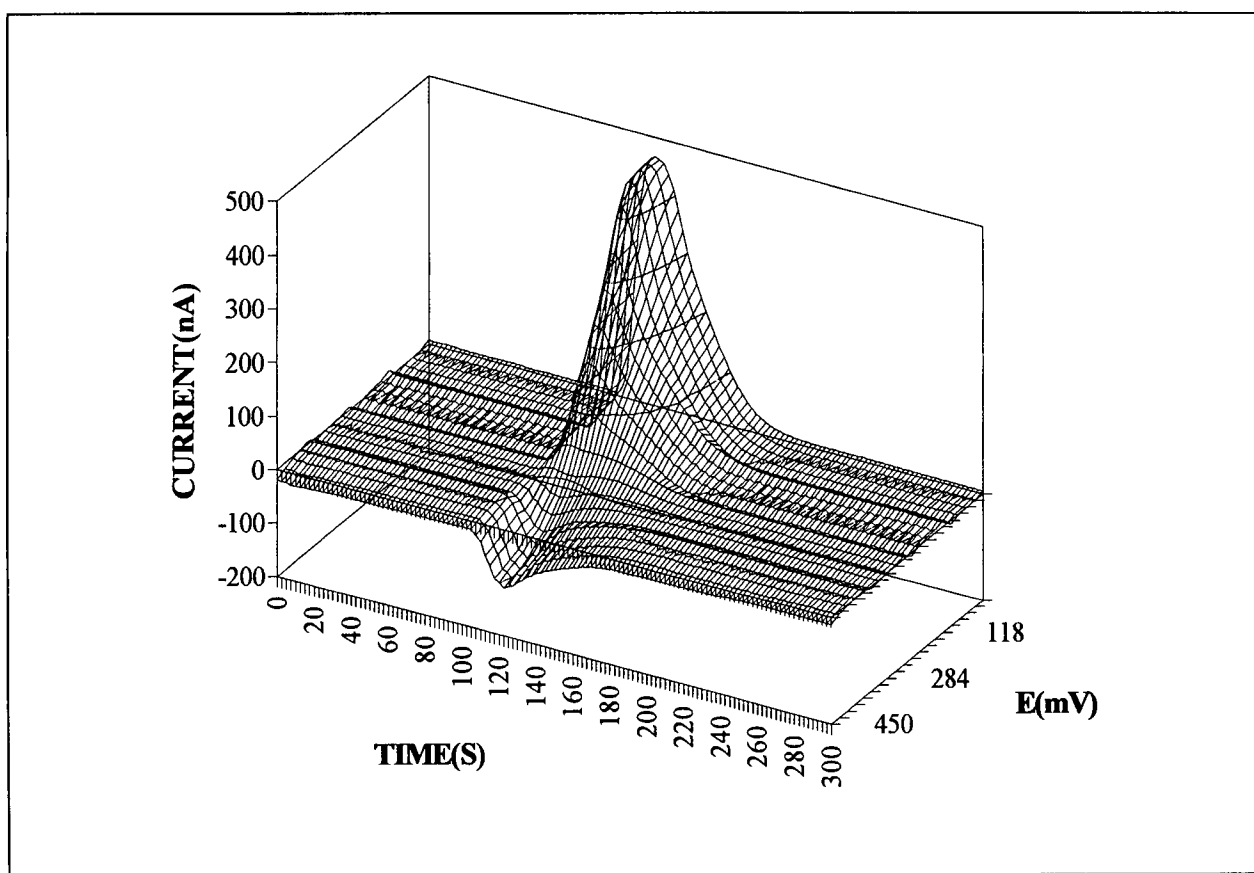


Figure 7.6(a) 3-dimensional post-run presentation (Microsoft Excel) of a potassium ferricyanide(1×10^{-3}) hydrodynamic voltammogram in 0.05M phosphate buffer

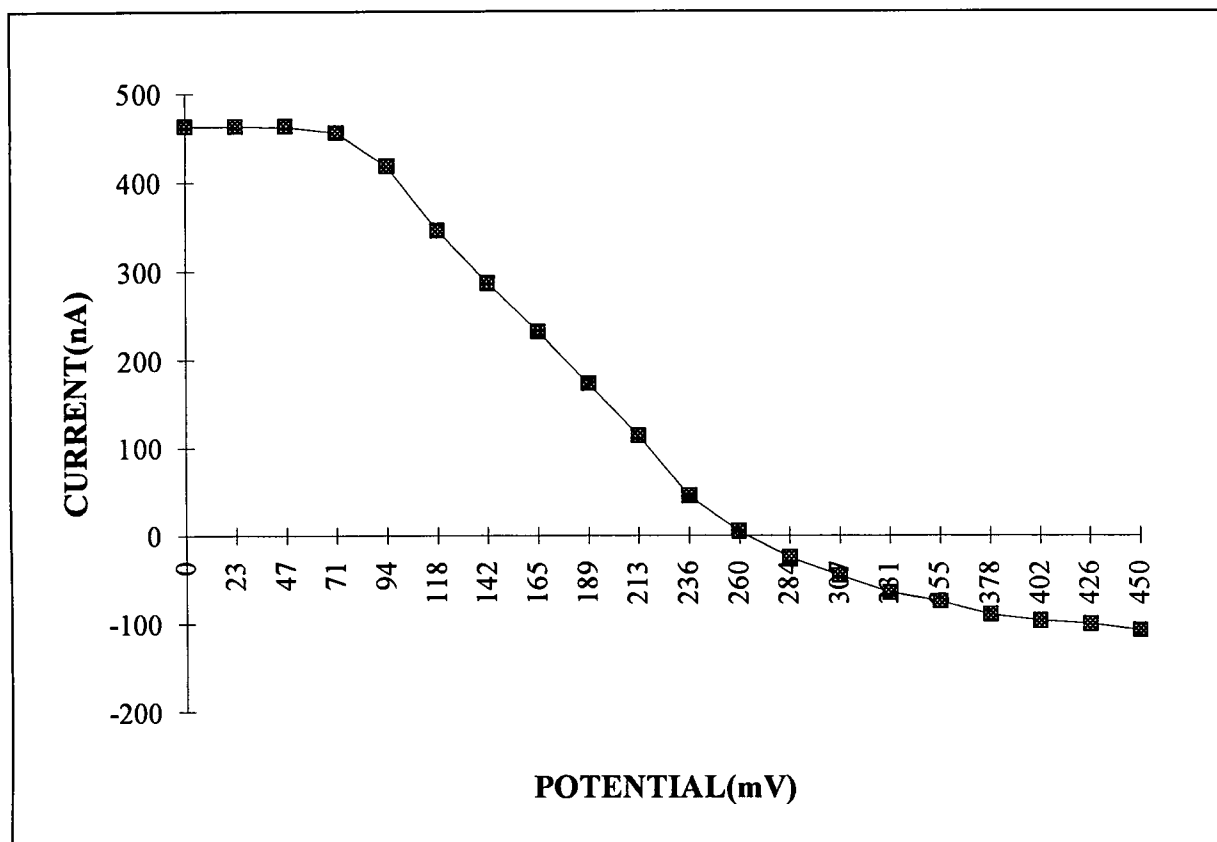


Figure 7 6(b) Hydrodynamic voltammogram of potassium ferricyanide taken from Figure 6(a) at 122 5 seconds covering the potential range 0 to 450 mV

This facility increases the amount of available information for each voltammogram and is important when calculating of the halfwave potential for qualitative work which is displayed with increased clarity in a 2-dimensional format The 2-dimensional hydrodynamic voltammogram of Figure 7 6(a) is shown in Figure 7 6(b) The data at time 122 5 sec were selected as they correspond to both the oxidation and reduction maxima visible on the 3-d display The halfwave potentials obtained from the hydrodynamic voltammogram in Figure 7 6(b) are comparable to those obtained using batch analysis with commercial instrumentation (Bioanalytical Systems CV50W)

- Oxidation halfwave potential 313mV 290mV (CV50W)
- Reduction halfwave potential 157mV 50mV (CV50W)

The shifts in potentials are assumed to be a result of the differences in the two techniques. The highly reversible nature of hydroquinone electrochemistry is shown in Figure 7.7. Oxidation and reduction peaks of almost equal height are obtained. A carrier stream (flow rate 0.4 ml/min) of 0.05 M phosphate buffer (pH 7.4) was used.

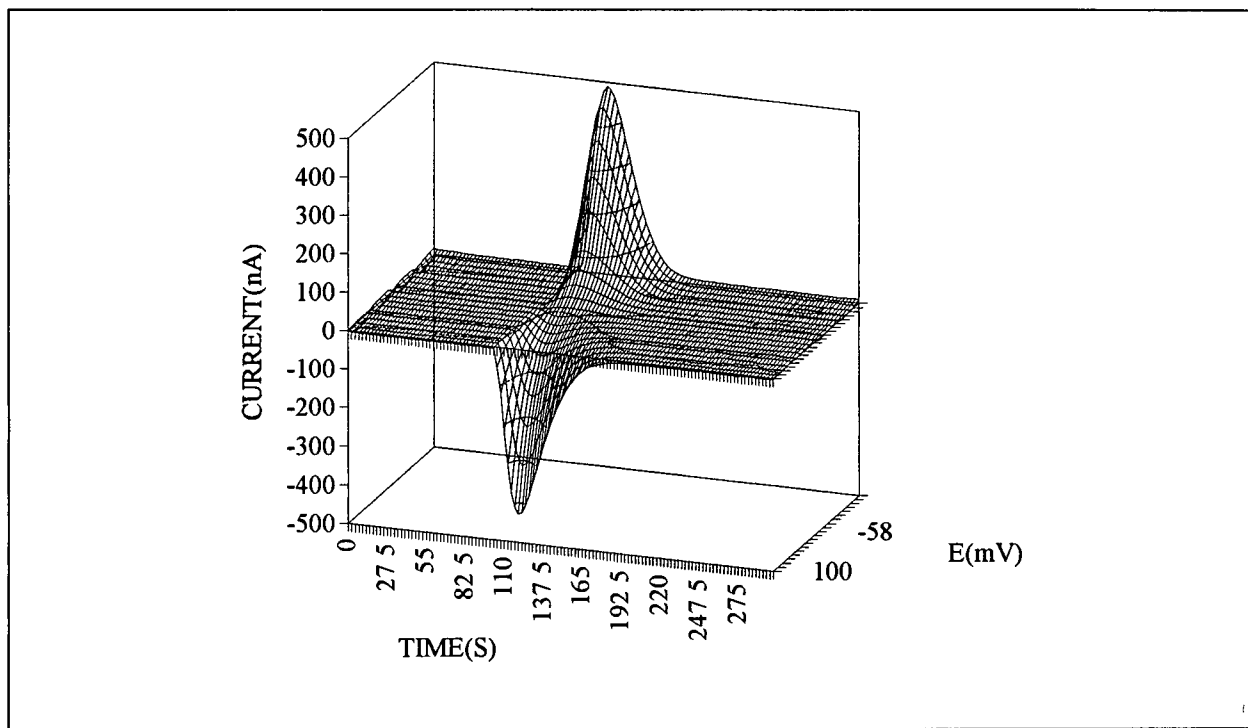


Figure 7.7 3-dimensional hydrodynamic voltammogram of hydroquinone (0.1 M) in 0.05 M phosphate buffer

7.2.6 Metal Analysis

The array was applied to the determination of Cu^{2+} , Fe^{2+} and mixtures of both. Flow injection analysis normally does not afford any selectivity therefore individual components in a mixed injection cannot be resolved individual only a signal corresponding to the total response is obtained. The problem can be overcome by inclusion of a chromatographic step which achieves the necessary separation. However

the combination of FIA with an amperometric array can be used to determine the individual components in a mixed species situation without prior separation

Cu^{2+} , Fe^{2+} and mixtures of both at a concentration of 250 ppm were prepared from a standard solution of 1000 ppm concentration. The array was polarised between +50 mV and -250 mV. The 3-dimensional hydrodynamic voltammograms (chronovoltammograms) of the respective metals are presented in Figure 7.8

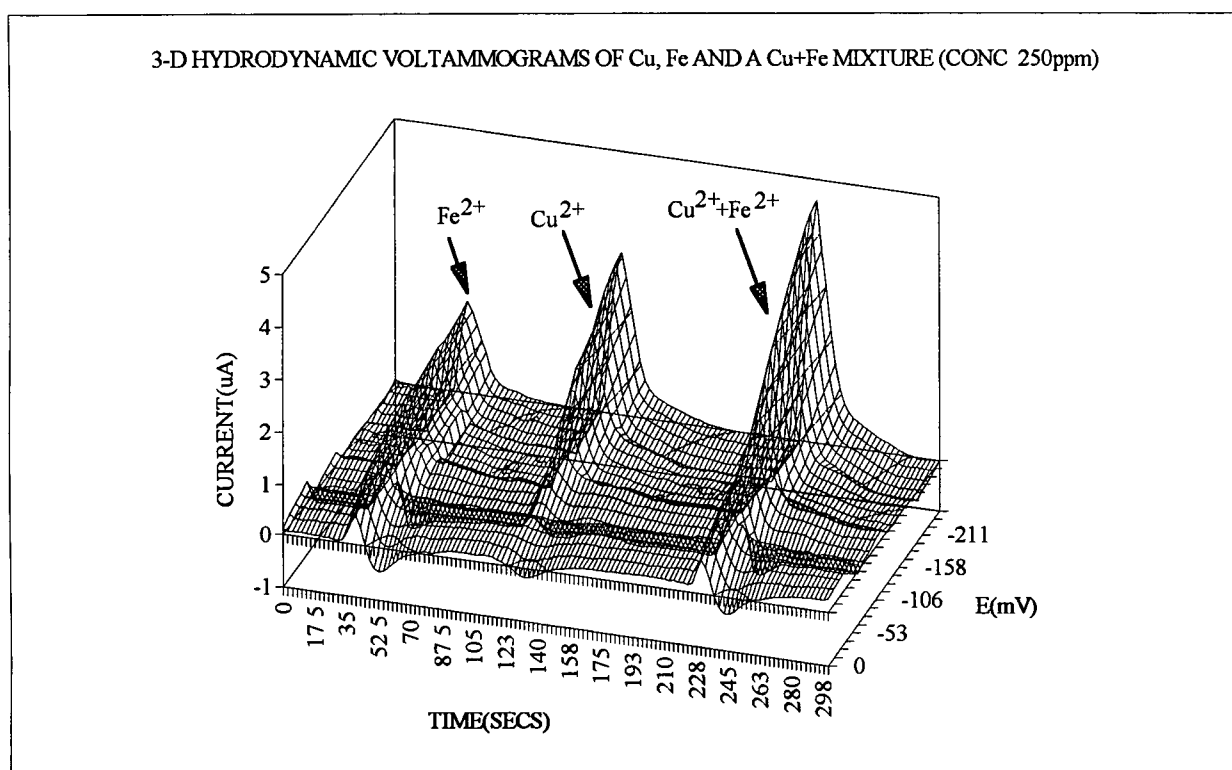


Figure 7.8 3-dimensional hydrodynamic voltammograms of copper²⁺, iron²⁺ and a mixture of both at concentrations of 250 ppm mobile phase - 0.05M phosphate buffer

The corresponding 2-dimensional hydrodynamic voltammograms were extracted at the current maxima. The relationship between the individual and the mixed voltammograms was investigated. The individual voltammograms were found to be approximately 90% additive as compared to the mixed voltammogram. Subtraction routines were utilised in

an effort to obtain voltammograms corresponding to the individual from the combined voltammogram. Some samples results are shown in Figure 7.11(a) and 7.11(b). Good correlation between the voltammetric shapes is obtained. However, a significant difference in the current values exists. The use of a weighting factor for each data point could be used to normalise the responses, provided that the ratio between the respective responses remains constant (such as procedure can be carried out post-run). A linear response to copper injections was obtained in the range 500 ppm - 100 ppb.

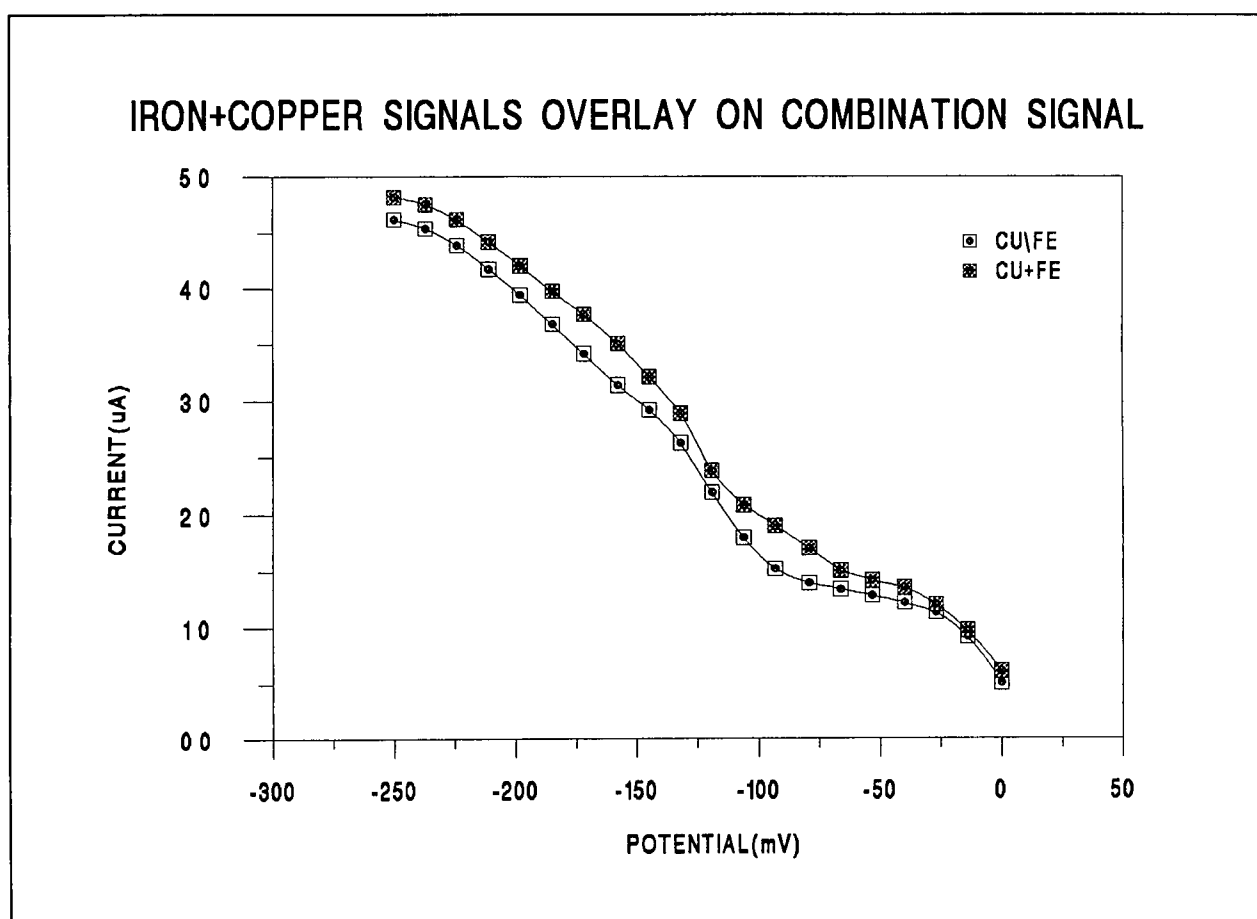


Figure 7.9 (a) A comparison between the 2-dimensional hydrodynamic voltammogram of the mixture and the addition of the individual metal voltammograms

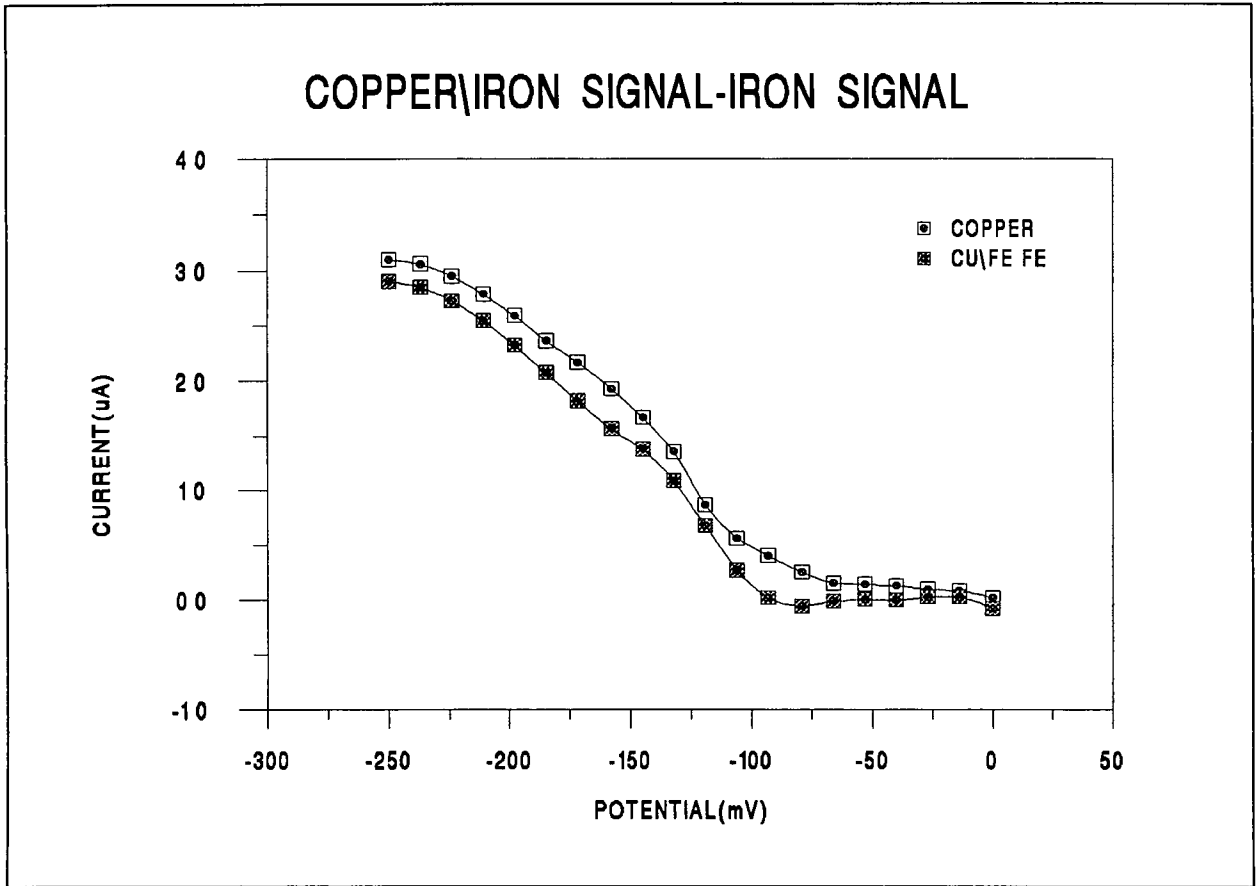


Figure 7 9(b) A comparison between the voltammogram obtain for copper by subtraction and the experimental result

CHAPTER 8

CONCLUSIONS AND FURTHER WORK

8.1 Conclusion

Amperometric arrays offer a significant improvement in electrochemical detection over single electrode configurations. These improvements are offered in both the qualitative and quantitative realms of analysis. Real time multi-component analysis is possible by careful selection of the working electrode potentials. The use of fixed as opposed to scanning DC voltammetry at a single working electrode can result in a significant increase in the amount of electrochemical information obtained such as data on reversibility. Data acquisition times are reduced and therefore suited to FIA and short time HPLC. High speed data acquisition which is equivalent to high speed scan rates can be carried out routinely without the undesired effects of charging currents and distortion of the voltammogram which occurs at high scan rates with a single electrode. Use of an array makes it possible to implement data redundancy regimes and therefore enhance the reliability and accuracy of the data obtained. The most important feature in the development of multichannel detection is the fabrication of low noise, reproducible working electrodes which are also robust and sensitive. Non-ideal behaviour of the working electrode arrays necessitates the development of normalisation procedures to compensate for this problem.

The results demonstrate the advantages of the multichannel potentiostats which can be utilised for numerous analytical applications.

8.2 Further Work

The present configuration of the system allows for possible development in a number of areas. Fabrication of the potentiostat circuits on a PCB board is desirable to increase the reliability of the electronic performance. A board that is capable of controlling eight working electrodes which fits into a PC expansion slot has been designed. The design utilised neglects the use of the RTI cards by incorporating both its own ADC (successive approximation 12-bit resolution) and digital I/O. Additional boards allow ease of expansion to accommodate larger working electrode array. Software control of these boards could be effected by Labview ® for Windows. This is a powerful and software development environment in which normal line code programming could be replaced by an object oriented approach. This employs the use of icons which represent the software instructions which are linked together and executed in a manner similar to a program flowchart. This environment facilitates the development of virtual instrumentation panels thus removing the tedious and difficult task of creating a "pleasing" graphical display.

The use of microband electrodes could offer a possible improvement in array performance and reproducibility. These can be fabricated by conventional photolithography or screen-printing. The arrays can therefore essentially be treated as disposable, removing any problems of electrode poisoning. This could prove very useful when dealing with biological samples where protein deposition can be a considerable problem.

Modifications of the flow cell designs would include housing the reference electrode together with working and counter electrodes in a single cell body. This would minimise any sample dispersion presented to the reference electrode. Closer proximity of the reference electrode to the working electrode array may improve potentiostat control.

REFERENCES

- 1 Willard, H H , Merrit, L L , Dean, J A and Settl, F A , *Instrumental Methods of Analysis*, Belmont, Wadsworth Inc, 1988
- 2 Skoog, A D , West, D M and Holler, F J , *Fundamentals of Analytical Chemistry*, New York, Saunders College Publishing, 1988
- 3 Heyrovsky, J , *Chem Listy* , 16, (1922), 256
- 4 Bond, A M , *Modern Polarographic Methods in Analytical Chemistry*, New York, Dekker, 1980
- 5 Osteryoung, J G and Osteryoung, R A , *Anal Chem* 57, (1985), 101A
- 6 Blutstein, H , Bond, A M and Norris, A , *Anal Chem* 46, (1974), 1754
- 7 Nicholson, R S and Shan, I , *Anal Chem* 36, (1964), 706
- 8 Vassos, B H and Ewing, G W , *Electroanalytical Chemistry*, New York, Wiley-Interscience, 1983
- 9 Plambeck, J A , *Electroanalysis Chemistry, Basic Principles and Applications*, New York, Wiley-Interscience, 1982
- 10 Christian, G D , *Analytical Science*, New York, Wiley, 1986
- 11 Bard, A J and Faulker, L R , *Electrochemical Methods, Fundamentals and Applications*, New York, Wiley, 1980
- 12 Schwarz, W M and Shan, I , *Anal Chem* 35, (1963), 1770
- 13 Floyd, T L , *Electronic Devices*, Columbus, Merrill, 1986
- 14 Osteryoung, J , *Science*, 218, (1982), 261
- 15 Enke, C G , *Science*, 218, (1982), 785
- 16 Bond, A M and Grabařic, B S , *Anal Chem* 51, (1979), 337
- 17 Bond, A M , Greenhill, H B , Heritage, I D and Reust, J B , *Anal Chim Acta* 165, (1984), 209

- 18 Wieck, H J , Heider, G H, Yacynych, A M , *Anal Chim Acta* 166, (1984), 315
- 19 Stefani, S and Seeber, R , *Anal Chim Acta* 187, (1986), 213
- 20 He, P and Faulkner, L R , *J Electroanal Chem* 224, (1987), 277
- 21 Ivaska, A , *Comtemporary Electroanalytical Chemistry*, New York, Plenum Press, 1990
- 22 Napp, D T , Johnson, D C and Brucenstein, S , *Anal Chem* 39, (1967), 481
- 23 Svenden, C N , *Analyst*, 118, (1993), 123
- 24 Stulick, K and Pacakova, V , *Electroanalytical Measurements in Flowing Liquids*, New York, Ellis Horwood, 1987
- 25 Kissinger, P T , *Anal Chem* 49, (1977), 447A
- 26 Kissinger, P T , Refshauge, C , Dreiling, R and Adams, R N , *Anal Lett* 6, (1973), 465
- 27 Anderson, J L and Chesney, D J , *Anal Chem* 52, (1980), 2156
- 28 Weisshaar, D E , Tallman, D E and Anderson, J L , *Anal Chem* 53, (1981), 1809
- 29 Anderson, J L , Weisshaar, D E and Tallman, D E , *Anal Chem* 53, (1981), 906
- 30 Radzik, D M , Brodbelt, J S and Kissinger, P T , *Anal Chem* 56, (1984), 2927
- 31 Kok, W Th , Hanekamp, H B , Bos, P and Frei, R W , *Anal Chim Acta* 142, (1982), 31
- 32 Samuelson, R , O'Dea, J and Osteryoung, J , *Anal Chem* 52, (1980), 2215
- 33 Reardon, P A , O'Brien, G E and Sturrock, P E , *Anal Chim Acta* 162, (1984), 175
- 34 Owens, D S , Johnson, C M , Sturrock, P E and Jaramillo, A , *Anal Chim Acta* 197, (1987), 249
- 35 Gunasingham, H , Tsy, B T and Ang, K P , *Anal Chem* 59, (1987), 262
- 36 Caudill, W L , Ewing, A G , Jones, S and Wightman, R W , *Anal Chem* 55, (1983), 1877
- 37 Wang, J and Dewald, H D , *Anal Chim Acta* 153, (1983), 325
- 38 Janata, J , Thogersen, N and Ruzicka, J , *Anal Chem* 55, (1983), 1986

- 39 Ruzicka, J Hansen, E H , Ghose, A K and Mottola, H A , *Anal Chem* 51, (1979), 199
- 40 Roston, D A , Shoup, R E and Kissinger, P T , *Anal Chem* 54, (1982), 1417A
- 41 Lunte, L E , Kissinger, P T and Shoup, R E , *Anal Chem* 54, (1982), 429
- 42 Anderson, L B and Reilly, C N , *J Electroanal Chem* 10, (1965), 295
- 43 Weber, S G and Purdy, W C , *Anal Chim Acta* , 148, (1985), 127
- 44 McClintock, S A and Purdy, W C , *Anal Lett* 14, (1981), 791
- 45 Lunte, C E , Wheeler, J F and Heineman, W R , *Anal Chim Acta* 200, (1987), 101
- 46 Roston, D A , Kissinger, P T and Shoup, R E , *Anal Chem* 54, (1982), 429
- 47 Allison, L A and Shoup, R E , *Anal Chem* 55, (1983), 8
- 48 Shoup, R E and Mayer, G S , *Anal Chem* 54, (1982), 1164
- 49 Aoki, A , Matsue, T and Uchida, I , *Anal Chem* 62, (1990), 2206
- 50 Sanderson, D G and Anderson, L B , *Anal Chem* 57, (1985), 2388
- 51 Lunte, L E , Wong, Sy We , Ridgeway, T H and Heineman W R , *Anal Chem* 188, (1986), 263
- 52 Cante, F , Rois A , Luque De Castro, M D and Valcarcel, M , *Anal Chim Acta* 211, (1988), 287
- 53 Albahadily, F N and Mottola, H A , *J Chem Educ* 63, (1986), 271
- 54 Matson, W R , Gamache, P G , Beal, M F and Bird, E D , *Life Science*, 41, (1987), 905
- 55 Matson, W R , Langlais, P , Volicer, L , Gamache, P H , Bird, E D and Mark K A , *Clin Chem* 30, (1984), 1477
- 56 Last, T A , *Anal Chem* 55, (1983), 1509
- 57 Saitoh, R and Suzuki, H , *Anal Chem* 51, (1979), 1683
- 58 Hershberger, L W , Callis, J B and Christian, G D , *Anal Chem* 53, (1981), 971
- 59 Wang, J , Rayson, G D , Lu, Z and Wu, H , *Anal Chem* 62, (1990), 1924
- 60 Mortia, M , Longmuire, M L and Murray, R W , *Anal Chem* 60, (1988), 2770

- 61 Anderson, J L , Whiten, K K , Brewester, J D , Ou, T Y , and Nonidez, W K ,
Anal Chem 57, (1985), 1366
- 62 DeAbreau, M and Purdy, W C , *Anal Chem* 59, (1987), 204
- 63 Fosdick, L E and Anderson, J L , *Anal Chem* 58, (1986), 2750
- 64 Anderson, J L , Ou, T Y and Moldoveanu, S , *J Electroanal Chem* 196, (1985),
213
- 65 Harrington, M S , Anderson, L B , Robbins, J A and Karweik, D H ,
Rev Sci Instrum 60, (1989), 3323
- 66 Matsue, T , Aoki, A , Ando, E and Uchida, I , *Anal Chem* 62, (1990), 407
- 67 Aoki, A , Matsue, T and Uchida, I , *Anal Chem* 64, (1992), 44
- 68 Hoogvliet, J C , Reijm, J M and van Bennekom, W P , *Anal Chem* 63, (1991),
2418
- 69 Fielden, P R and McCreedy, T , *Anal Chim Acta* 273, (1993), 111
- 70 Bearly, T H , Doshi, A K and Fielden, P R , *Anal Proc*, 26, (1989), 389
- 71 *RTI-800/815 User's Manual*, Analog Devices
- 72 *RTI-817 User's Manual*, Analog Devices
- 73 Don Lancaster, *Active-Filter Cookbook*, Indianapolis, 1975
- 74 Patrick H Garrett, *Analog I/O Design*, Reston Publishing company, 1981
- 75 M S Ghausi, and K R Laker, *Modern Filter Design*, Bell Telephone Laboratories
Inc , 1981
- 76 *Data-Acquisition Databook*, Volume 1, Integrated Circuits, Analog Devices
- 77 *Software Manual for the RTI-800, 802, 815, 817, 820*, Analog Devices
- 78 A Robinson, *Multichannel Time series Analysis with Digital Computer Programs*,
Holden-Day Inc , San Francisco, 1967
- 79 R W Hamming, *Digital Filter*, Prentice-Hall Inc , New Jersey, 1983
- 80 G F Dulaney, *Anal Chem* , 47, (1975), 27A
- 81 R Thompson, *J Chem Educ* , 62(10), (1985), 866

- 82 Shukla, S , and J Rusling, *Anal Chem* , 56(12), (1984), 1347A
- 83 Dulaney, G , *Anal Chem* , 17, (1975), 25A
- 84 Binkley, D , and R Dessy, *J Chem Educ* , 56, (1979), 148
- 85 Hari Gunasingham, *Anal Chem Acta*, 169, (1985), 309
- 86 A Savitsky and M J E Golay, *Anal Chem* 36, (1964), 1627
- 87 Howard A Strobel, and Willam R Heineman, *Chemical Instrumentation, A Systematic Approach*, New York, John Wiley & Sons, 1989

Multichannel Potentiostat Detection System For Flow Analysis

